

Norwegian University  
of Life Sciences

**Master's Thesis 2020 30 ECTS**

Faculty of Science and Technology

# **Influence of vegetation height on temperature measurements**

Påvirkning av vegetasjonshøyde på  
temperaturmålinger

**Johanne Wiborg**

Environmental Physics and Renewable Energy



# Preface and Acknowledgements

The following work is a master's thesis, which marks the end of my studies in Environmental Physics and Renewable Energy at the Norwegian University of Life Sciences (NMBU). The thesis is a part of a cooperation between the Norwegian Meteorological Institute and NMBU

First and foremost, I would like to thank my advisor Mareile Wolff for all her help and guidance throughout this process. Being a part of this project has been exciting and your expertise and insights have been invaluable.

I also want to thank everyone else that has provided me with the data and knowledge necessary for my thesis. I especially would like to thank Signe Kroken for providing me with all the data I asked for and more.

During my years at NMBU, I have made some great memories and met a lot of delightful people. I want to take this time to thank all my professors, especially Arne Auen Grimenes. My time at NMBU was wonderful, and knowing that I always had the support of my university has been so important to me. In addition to a top-notch education, I have made lifelong friendships. I am forever grateful to be a graduate of such a fantastic university and I will miss my time there greatly.

Lastly, I want to thank everyone who has helped me through this process. I knew that writing my thesis was going to be challenging, but I definitely never expected or imagined having to write it during a pandemic. The support of my friends and family has been extremely helpful. I want to thank Ingrid Marie Øiberg Lund for proofreading and for helpful grammar discussions. I want to thank my sisters, Helene and Rebecca, and my parents, Kersti and Trond, for being my biggest believers and my best supporters. Lastly, I want to thank Cody Pritchard for his patience and help throughout this process. Thank you for your help with the field controls, the writing, and proofreading, and for tolerating all my talk about the influence of grass on temperature for five months.

Johanne Wiborg  
NMBU, Ås  
15/6/2020



# Abstract

The environmental conditions surrounding a meteorological site influence the measurements taken at that site. To account for this, the World Meteorological Organization's (WMO) Commission for Instruments and Methods of Observation (CIMO) provides guidelines for how temperature, precipitation, wind, and radiation measuring sites should be classified in their Siting Classification for Surface Observing Stations on Land (SC). These guidelines are given in the appendix of WMO CIMO's guide. The classifications given in the SC for temperature measuring sites take into consideration the factors of distance from heat sources and water bodies, slope, shade, and height of vegetation. A site's classification impacts the way its measurements are interpreted, including adding additional estimated uncertainty to the measurements to account for the site's environmental conditions. As an increasing number of countries are utilizing the SC, issues therein have been identified, and recommendations have been made to conduct further analysis of the SC criteria. These recommendations included, among other aspects, the category height of vegetation.

This thesis aimed to analyze and examine the influence of increased vegetation height on temperature measurements. The data used are from an experiment conducted in Ås, Norway, where air temperature and humidity data were collected hourly at two locations; one where the grass was cut (C) and one where the grass remained uncut (U). Data were collected at three heights in order to better understand the temperature profile. The grass at U was 40-50 cm tall throughout the majority of the experiment's duration. The SC currently estimates the additional estimated uncertainty of vegetation taller than 25 cm to be 2 °C.

This thesis' analysis of the observations showed that the most common difference between temperature measured at the two locations at 2 m was 0.0 °C and that 97.4% of the differences in temperature between U and C were in the interval [-0.3 °C, 0.3 °C]. Furthermore, the largest observed difference in temperature between U and C at 0.55 m was 1.4 °C. Of these values, 88.5% were in the  $\pm 0.3$  °C-interval.

As expected, the analysis also showed that weather impacted how strongly the influence of surface properties affected air temperature. Low wind and cloud cover increased the influence and made the difference between air temperature measured at U and C larger.

It is a well-known fact that increased vegetation density results in subdued diurnal temperature variation. When evaluating the difference in daily maximum and minimum temperature, this notion was demonstrated. The daily maximum temperature was generally lower over uncut grass than over cut grass, and the daily minimum was generally higher. However, the difference in daily maximum and minimum temperature between U and C at 2 m had median values of 0.0 °C and 0.1 °C respectively, making the differences smaller than would be expected based on the current SC guidelines.

The findings of this study indicate that increased vegetation height influences air temperature to a lesser degree than WMO CIMO suggests, and that the limits for vegetation height in the SC might be too strict.



# Sammendrag

Miljøforholdene rundt en meteorologisk stasjon påvirker målingene som blir gjort der. Verdens meteorologiorganisasjons (WMO) kommisjon for instrumenter og metoder for observasjon (CIMO), redegjør for dette ved å gi retningslinjer for hvordan målestasjoner for temperatur, nedbør, vind og stråling skal klassifiseres. Disse retningslinjene finnes i deres Siting Classification Guide (SC). Klassifiseringene som blir gitt for målestasjoner for temperatur tar hensyn til følgende kategorier for påvirkning: avstand fra varmekilder og vannmasser, helning, skygge og vegetasjonshøyde. Klassifiseringen av en målestasjon påvirker tolkingen av målingene. Dette skjer gjennom blant annet at målingene blir gitt en ytterligere estimert usikkerhet for å redegjøre for stasjonens miljøforhold. Ettersom stadig flere land tar i bruk SC er det blitt identifisert problemer med guiden, og ytterligere analyse av kriteriene i SC har blitt anbefalt. Disse anbefalingene inkluderer blant annet å gjennomføre en analyse av vegetasjonshøydekategorien.

Målet med denne oppgaven er å analysere og undersøke påvirkningen av økt vegetasjonshøyde på temperaturmålinger. Dataene som ble brukt er fra et eksperiment utført i Ås i Norge, der lufttemperatur- og fuktighetsmålinger ble samlet inn hver time på to steder. På det ene stedet ble gresset klipt (C) og på det andre stedet forble gresset uklipt (U). Data ble samlet inn i tre høyder for å få en bedre forståelse av temperaturprofilen. Gresset ved U var 40-50 cm høyt gjennom mesteparten av eksperimentet. SC anslår at den ekstra estimerte usikkerheten til stasjoner med vegetasjon høyere enn 25 cm er  $2^{\circ}\text{C}$ .

Resultatene som presenteres i oppgaven viser at den vanligste forskjellen mellom temperatur målt på de to stedene i 2 m var  $0,0^{\circ}\text{C}$ , og at 97,4% av temperaturforskjellene mellom U og C var i intervallet  $[(-0,3^{\circ}\text{C}), (0,3^{\circ}\text{C})]$ . Videre var  $1,4^{\circ}\text{C}$  den største observerte temperaturforskjellen mellom U og C i 0,55 m og 88,5% av disse temperaturforskjellene var mellom  $-0,3^{\circ}\text{C}$  og  $0,3^{\circ}\text{C}$ .

Som forventet viste analysen også at været hadde innflytelse på hvor sterk overflatens påvirkning var på lufttemperaturen. Lav vind og lavt skydekke økte påvirkningen og gjorde forskjellen mellom lufttemperatur målt ved U og C større.

Det er et kjent faktum at økt vegetasjonstetthet resulterer i mindre daglig temperaturvariasjon. Ved evaluering av forskjellen i daglig maksimums- og minimumstemperatur ble dette observert. Den daglige maksimale temperaturen var generelt lavere over uklippet gress enn over klippet gress, og det daglige minimum var generelt høyere. Forskjellen i daglig maksimal og minimumstemperatur mellom U og C ved 2 m hadde imidlertid medianverdier på henholdsvis  $0,0^{\circ}\text{C}$  og  $0,1^{\circ}\text{C}$ . Disse forskjellene er mindre enn forventet basert på gjeldende retningslinjer i SC.

Funnene fra denne studien indikerer at økt vegetasjonshøyde påvirker lufttemperaturen i mindre grad enn WMO CIMO antyder, og at grensene for vegetasjonshøyde i SC kan være for strenge.





# List of symbols and acronyms

## Symbols

<b>C</b>	The location with cut grass
<b>U</b>	The location with uncut grass
<b>2m</b>	Represents the sensors at 2.00 m at one of the two locations (U or C)
<b>1m</b>	Represents the sensors at 1.25 m at one of the two locations (U or C)
<b>0.5m</b>	Represents the sensors at 0.55 m at one of the two locations (U or C)
<i>T</i>	Temperature
<i>RH</i>	Relative humidity
$\rho$	Absolute humidity

## Acronyms

<b>MET</b>	Norwegian Meteorological Institute
<b>SC</b>	Siting Classification for Surface Observing Stations on Land
<b>WMO</b>	The World Meteorological Organization
<b>WMO CIMO</b>	The World Meteorological Organization's Commission for Instruments and Methods of Observation



# Contents

Preface and Acknowledgements . . . . .	I
Abstract . . . . .	III
Sammendrag . . . . .	V
List of symbols and acronyms . . . . .	VII
<b>1 Introduction</b>	<b>1</b>
1.1 Background . . . . .	1
1.1.1 Motivation . . . . .	1
1.2 Research question . . . . .	2
1.3 The data . . . . .	2
<b>2 Theory</b>	<b>3</b>
2.1 The vertical structure of the troposphere . . . . .	3
2.2 Energy balance . . . . .	4
2.2.1 Radiation . . . . .	4
2.2.2 Radiation and energy budget . . . . .	5
2.3 Diurnal variations and surface influence . . . . .	6
2.4 Influence of wind and solar radiation . . . . .	9
2.4.1 Cloud cover . . . . .	9
2.4.2 Wind speed . . . . .	9
2.5 Relative and absolute humidity . . . . .	9
2.5.1 Converting from relative to absolute humidity . . . . .	10
2.6 Siting classification . . . . .	10
2.7 Evaluating other categories in the Siting Classification . . . . .	12
2.8 Use of temperature measurements . . . . .	13
<b>3 Method</b>	<b>15</b>
3.1 Climatology of the test site and experiment setup . . . . .	15
3.2 Field control . . . . .	20
3.2.1 Equipment . . . . .	20
3.2.2 Execution . . . . .	21
3.2.3 Results from the field controls . . . . .	21
3.2.4 The measuring instruments' uncertainties . . . . .	23
3.3 Data processing . . . . .	26
3.4 Weather in 2018 and 2019 . . . . .	30
3.4.1 2018 . . . . .	30
3.4.2 2019 . . . . .	31
3.5 The use of the 2018 data set . . . . .	31
3.6 Statistical tests . . . . .	32
3.7 Box and whisker plot . . . . .	33
3.8 Weather categories . . . . .	34
3.9 Weather's influence . . . . .	36

<b>4</b>	<b>Results</b>	<b>37</b>
4.1	Overview of the data . . . . .	37
4.1.1	Timelines of temperature measurements . . . . .	37
4.1.2	Difference in temperature over uncut and cut grass in 2019 . . . . .	39
4.2	Comparisons of data from 2018 and 2019 . . . . .	40
4.2.1	Difference in temperature over uncut and cut grass . . . . .	40
4.2.2	Test statistics to evaluate how different the years were . . . . .	40
4.2.3	The difference in temperature at three heights . . . . .	41
4.3	Diurnal variation in temperature difference . . . . .	43
4.3.1	Overview . . . . .	43
4.3.2	Radiation categories . . . . .	45
4.3.3	Wind categories . . . . .	48
4.3.4	High influence conditions . . . . .	50
4.4	Difference in daily values . . . . .	50
4.5	Day and night . . . . .	53
4.6	Individual events . . . . .	55
4.6.1	Vertical temperature profiles . . . . .	55
4.6.2	Temperature values on individual days . . . . .	60
4.7	Humidity . . . . .	62
4.7.1	Difference in humidity values . . . . .	62
4.7.2	Vertical profiles . . . . .	65
<b>5</b>	<b>Discussions</b>	<b>69</b>
5.1	Overview of the data . . . . .	69
5.2	Comparing data from 2018 and 2019 . . . . .	70
5.2.1	Average and standard deviation . . . . .	70
5.2.2	Statistical tests . . . . .	70
5.2.3	The difference in temperature at three heights . . . . .	71
5.3	Diurnal variation in temperature difference . . . . .	71
5.3.1	Overview . . . . .	71
5.3.2	Solar radiation . . . . .	72
5.3.3	Wind speeds . . . . .	73
5.3.4	High influence conditions . . . . .	73
5.4	Difference in daily values . . . . .	73
5.5	Day and night . . . . .	74
5.6	Vertical temperature profiles . . . . .	75
5.7	Different effects in the same class . . . . .	76
5.8	Humidity . . . . .	76
<b>6</b>	<b>Conclusions and Outlook</b>	<b>79</b>
6.1	What is the influence of vegetation height on temperature measurements? . . . . .	79
6.2	Final suggestions . . . . .	80
6.3	Improvements . . . . .	81
6.4	Further investigations . . . . .	82
	<b>Bibliography</b>	<b>86</b>
	<b>Appendices</b>	<b>87</b>
	<b>A Travelling normal calibration</b>	<b>88</b>
	<b>B The field controls' results</b>	<b>89</b>
	<b>C Diurnal box and whisker plots for 2018</b>	<b>90</b>

<b>D Monthly difference in temperature</b>	<b>92</b>
<b>E Radiation category plots for 2018</b>	<b>95</b>
<b>F Diurnal difference in humidity</b>	<b>97</b>
<b>G Difference in temperature in two time periods</b>	<b>100</b>



# Chapter 1

## Introduction

### 1.1 Background

Air temperature is one of the most frequently measured meteorological variables (Huwald et al., 2009) and important climate parameters (IPCC, 2014). Because it is logged at almost all standard automatic weather stations (Huwald et al., 2009) and is a variable that has been logged for over a century, its applications are many. Air temperature is, for example, used in climate research, where the long time-series makes it possible to analyse trends over time (Musacchio, Coppa, and Merlone, 2019). It is also commonly used in weather analysis.

The environmental conditions, both natural and artificial, in close vicinity of a meteorological station influence the air temperature measurements. The representativeness of the measurements can be influenced by, for example, nearby heat sources or shading. The World Meteorological Organization’s Commission for Instruments and Methods of Observation (WMO CIMO) gives guidelines for how a site for temperature measuring instruments should be. The commission provides a Siting Classification for Surface Observing Stations on Land (SC). The SC is given in the appendix in WMO CIMO’s guide (WMO, 2018) and is a template for evaluating the reliability of non-ideal weather stations. It provides guidelines for classifying the influence of a station’s surroundings. For air temperature and humidity stations, the influence categories are slope, height of vegetation, distance to heat sources and water bodies, and shading (WMO, 2018).

#### 1.1.1 Motivation

In a report done by the Cooperation of National Weather Services in the Nordic countries (NordObs) in 2014, it was recommended that further investigations should be done to evaluate the effects that certain terrain features have on temperature measuring instruments (Wolff, Haapa, et al., 2014). Further analysis of height of vegetation was recommended. This need was reinforced in a conference paper in 2018 (Wolff, Nygård, et al., 2018). According to WMO CIMO’s SC, the vegetation height under a measuring instrument is supposed to be “maintained in a ‘routine’ manner” and be representative of the region (WMO, 2018). NordObs states in their evaluation that at many of the sites they have evaluated, it is impossible to maintain vegetation as low as SC requires, and that many of the sites have vegetation just over the class 3 requirement of 25 cm (Wolff, Nygård, et al., 2018). Another limitation to which attention was drawn by NordObs in their report is that the highest class in any category determines the overall class of a site. It is therefore critical that the impact on the temperature measurements is equal for the same class in all the different categories. The report found that this does not seem to always be the case (Wolff, Nygård, et al., 2018). Moreover, it has been questioned whether the vegetation height requirements that determine the class in the vegetation category are too strict and rigid (Wolff, Haapa, et al., 2014).

These concerns regarding the SC and its trustworthiness lead to an interest in a thorough evaluation of the influence of vegetation height on temperature measurements.

## 1.2 Research question

This thesis' leading research question is the following:

### **What is the influence of vegetation height on temperature measurements?**

The goal, therefore, is to evaluate the effect of increased vegetation, specifically grass, on near-surface temperature measurements. The analysis involves comparing the temperature over uncut and cut grass as well as evaluating and understanding the vertical temperature profile over surfaces with increased vegetation height and density. The project also aims to understand what factors increase or decrease the influence of the increased vegetation height and to what degree.

Additionally, the effect of increased vegetation height on humidity measurements will be addressed in this project, but due to missing and low-quality data, fewer conclusions will be drawn with regards to this question.

## 1.3 The data

The data used to evaluate the research question of this project are from an experimental setup at Søråsfeltet in Ås, Norway. The experiment started in July 2018, but the most valuable data were collected in the summer of 2019. Hourly data from air temperature and relative humidity measuring instruments at three heights at two locations, were used in the analysis. Throughout the summer of 2019, the grass at one location was regularly cut short, while the grass at the other location was allowed to grow tall. Other than the minor differences in the distances to their surroundings and the different grass heights, the only aspect that differentiated the meteorological data logged at the two locations was the 25 m that separated them. Therefore, the data used in this experiment are perfectly suitable for analyzing the effect that increased grass height has on temperature measurements, and relate this to the recommendations given by WMO CIMO in their SC Guide.



# Chapter 2

## Theory

This chapter describes the dynamic between the air and the surface and how they influence each other. Firstly, the influence that the earth's surface properties have on the different layers of the troposphere, and the radiation and energy balance at the surface, is explained. The radiation and energy balance at the surface is heavily influenced by diurnal variations, and this chapter will describe how this affects air and ground temperature. Additionally, the effect that weather conditions have on surface properties' influence on air temperature will be explained. Theory regarding influence of increased vegetation on the temperature is also included.

The motivation behind this thesis is to evaluate the influence of increased vegetation height on air temperature, and compare it to the limits of vegetation height given in the SC. The theory behind the SC is therefore laid out in this chapter, as well as results from studies evaluating other categories in the SC.

If not otherwise specified, the theory in this chapter is from Dannevig, Harstveit, and Seter (2020), Elert (2020), Foken (2008a), Foken (2008b), Geiger, Aron, and Todhunter (2003), Oke (2002a), Oke (2002b), Vilà-Guerau de Arellano et al. (2015), Wallace and Hobbs (2006), and WMO (2018).

### 2.1 The vertical structure of the troposphere

The lower part of the atmosphere, called the troposphere, is the section of the atmosphere affected by the surface. The troposphere has a height of about 10 km and its vertical structure and layers are shown in figure 2.1. The shallower zone, called the planetary boundary layer, is influenced by the surface on a time scale of about 1 day. This layer is characterized by “well-developed mixing” (Oke, 2002a). During the day, the height of this layer is about 1-2 km, while at night it can drop down to around 100 m. This happens as a result of convection, a process where the sun heats the surface during the day and heat is transported into the colder atmosphere. At night, the surface cools down to a temperature below that of the atmosphere which results in downward convection. The height is also heavily affected by large-scale weather systems. The turbulent surface layer is characterized by “strong small-scale turbulence” (Oke, 2002a) caused by the surface roughness and convection. This layer's height can be about 50 m during the day and drop down to a few meters at night. On a small timescale of about 1 second, the horizontal structure can vary greatly; but on a longer time scale of about 10 minutes, the layer is believed to be stable. The roughness layer extends over the elements of the surface at about 1-3 times the height of these elements. This layer is very strongly affected by the surface and its properties, and has a turbulent flow. The lowest layer is the laminar boundary layer, which is in direct contact with the surface. It only extends a few millimeters vertically and it has a laminar flow.

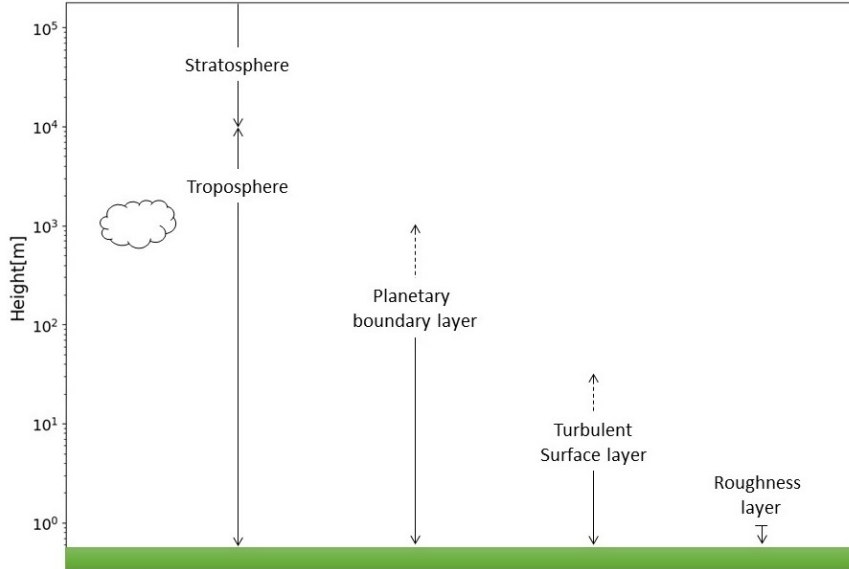


**Figure 2.1:** A visual representation of the vertical structure of the atmosphere where the  $y$ -axis is logarithmic. Adapted from Oke (2002a).

## 2.2 Energy balance

The energy balance of the earth-atmosphere system is driven by the radiation budget. Properties of the surface determines how much of the incoming, high-energy solar radiation gets transferred through heat fluxes. The amount of solar radiation that reaches the surface is decided by cloud cover. These factors influence the total energy in the energy balance at the earth's surface. Understanding what influences the energy balance is essential in order to understand how the air temperature is affected by the surface.

### 2.2.1 Radiation

Everything with a temperature over 0 K emits radiation. The temperature of a given body and the characteristics of the radiation it emits are related. A higher temperature yields a higher proportion of radiation of shorter-wavelengths. Planck's law shows how the spectral radiance of a black body at a given temperature:

$$E_{\lambda} = \frac{8\pi hc^2}{\lambda^5} \frac{1}{e^{hc/\lambda kT} - 1} \quad (2.1)$$

This version of Planck's law gives the power per unit area per unit wavelength [W/m<sup>2</sup>m].  $h$  is Planck's constant, which has the value  $6.626 \times 10^{-34}$  J s,  $c$  is the speed of light in vacuum with an approximate value of  $3.0 \times 10^8$  m/s,  $\lambda$  is the wavelength,  $k$  is the Boltzmann constant with a value of  $1.386 \times 10^{-23}$  J/K, and  $T$  is the surface temperature in Kelvin. Planck's law shows that a body radiates radiative energy in a spectrum of wavelengths, not just at discrete wavelengths.

From Planck's law, Wien's displacement law can be derived. This law reads:

$$\lambda_{max} = \frac{2.88 \cdot 10^{-3}}{T} \quad (2.2)$$

In equation (2.2),  $\lambda_{max}$  is the wavelength of peak emission in meters. The expression shows that a black body with a given surface temperature has a wavelength in which the body emits the most radiative energy of. The concepts of Planck's law and Wien's displacement law are demonstrated in figure 2.2, where Planck's law is plotted for temperatures of 300 K (figure 2.2a) and 6000 K (figure 2.2b). 300 K is approximately the

surface temperature of the earth and 6000 K is approximately the surface temperature of the sun. It is important to note that the scales of the y-axes are different in figure 2.2a and figure 2.2b. From figure 2.2, one can see that a body of higher temperature emits radiation with shorter wavelengths and higher energy values than a body of lower temperature.

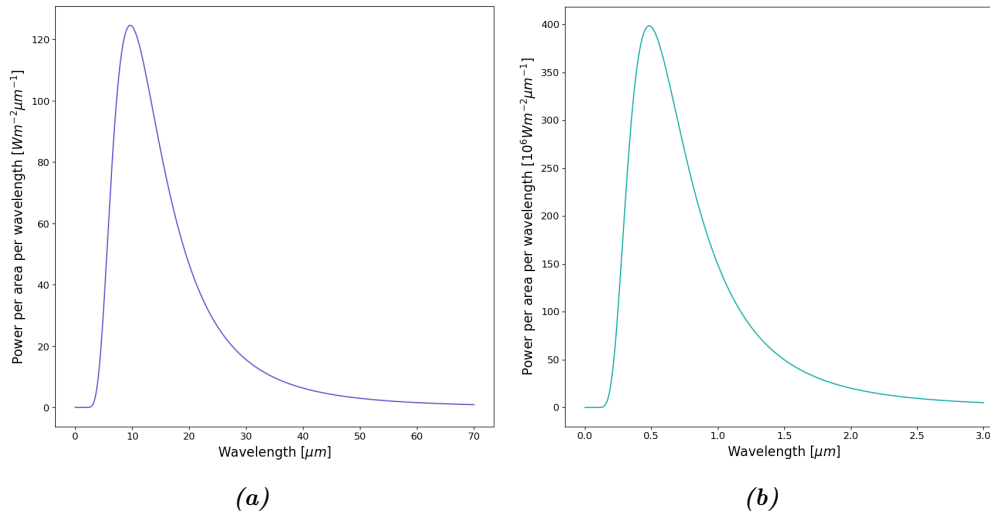


**Figure 2.2:** These figures are plots of Planck's law (equation 2.1), showing the spectral distribution of radiative energy emitted (a) by a black body with a temperature of 300 K and (b) by a body with a temperature of 6000 K. The y-axes have different scales.

The radiation emitted by the sun, called solar or short-wave radiation, usually has wavelengths between approximately 0.15 and 3.0  $\mu\text{m}$ . Long-wave radiation emitted by the earth-atmosphere system usually has wavelengths between 3.0 and 100  $\mu\text{m}$  (Oke, 2002a). As illustrated in figure 2.2, solar radiation is more energy-rich than the long-wave radiation emitted by the earth.

Radiation is either reflected ( $\alpha_\lambda$ ), transmitted ( $\Psi_\lambda$ ), or absorbed ( $\zeta_\lambda$ ) when it is incident on a surface. The sum of  $\alpha_\lambda$ ,  $\Psi_\lambda$ , and  $\zeta_\lambda$  for a specific wavelength is 1. This means that if, for example,  $\alpha_\lambda$  gets smaller or larger, then the proportion being transmitted or absorbed will also change.

The properties and characteristics of the surface the radiation is incident upon, determines the proportions of radiation that is reflected, transmitted, or absorbed. The amount of radiation that is reflected depends on the surface's albedo. Typical albedo values for grass are in the interval 0.16-0.26. The exact value depends on, among other factors, the length of the grass. Shorter grass has higher albedo. The change in albedo due to surface property changes may affect both ground and air temperature.

### 2.2.2 Radiation and energy budget

The earth's surface is the area where the majority of the atmospheric energy transfer happens. Incoming solar radiation (shortwave radiation),  $S_\downarrow$ , is either absorbed by the surface, which results in heating, or it is reflected. The shortwave radiation reflected by the surface is called outgoing shortwave radiation,  $S_\uparrow$ . The proportion reflected depends on the surface's albedo. Clouds, aerosols, and gases in the atmosphere emit longwave radiation,  $L_\downarrow$ , that is absorbed by the surface. At the same time, longwave radiation is emitted by the surface into the atmosphere,  $L_\uparrow$ . During the day hours, the sum of the four components of the radiation budgets results in net radiative energy being absorbed by the surface. Since all shortwave radiation in the earth-atmosphere system is solar radiation, there is no shortwave radiation during the night. There is more longwave radiation being emitted by the surface than is coming in from the atmosphere, and this

results in net radiative energy leaving the surface at night.

Shortwave radiation can be divided into two categories; diffuse radiation and direct radiation. Diffuse radiation is solar radiation scattered by atmospheric particles before it reaches the surface, while direct solar radiation does not get scattered.

The net radiative energy coming into the earth's surface during daylight hours is transferred through the turbulent energy fluxes; sensible heat flux,  $Q_H$ , and latent heat flux,  $Q_E$ . Ground heat flux transfers energy into the soil ( $Q_G$ ), which is stored in surface elements such as vegetation and buildings ( $\Delta Q_S$ ). Figure 2.3 shows a sketch of all the energy fluxes at the surface .

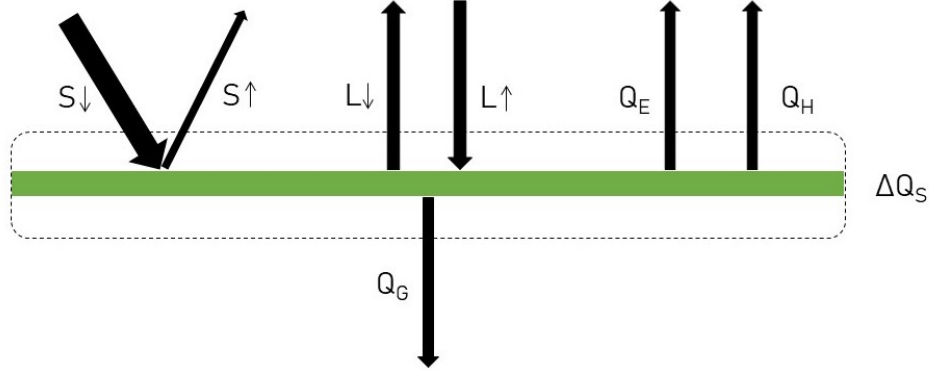


**Figure 2.3:** A visual representation of the components of the radiation and energy budget at the surface. Adapted from Foken (2008a).

The net radiative energy flux equals the net energy flux, and the energy balance at the earth's surface can be expressed the following way:

$$S\uparrow + S\downarrow + L\downarrow + L\uparrow = Q_E + Q_S + Q_G + \Delta Q_S \quad (2.3)$$

A convention for the signs of the fluxes is needed, and it is common in micrometeorology that radiation and energy fluxes are considered positive when they transfer energy away from the earth's surface (Foken, 2008a). In the context of this thesis, this convention will be used. This means that fluxes are positive if they go from the surface either into the atmosphere or the ground, and conversely, are negative if they go from the atmosphere or the ground to the surface.

## 2.3 Diurnal variations and surface influence

The vertical temperature profiles over the surface in the lowest few meters of the atmosphere are affected by surface properties and by diurnal variations. The transfer of heat between the soil and the air closest to the ground is proportional to the mean heat concentration gradient and the molecular diffusivity of the soil, which is the soil's ability to transfer heat. During the day, it is at the surface that most absorption of energy happens, while at night, it is where most of the depletion happens. The daily radiative energy budget, and how it affects diurnal variations in the energy balance at the earth's surface, institutes a downward temperature gradient in the air and soil during the day and upward temperature gradient at night. The magnitudes of the temperature gradient and soil heat flux decrease with distance away from the surface.

The variation in vertical temperature profiles during the day and night hours can be seen in figure 2.4. The plot displays data from this thesis' experiment from 21/9/2019, which was a sunny day with low wind ( $< 5$  m/s). The ground receives radiative energy and is heated during the day, which results in the heating of the air. At night, the energy exchange is in the opposite direction, which results in the night inversion seen in figure 2.4. The plot shows how the air closest to the ground is more affected by the surface and

the energy exchange occurring there, while the temperatures at the other three heights are more similar to each other. This shows how the temperature gradient decreases as distance from the surface increases.

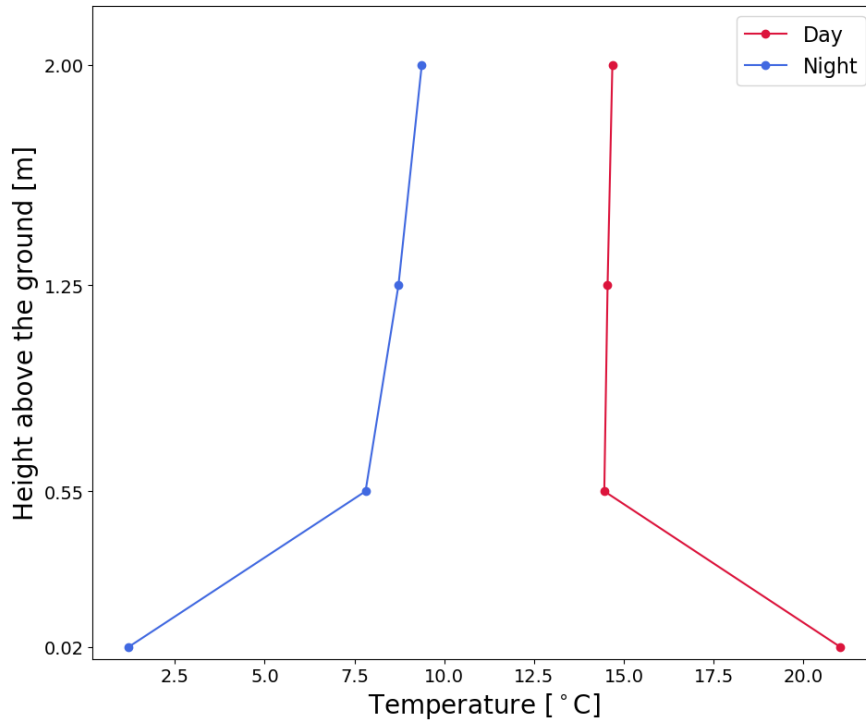


**Figure 2.4:** This figure displays a plot of the vertical temperature profile for day and night hours on 21/9/2019 from Søråsfeltet test site in Ås, Norway. Day hours are 06:00-17:00, night hours are 18:00-05:00, and the plot displays the mean value for each height for those 12 hours. Data from four heights were used: 2 m, 1.25 m, 0.55 m, and 0.02 m. The highest three instruments are from the location C in this thesis’ experimental setup, while the temperature logged at 2 cm is provided by BIOKLIM. This value is called the grass temperature and the mean value is logged every ten minutes. The hourly data logged are the average value of these six mean values. Unlike the measuring instruments used in this thesis’ experiment, the instrument logging this value is not protected against radiation.

The properties of the ground affect the interaction between the ground and the air as well as the heat transportation in the ground. Different soil types have different thermal conductivity values. This variable varies with depth and time. Moisture content in the soil affects the thermal conductivity where an increase will result in enhancement of the soil’s conductivity and heat capacity. In short, many factors impact the soil’s response to addition of heat and it’s ability to transport it.

The ground’s daily temperature variation decreases with increased depth. From around 0.75 m depth, the daily variation in temperature is approximately zero. Even though the temperature in the soil varies throughout the day, the thermal conductivity in air is much larger than in soil, which results in greater diurnal temperature variations in the air than in the ground. For turbulent air at 10°C, the thermal conductivity is  $\approx 125$  W/mK, while for soil it varies between 0.06 and 2.20 W/mK, depending on the soil type and the moisture content (Foken, 2008b). This results in the daily variations in air and ground temperature as illustrated in figure 2.5. In this figure, the daily variation in air temperature is evident, varying from 8.6°C to 22.8°C at 2.0 m above the surface. The ground temperature fluctuates much less throughout the day, ranging between 15.8°C and 21.1°C at 2 cm into the ground. One can also see from this figure the decrease in daily temperature variation with increased soil depth.

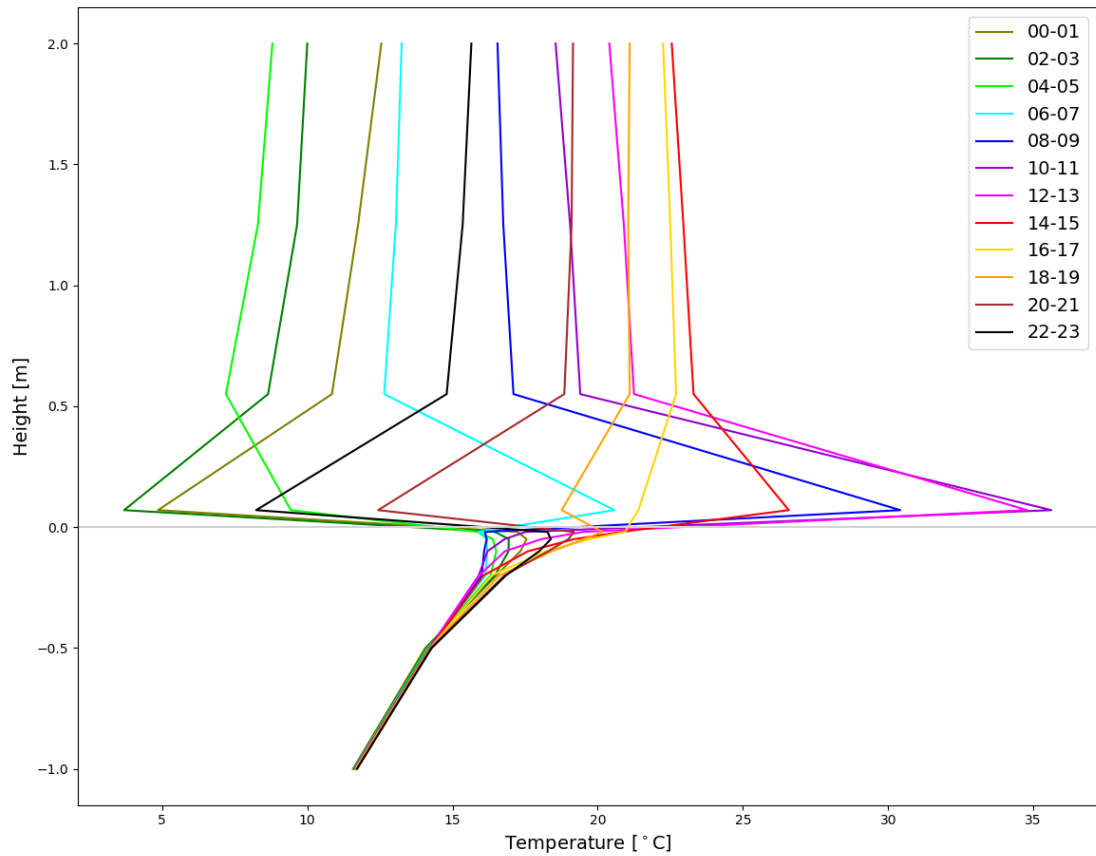


**Figure 2.5:** The plot shows bihourly temperature values above and below the ground on 28/6/2019 from Søråsfeltet test site in Ås, Norway. Data from heights 2 m, 1.25 m, and 0.55 m are from the location C in this thesis' experimental setup, while while the temperatures logged at 0.02 m, -0.02 m, -0.05 m, -0.1 m, -0.2 m, -0.5 m, and -1 m are provided by BIOKLIM. The temperature at 2 cm is called the grass temperature and the mean value is logged every ten minutes. The hourly data logged are the average value of these six mean values. Unlike the measuring instruments used in this thesis' experiment, the instrument logging this value is not protected against radiation.

Characteristics and properties of the surface further affect the air temperature. The daily temperature variations are subdued with increased vegetation cover and density, which means a lowering of the maximum temperature and an increase of the minimum temperature.

## 2.4 Influence of wind and solar radiation

Weather influences the effect of surface properties on air temperature and the vertical temperature profile close to the ground. This section will explain how cloud cover influences the energy balance at the surface and how different wind speed values influence the mixing of air.

### 2.4.1 Cloud cover

As explained in section 2.2, almost all solar radiation reaching the earth is shortwave radiation. In the earth's atmosphere, 18% of solar radiation is absorbed by ozone and water vapor (Barry and Chorley, 2009). Global radiation is the sum of the direct and the diffuse radiation, and the ratio of diffuse to total radiation increases with increased cloud cover. According to Barry and Chorley (2009), the proportion of radiation that is diffuse on a cloud-free day "is about 0.15-0.20 at the surface. For average cloudiness, the ratio is about 0.5 at the surface".

The energy balance at the surface is heavily influenced by solar radiation. Days with clear skies will have more solar radiation reaching the ground, which will result in more energy being transported from the ground into the air. In this way, cloud cover influences the effect the surface has on the air temperature.

### 2.4.2 Wind speed

When wind speed is high, the air is well-mixed and the surface's influence on air temperature is smaller. Conversely, when wind speed is low, the air close to the ground is more subject to the surface's influence. Wind speed values below 5 m/s are considered low wind speeds and values from 0 to 2-3 m/s result in windless conditions.

Wind speed is generally lower during the night than during the day. This is because the surface and the air closest to the surface cools faster after sunset than the air higher up in the atmosphere. The colder the air is, the more dense it is. This temperature inversion that occurs during the night therefore results in strong static stability and less mixing of the air between the layer, which makes the air less susceptible to influence by the air higher up. This results in a reduction in the wind speed.

## 2.5 Relative and absolute humidity

Air humidity is a measure of how much water vapor air contains. While absolute humidity,  $\rho$ , tells the number of grams of water vapor a cubic meter of dry air contains, relative humidity,  $RH$ , is the ratio of the water vapor content of the air to the maximum capacity the air has for water vapor.  $RH$  is therefore given in percent. This capacity is dependent on temperature. When the air is saturated, the relative humidity is 100%. More specifically, the relative humidity is the relationship between water vapor pressure ( $e$ ) and saturated water vapor pressure ( $e_0$ ):

$$RH = \frac{e}{e_0} \cdot 100\% \quad (2.4)$$

$e_0$  increases when the temperature increases ( $e_0 \propto T$ ), and figure 2.6 shows the relationship between saturated water vapor pressure and temperature. This means that relative humidity is inversely proportional to temperature. Consequently, the relative humidity

will decrease if nothing else changes other than an increase in temperature, and vice versa. Furthermore, if the volume is unchanged, the absolute humidity remains constant if temperature changes.

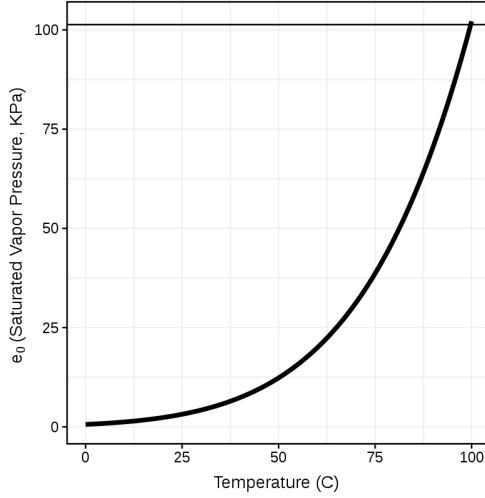


**Figure 2.6:** The figure shows the development of saturation water vapor pressure water according to the Tetens equation. The horizontal line represents the atmospheric pressure. Figure by Dylan W. Schwilk - Own work, CC BY-SA 4.0, <https://commons.wikimedia.org/w/index.php?curid=58144515>.

### 2.5.1 Converting from relative to absolute humidity

In this experiment, relative humidity was logged by the humidity instruments. As explained, relative humidity is inversely proportional to temperature and is therefore affected by temperature change. Absolute humidity, on the other hand, is independent of temperature if the volume remains unchanged. In order to look at the humidity at the site independent of the temperature, relative humidity need to be converted to absolute humidity. The most accurate way to do this conversion is to use tables for the saturation values. However, for simplicity and practicality, a numerical approach was used in this thesis. The equation used was (Engineering ToolBox, 2004):

$$\rho = \frac{RH}{100} \cdot \frac{2.2e^{77.345+0.0057T-7235T^{-1}}}{T^{9.2}} \quad (2.5)$$

In this equation,  $\rho$  is calculated by using  $RH$  and  $T$  [K]. A Python function was created where the relative humidity and temperature values from the data sets were input values and the absolute humidity was the output.

## 2.6 Siting classification

The surroundings of a site, the environmental conditions, can influence the measurements performed at the site. It is necessary to know and understand the influence of a site's surroundings on meteorological data recorded at the site. It is particularly important to consider a site's environmental conditions when it is supposed to be representative of a large area i.e. 100-1000 km. Siting classification is a tool that is used to take these factors into account. Meteorological sites are assigned a class between 1 and 5 in different categories depending on how large the influence of environmental surroundings are. Class 3, 4, and 5 have additional estimated uncertainties associated with them, as shown in table 2.1.

A site that records air temperature and humidity data gets classified in four categories: height of vegetation, slope, shade on the measuring instrument due to obstacles,



**Table 2.1:** Additional estimated uncertainty given to a site recording air temperature with class 3, 4 or 5 according to SC.

Class	Additional estimated uncertainty
3	1 °C
4	2 °C
5	5 °C

and distance away from heat sources and water bodies. The requirements in each class are shown in figure 2.7. The instruments must be mounted between 1.25 m and 2 m.

CLASS	1 PERFECT	2 SMALL INFLUENCE	3 SOME INFLUENCE	4 SIGNIFICANT INFLUENCE	5 INAPPROPRIATE
HEAT SOURCES/ WATER BODIES	Measurement point is situated more than 100 m from HS/WB	Measurement point is situated more than 30 m from HS/WB	Measurement point is situated more than 10 m from HS/WB	HS/WB occupies less than <50% of a 10 m circle and less than <30% of a 3 m circle	N/R
SLOPE	Flat horizontal land, surrounded by an open space, slope less than ¼ (19°)		N/R		
VEGETATION UNDER SENSOR	Ground covered with natural and low vegetation (<10 cm) representative of the region		Ground covered with natural and low vegetation (<25 cm) representative of the region	N/R	
SHADE	Sensor is no longer than 1 h in the shade when the sun is above 7°. Shade from topography is not included			Sensor is no longer than 1 h in the shade when the sun is above 20°. Shade from topography is not included	N/R

**Figure 2.7:** The figure shows the different requirements for the five classes in the different categories in WMO CIMO’s SC. A category is not able to get a class if the field is marked yellow or blue. In the yellow fields, the requirement is the same as what is described for class 1. If the field is blue, there is no description for that class in the SC. The no requirement fields are the highest class the categories can get.

As can be seen in the overview of the SC in figure 2.7, there is only one category where it is possible to get all five classes, and that is in the distance to heat source and water body category. In the other three categories, there are classes you cannot get because the SC does not have limits for them. This makes it impossible to compare certain classes between two categories. Some examples of this are that class 2 can only be given in the distance to heat source and water body category, and the shade category has no description for class 3, while the other three do.

This thesis looks at the height of vegetation category, and in the SC, it says that the vegetation under an instrument measuring temperature or humidity is expected to be maintained routinely. It also says that the vegetation must be representative for the area. This varies greatly between countries and regions, and different vegetation types have different albedo values. As mentioned, the albedo affects the radiation balance and will influence the vertical temperature gradient. According to the SC, the height must be below 10 cm to get class 1 or 2 and under 25 cm to get a class 3. Class 4 and 5 have no requirements for vegetation height. This is summed up in table 2.2 and means that a site can only get class 1, 3, or 4 in this category. It is important to note here that the height of the instrument does not affect the class if it’s within the 1.25 m to 2 m interval. Therefore, the distance between the vegetation and the measuring instrument is not taken into account. This could result in an instrument at 1.25 m getting class 3,

while being closer to the vegetation than a class 4 measuring instrument at 2 m.

**Table 2.2:** *The class given to a site recording air temperature and/or humidity in the category for height of vegetation according WMO CIMO’s Siting Classification.*

Class	Vegetation height
1	<10 cm
2	<10 cm
3	<25 cm
4	No requirement
5	No requirement

## 2.7 Evaluating other categories in the Siting Classification

Since it is the highest class in any category that is registered in global classification systems, it is important that the same class in two different categories influence the temperature measurements by an equal amount. Questions have been raised as to whether this is the case, and it has been suggested by for example Wolff, Haapa, et al. (2014) that separate investigations into each category are needed. In this section, results from projects evaluating the effects of nearby heat sources and water bodies are presented and their results are summed up in table 2.3.

An experiment was conducted in Tsukuba, Japan between June 2010 and January 2011 where the influence of distance away from an asphalt road on temperature measurements was evaluated. The road was 10 m wide and measuring instruments were put up in three heights (0.5 m, 1.5 m, and 2.5 m) at four different distances away from the asphalt road: 0.8 m, 3.2 m, 6.2 m, and 10 m. These distances correspond to classes 5, 4, 3, and 3 respectively in the WMO SC guide. According to SC, an additional estimated uncertainty of up to 1 °C should be given to the instruments at 6.2 m and 10 m away from the road, up to 2 °C for the instrument 3.2 m away, and up to 5 °C for the instrument only 0.8 m away from the road. The report concluded that positive biases between 0.2 °C and 0.5 °C were observed for the instruments mounted at 0.5 m, where the bias decreased with increasing distance away from the road. For 1.5 m, which is in the height interval recommended by WMO CIMO, the bias was around +0.1 °C (Hamagami et al., 2012). From the data at 2.5 m, the report says negative biases were found. Because of this, they concluded that even though advection of heated air can explain some of the biases registered, the road’s influence on temperature is complex. In general, the biases at 1.5 m were much smaller than at 0.5 m, and the report from the experiment says that “At a height of 1.5 m,  $\delta T$  ranges from 0.0 °C to 0.2 °C regardless of the distance from the road” (Kumamoto et al., 2013). This is in direct conflict with WMO CIMO’s guidelines and assertions in SC.

Other projects have evaluated the effect of nearby heat sources in different ways. A project in Rygge, Norway in 2016 evaluated the effect of a flat heat source on a measuring instrument in class 4. The estimated uncertainty for class 4 in the SC is 2 °C. Their results showed temperature deviations between 0.5-1.0 °C during the day and as low as -2.0 °C at night (Wolff, Kielland, et al., 2016). A study in Helsinki, Finland in 2009 showed that where a measuring instrument was located in relation to an elevated heat source influenced the impact that the heat source had on the temperature measurements. When an instrument was located on the south side, the class 4 instrument could experience temperature deviations up to 1.7 °C and the class 5 instrument could experience temperature deviations up to 4.0 °C. These values were only 0.3 °C and 1.0 °C away from the additional estimated uncertainties given in SC (see table 2.1). The instrument located on the north side, however, only experienced deviations as large as

$\pm 0.1$  °C for a class 5 instrument. This deviation is 4.9 °C away from that site’s additional estimated uncertainty.

In 2012, an experiment was conducted in the Zhejiang province in China where the influence of a water body on temperature measurements was evaluated. In the experiment, measuring instruments were placed 0 m, 50 m, 100 m, 200 m, and 300 m away from a water body and these instruments were in class 4, 2, 2, 1, and 1, respectively. Evaluation of the data from the experiment showed that the impact of the water body on the temperature measurements weakened with distance away from it. Specifically, the instruments at 200 m and 300 m away from the water were much less impacted by the water body than the instruments 0, 50, and 100 m away (Jianxia et al., 2012). One of the most notable observation from this project was that the maximum monthly mean deviation was found to be about 0.75 °C. This was for the instrument 0 m away from the water, which gives it a class 4 or 5. The instrument 50 m away (class 2) had a maximum monthly mean deviation of around 0.45 °C. According to the SC, these two instruments should have vastly different additional estimated uncertainty associated with them, but the difference between their maximum monthly mean deviation is only 0.3 °C (Wolff, Kielland, et al., 2016).

**Table 2.3:** A summary of the studies by Kumamoto et al. (2013) and Jianxia et al. (2012) and studies summarized in Wolff, Kielland, et al. (2016) where the effect of distance away from heat sources and water bodies were evaluated in relation to the classes given by WMO CIMO in the SC.

Observed temperature differences [°C]	Class 1	Class 2	Class 3	Class 4	Class 5
Flat heat source from Kumamoto (2013)			[0.0, 0.2]	[0.0, 0.2]	[0.0, 0.2]
Water body (experiment) from Jinaxia (2014)	[-0.2, 0.25]	[-0.25, 0.45]		[-0.25, 0.75]	
Flat heat source, study in Norway (2016)				[0.5, 1.0], -2 (night)	
Elevated heat source (S), study in Helsinki (FMI, 2009)			0.0	[0.0, 1.7]	[0.4, 4.0]
Elevated heat source (N), study in Helsinki (FMI, 2009)			0.0		$\pm 0.1$

## 2.8 Use of temperature measurements

Weather data are used in different ways depending on the application. Because of this, there can be several ways to evaluate the correctness of this type of data. Some examples of this can be seen in the IPCC Fifth Assessment Report published in 2014, where temperature data were evaluated by for example annually averaging it, looking at the average for a decade, and daily temperature extremes (IPCC, 2014). When WMO calculate their climatological normals, they look at the monthly mean of daily maximum, minimum, and mean temperature values, the mean number of days with maximum temperature over a certain limit, and the mean number of days with minimum temperature below 0 °C, among many other temperature parameters (WMO, 2017). These are examples of how hourly data are not used directly, but as tools to calculate parameters on larger time scales. Weather analysis and evaluations of temperature records are examples of applications that use hourly temperature data (Mareile Wolff, personal communication, 14/4/2020).



# Chapter 3

## Method

This chapter has two main parts. The description of the test field and the data sets used in the thesis can be found in part 1, which contains sections 3.1 through 3.5. Analysis methods are described in part 2, which contains sections 3.6 through 3.9. The chapter aims to give thorough descriptions of methods used both for the initial processing of the raw data as well as the ones for analysis of it.

### Part 1

The chapter's first part focuses on the test site itself, the data logged at the test site, and the steps taken to make the data usable. Setup of the experiment and the test site's climatology is described in detail in section 3.1. A description of the method for field controls and the results of those can be found in 3.2. Section 3.3 thoroughly describes how quality control of the data was done. Finally, section 3.4 details the differences in the weather in 2018 and 2019, the two years this thesis has data from, and 3.5 follows up with how the data set from 2018 can be used.

### 3.1 Climatology of the test site and experiment setup

The experiment in this thesis was set up with the goal of evaluating the influence of vegetation height on temperature measurements. The setup is at the Field Station for Bioclimatic Studies (Feltstasjon for bioklimatiske studier - BIOKLIM) at Søråsfeltet by NMBU in Ås, Norway. The coordinates for BIOKLIM are N59°39'37" E10°46'54" and it is located 93.9 m above sea level (NMBU, 2019). For this experiment, two poles were placed 25 m apart. In this thesis, these poles are named C and U and are used to represent measurements from the two locations. C stands for cut and U stands for uncut. The grass was cut weekly at C, while there was a 6 m by 6 m square of grass around U that was uncut. Each pole had temperature and humidity measuring instruments at three heights: 2 m, 1.25 m, and 0.55 m. The measuring instruments at the height 2 m are referred to with zero decimal places in the height measurement because the exact height of these instruments cannot be stated with any more magnitudes of certainty. In contrast, the measurement values for heights of the instruments at 1.25 m and 0.55 m are given with two decimals. The first measurement was done 7/7/2018 at 12:00.

The temperature measuring instrument type used in this experiment is Pt100 1/10 DIN. Its specifications are given in table 3.1. Three temperature values were logged every hour by the instruments: maximum and minimum temperature of the last hour and the average temperature value the last minute of every hour. This last value will from now on be referred to as the hourly temperature. The humidity instruments used are HMP155 by Vaisala and the specifications are given in table 3.2. The humidity values logged are the average humidity values the last minute of every hour, and these values will from now on be referred to as hourly humidity.

**Table 3.1:** Specifications for the type of temperature measuring instrument used in this thesis' experiment are given in this table.

Instrument type	Pt100 1/10 DIN	
Interval	-50 °C to +250 °C	
Accuracy	-10 °C	±0.03 °C
	0 °C	±0.03 °C
	10 °C	±0.04 °C
	20 °C	±0.04 °C
	30 °C	±0.05 °C

**Table 3.2:** Specifications for the type of humidity measuring instrument used in this thesis' experiment is given in this table.

Instrument type	HMP155	
Manufacturer	Vaisala	
Accuracy	At +15 °C to 25 °C:	±1% RH (0-90% RH)
		±1.7% RH (90-100% RH)
	At -20 °C to +40 °C:	±(1.0 + 0.008 × reading)% RH

Figure 3.1 shows the test site BIODKLIM with the locations of C and U marked with a blue and red circle respectively, where U is north of C. Apart from the uncut grass at U during the experiment's duration, the distance to C and U's surroundings are what differentiates the two locations. An outbuilding can be seen west of C in figure 3.1. The distance between C and the outbuilding is 16 m, and between the outbuilding and U there is about 30 m. The outbuilding is a heat source. Its proximity to C gives the measuring instruments at that location a class 2 in the category of distance to a heat source. In the other three categories, C gets a class 1. In the category of distance to a heat source, a station gets class 1 or 23 if it is more than 100 m or 30 m away from the station. With the outbuilding being 30 m away from U, and the two objects north and northwest of U not being there during the experiment, U got class 1 in every categories before the grass stopped being cut.

A picture of the field station BIODKLIM and its surroundings can be seen in figure 3.2. The station disposes an area of about 120 m<sup>2</sup> and is surrounded by about 5000 m<sup>2</sup> of farmland. This surrounding farmland slopes slightly, about 1%, to the west. Surrounding the farmland are forest and residential developed areas. The shortest distance from non-farmland to the field station is 200 m (NMBU, 2019).

According to NMBU staff responsible for maintaining the test field, the grass was cut weekly between the beginning of May until the end of September in 2019. The grass was cut under both U and C on 7/5/2019 and this was the last time the grass was cut under U that summer. The grass heights were equal until the next time it was cut. Records from the site says that it was cut again on 22/5/2019, but according to the staff it was cut once between 7/5 and 22/5. Because we cannot know when in that time period it was cut and when on 22/5 it was cut, 23/5 was chosen as the start date in the data set. This is the first day we know that the grass under U and C differed in height.

An approximation of the grass heights at U and C and the difference between them is presented in figure 3.3. Figure 3.3a shows the estimated heights of the grass at U and C, while figure 3.3b shows the difference in grass height. The plot was created based on Åshild Ergon's expertise regarding how fast grass grows and maximum height of grass. According to Ergon, the grass grows the fastest in May and June and it can therefore be assumed that the grass reached maximum height by the end of June at the latest



*Figure 3.1:* A picture of the test site BIOKLIM. The red circle is marking the location where the grass remained uncut through the summer of 2019 and the blue circle is marking the location where the grass was cut. The picture was taken with a screen shot of Google Maps and the circles were added by me.



*Figure 3.2:* A picture of the field station BIOKLIM (inside the red circle) and its surrounding farmland, forest, and residential areas where up, right, down, and left correspond to the cardinal directions north, east, south, and west. The picture was taken with a screen shot of [www.norgeskart.no](http://www.norgeskart.no) by Kartverket and the circle was added by me.

(Åshild Ergon, personal communication, 21/4/2020).

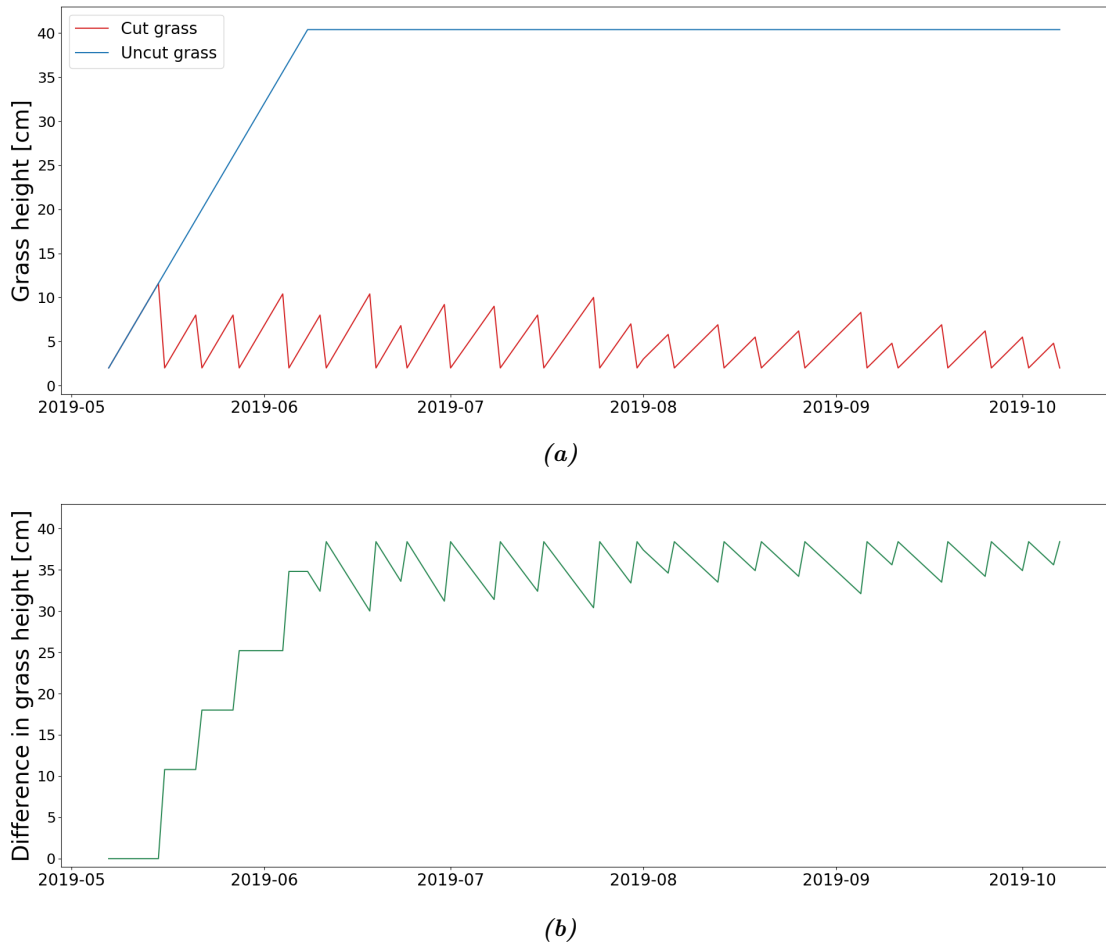


**Figure 3.3:** The plots display an estimation what happened to the grass at the two locations in this thesis' experiment in 2019. (a) shows the estimated grass heights at this thesis' two locations throughout 2019 and (b) shows the difference in estimated grass height. The grass was cut weekly at one location (cut) and only cut in the beginning of May at the other location (uncut). The plots were created based on the expertise of Åshild Ergon' regarding how fast grass grows and maximum height of grass (Åshild Ergon, personal communication, 21/4/2020).

Figures 3.4 and 3.5 are pictures of U on 5/8/2019. The two pictures show how tall the grass grew in 2019. The picture in figure 3.5 demonstrates that the grass will not necessarily stand straight up when it grows tall it . This variation in height, depending on wind and rainfall, among other factors, can make it difficult to pinpoint the exact height of vegetation.

A white logger cabinet hangs at about the same height as the measuring instruments at 1.25 m at U. It can be seen on the left side of the pole in figure 3.5. The logger cabinet contains the logger and power supply for the instruments at U. Because of the cabinet's color, it has a high albedo which means it reflects a large part of the solar radiation, affecting the radiation budget of the instrument. Despite its high albedo, the cabinet will also absorb some of the incoming radiation and will heat up the surrounding air. The logger cabinet has most likely affected the air temperature and relative humidity measurements at 1.25 m at U. This makes it more difficult to evaluate the temperature profile at U than at C.





**Figure 3.4:** Photo of the location where grass was uncut on 5/8/2019. Credit: Mareile Wolff.



**Figure 3.5:** Close-up photo of the measuring instruments and grass at the location where the grass was uncut from 5/8/2019. Credit: Mareile Wolff.

## 3.2 Field control

The field controls done for this thesis' experimental setup were essential for the data analysis. The aim of the thesis was to use observational data to determine and quantify the influence of vegetation height on temperature and humidity measurements. For the necessary analysis to be possible, the uncertainty range of the measurements needed to be trusted. The field controls and their results were therefore important. The accepted interval of mean deviation for temperature instruments is  $\pm 0.3^\circ\text{C}$  and for humidity instruments it is  $\pm 5\%$ . Everything within these intervals are accepted by Norwegian Meteorological Institute (MET), and if an instrument's deviations are not within the interval, it must be replaced. Furthermore, the results from the field controls determined the uncertainty of the experiment's measuring instruments.

### 3.2.1 Equipment

This section details the equipment used in the field controls, the calibration of these instruments, and the calibration of the references that the instruments are calibrated against.

In a field control, a travelling normal is a device used to measure data in the same conditions and locations as the measuring instruments being evaluated. It is a handheld, portable temperature and humidity gauge with a calibrated standard. The travelling normal used in this thesis' field control is a converted Vaisala HMP77. It has a Pt100 mounted onto it, which secures the same response time as the other instruments at the station. The hand-held indicator is a Vaisala HM70, which is digital. The HMP77's humidity measurements' accuracy is  $\pm 1.0\%$  for relative humidity (*RH*) measurements in the interval  $[0\%, 90\%]$ , and  $\pm 1.7\%$  for *RH* measurements in the interval  $[90\%, 100\%]$ . The Pt100's accuracy was presented in table 3.1.

### Calibration of the travelling normal

The travelling normal is regularly calibrated at the MET institute. To calibrate the humidity measuring instrument, the instrument is set up with analog output (0-1 V). This is then connected to a multimeter. The instrument reading, reference and setpoint management are done by a Linux program. The environmental conditions are set in a climate chamber. The humidity interval that the calibration tested for was  $[10\%, 90\%]$ . The voltage levels tested were between 0.1 V and 0.9 V, with intervals of 0.1 V. 0.1 V corresponded to *RH* value of 10% and 0.9 V corresponded to *RH* value of 90%. The correction value decreased in absolute value with increased voltage level, as can be seen in appendix A. Three series of measurements were done, two with descending values and one with ascending values. The uncertainties of the humidity instrument are from the normal (the reference the instrument is calibrated against), the homogeneity and stability of the climate chamber, repeatability, and hysteresis. The homogeneity and stability of the climate chamber is a value given by the manufacturer, while the other values are empirical (Svein Olav Sundal, personal communication, 5/5/2020).

The temperature calibration is done by manual reading where the environmental conditions are set in a climate chamber. The temperature interval tested for was  $[-15^\circ\text{C}, 30^\circ\text{C}]$  with intervals of  $15^\circ\text{C}$ . One series of measurements was done. The uncertainties at the individual setpoints for the instrument are from the normal (the reference the instrument is calibrated against), uncertainty related to the reading, and the homogeneity and stability of the climate chamber. The homogeneity and stability of the climate chamber is a value given by the manufacturer, while the other values are empirical (Svein Olav Sundal, personal communication, 5/5/2020).

The calibration of the travelling normal was done in October 2019 and is valid until July 2020. The combined uncertainties are calculated by using the method of adding the

uncertainties in quadrature:  $\delta x = \sqrt{x_1^2 + x_2^2 + \dots + x_n^2}$ . In this method, the coverage factor,  $k$ , is equal to 1.  $k=2$  is used, and it gives the results a certainty of 95%. The results, therefore, had to be multiplied by 2 to find the instruments' uncertainty. The combined total uncertainty of the travelling normal's humidity instrument was determined to be  $\pm 1.2$  for the coverage factor,  $k$ , equal to 1 and  $\pm 2.5$  for  $k=2$ . The combined total uncertainty the travelling normal's temperature instrument was determined to be  $\pm 0.1$  °C for  $k=2$  at all setpoints (Svein Olav Sundal, personal communication, 5/5/2020).

### Calibration of reference instruments

The reference instrument used in the calibration of the humidity measuring instrument of the travelling normal was a MBW 473 Dew Point Mirror. The instrument was calibrated by comparing it to a reference dew point mirror. It was placed in a climate chamber and connected to the air flow from the reference dew point generator of the chamber. The reference dew point mirror was connected in parallel to the same airflow. The calibration was performed by comparing the dew point value of the reference instrument with the value the calibration instrument showed. The air flow through the instrument for calibration was around 0.5 L/min. The reading was taken about two hours after there were sufficiently stable conditions in the climate chamber. No commissioning of the instrument was done (Justervesenet, 2019).

The reference instrument used in the calibration of the temperature measuring instrument of the travelling normal was a milliK Precision Thermometer Indicator from Isotech. The instrument was calibrated by the manufacturer. The milliK has three input channels: two for sensor and one for current. In the calibration of the milliK, three signals were applied to all three inputs. By doing this, signals were simulated "over a representatives range for all measurement configuration" (Isotech, 2018). These signals were generated by sources that have calibration "traceable to recognize National standards" (Isotech, 2018).

### 3.2.2 Execution

In order to compare the temperature and humidity registered at U and C to what the traveling normal registered, the values had to be registered at the same time. A portable keyboard and display tool, CR1000KD, was used to register what U and C logged. For each instrument, the temperature and humidity were read three times with approximately 1-2 minutes in between each reading. This was done three times with a time interval of minimum 10 minutes between each time at all three heights, (2 m, 1.25 m, and 0.55 m), at both two locations, U and C. This method is standard for MET's operational routines.

Two field controls were done of the experimental setup. The first field control was done 18/7/2018 and the second one was done 27/2/2020. The deviations between what the experiment's instruments measured and the values that the travelling normal measured from both field controls are given in appendix B. The second field control was lead by the author of this thesis, who is not experienced with this type of work. Due to the sensitive nature of carrying out these field controls, it cannot be ruled out that mistakes were made during the execution of the second field control. This must be taken into consideration when considering the results from this field control and the conclusions drawn.

### 3.2.3 Results from the field controls

This section will present the results from the field controls and show how they were used to calculate the measuring instruments' uncertainties. The values of the difference

between the measuring instruments' readings and the values from the travelling normal are given in appendix B.

In the field control analysis sheet provided by MET, the mean deviations of temperature and humidity are calculated by averaging all the differences between the measuring instruments' readings and the values from the travelling normal. Table 3.3 shows the results from using this approach on the field control results form 18/7/2018. The mean temperature deviations are all negative and within MET's  $\pm 0.3^\circ\text{C}$  interval. The mean humidity deviations are all positive and within MET's  $\pm 5\%$  interval.

**Table 3.3:** Results from field control of temperature and humidity measuring instruments in this report's experimental setup done on 18/7/2020.

Instrument	Height [m]	Mean deviation, temperature [ $^\circ\text{C}$ ] $\pm 0.1^\circ\text{C}$	Mean deviation, humidity [%] $\pm 1.2\%$
C (cut grass)	2	-0.13	1.98
	1.25	-0.10	3.07
	0.55	-0.13	3.10
U (uncut grass)	2	-0.05	1.36
	1.25	-0.01	3.72
	0.55	-0.07	3.70

Table 3.4 shows the results from the field control done 27/2/2020 and 5/4/2020 where the approach in the analysis sheet provided by MET was used. The field control from February resulted in a mean deviation of  $-0.36^\circ\text{C}$  for the temperature measuring instrument at C at 0.55 m, which was outside of MET's uncertainty interval of  $\pm 0.3^\circ\text{C}$ . Due to the suspicion that the inconsistencies that caused this large mean deviation value could be due to the fast temperature changes during the measurements, a field control of this measuring instrument was done in May 2020. When redoing the control in May, the mean deviation was equal to  $-0.10^\circ\text{C}$ , which is within MET's uncertainty interval.

**Table 3.4:** Results from field control of temperature and humidity measuring instruments in this report's experimental setup done on 27/2/2020. p.p. is the abbreviation for percentage point.

\* = result from field control on 5/4/2020.

Instrument	Height [m]	Mean deviation, temperature $\pm 0.1^\circ\text{C}$ [ $^\circ\text{C}$ ]	Mean deviation, humidity [p.p.] $\pm 1.2\%$
C (cut grass)	2	0.04	-20.59
	1.25	-0.06	2.20
	0.55	-0.36 / -0.10*	1.33 / 1.28*
U (uncut grass)	2	-0.05	3.01
	1.25	0.16	2.08
	0.55	-0.09	2.71

The field control done on 27/2/2020 revealed problems with the humidity instrument at 2 m at C, which deviated more than 20 percentage points (p.p.) from the travelling normal. A closer look at the data showed that humidity data at this height started to deviate periodically from the other instruments on 23/9/2019. Due to its unreliability, it was decided not to use this data after 23/9/2019. This will be discussed in more detail in section 3.3.

Other than the two issues discussed, the result from the field control showed that all other mean deviations for temperature and humidity were within MET’s accepted intervals, just like the results from 18/7/2018 showed. The mean deviations are within these intervals also when applying the traveling normal’s uncertainty.

### 3.2.4 The measuring instruments’ uncertainties

This section will explain how the uncertainties of the air temperature and relative humidity measurements in this thesis’ experiment were found based on the results from the field controls. Absolute values of the difference between the values registered by the experiment’s instruments, and the values measured by the travelling normal, were used instead of the real values.

The air temperature measurements’ uncertainty was found by calculating the expanded uncertainty. This approach is described in chapter 1.6 in WMO (2018) and can be used when observational errors follow the Gaussian distribution or a near-Gaussian distribution. The true value of a measurement can then be expressed as the measured value in combination with its expanded uncertainty:

$$\begin{aligned} \langle \text{true value} \rangle &= \langle \text{measured value} \rangle \pm \langle \text{expanded uncertainty} \rangle \\ &= \langle \text{measured value} \rangle \pm k \times \sigma \end{aligned} \quad (3.1)$$

In equation (3.1),  $k$  is the coverage factor. In this thesis’ application of equation 3.1,  $k=2$  because it is common in metrology to test on a 95% confidence interval (WMO, 2018). We see from the equation that the expanded uncertainty is equal to  $k \times \sigma$ , where  $\sigma$  is the variance. The variance is equal to the square root of the standard deviation, which is calculated as shown in equation (3.2):

$$\hat{\sigma}^2 = \frac{\sum_{i=1}^n (X_i - \bar{X})^2}{n - 1} \quad (3.2)$$

In equation (3.2),  $(X_i - \bar{X})$  is the difference between the temperature measured by the experiment’s instruments and the temperature measured by the travelling normal. Since nine values were recorded in 2018 and in 2020,  $n = 18$ .

Table 3.5 shows the differences between air temperature measured by the experiment’s instrument and the travelling normal,  $(X_i - \bar{X})$ , at 0.55 m at the location with uncut grass (U) from the field controls in 2018 and 2020. The first three  $(X_i - \bar{X})$  values from 2020 were very different from the other deviation values that day, both in absolute value and in sign. The three values are underlined and are between  $-0.72^\circ\text{C}$  and  $-0.52^\circ\text{C}$ . The six next deviation values from the field control in 2020 have similar values, only varying between  $0.14^\circ\text{C}$  and  $0.24^\circ\text{C}$ . The measurements for these deviations were done approximately 10 and 20 minutes after the first three measurements. The large difference between the three underlined values in table 3.5 and the other six from 2020, might be due to not giving the travelling normal enough time to acclimatize when shifting it’s position from 1.25 m to 0.55 m, or some other unknown factor. Due to the large difference between these three values and the other  $(X_i - \bar{X})$  values from that day, uncertainties were calculated both including and excluding these values.

Absolute values of the deviation values from the field controls of the temperature measuring instruments have been used to calculate the values in table 3.6. The maximum and mean value of the deviations are shown, as well as the expanded uncertainties. One can see that for the measuring instrument at U at 0.55 m, the different uncertainty values are notably higher than than for the other five instruments when including the underlined values in table 3.5. Moving forward, the non-underlined uncertainty values for this instrument will be used instead. The expanded uncertainties for the measuring instruments at both locations (U and C) at all three heights (2 m, 1.25 m, and 0.55 m) are therefore all equal to or smaller than  $0.28^\circ\text{C}$ .

**Table 3.5:** This table shows the deviations between the air temperature measurements done at the location with uncut grass ( $U$ ) at 0.55 m by the experiment's measuring instrument and the travelling normal during the field control in 2018 and in 2020. The three underlined values deviate from the other values by a notable amount.

Date of field control	Temperature differences [ $^{\circ}\text{C}$ ]								
23/5/2018	-0.10	-0.10	-0.09	-0.14	-0.12	-0.09	-0.02	-0.06	0.08
27/2/2020	<u>-0.72</u>	<u>-0.59</u>	<u>-0.52</u>	0.14	0.17	0.15	0.16	0.24	0.18

**Table 3.6:** This table shows the maximum and mean values of the absolute values of the difference between air temperature measured by the experiment's instrument and by the travelling normal,  $(X_i - \bar{X})$ . The expanded uncertainty is calculated using these absolute values and by using equation 3.1.  $C$  represents the location with cut grass and  $U$  represents the location with uncut grass. The heights are the heights at which the instruments are mounted. All  $(X_i - \bar{X})$  values can be found in appendix B. In the rightmost column, the underlined values have been calculated by including the underlined values in table 3.5. The non-underlined values were found by excluding the underlined values in table 3.5.

Location and height	C, 2 m	C, 1.25 m	C, 0.55 m	U, 2 m	U, 1.25 m	U, 0.55 m
Maximum absolute value [ $^{\circ}\text{C}$ ]	0.19	0.13	0.22	0.24	0.30	<u>0.72</u> /0.24
Mean absolute value [ $^{\circ}\text{C}$ ]	0.08	0.08	0.12	0.06	0.10	<u>0.20</u> /0.12
Expanded uncertainty [ $^{\circ}\text{C}$ ]	0.21	0.18	0.26	0.17	0.28	<u>0.57</u> /0.28

When calculating the uncertainty of the difference between two values, their uncertainties are added together (Richmond, 2003). The combined expanded uncertainties of the difference between temperature at U and C measured by the instruments in the experiment behind this thesis are given in table 3.7.

**Table 3.7:** This table presents the combined expanded uncertainties of the difference between temperature values measured at the location with uncut (U) and cut (C) grass at the three heights in the experiment behind this thesis. The combined expanded uncertainties are based on the individual measuring instruments' expanded uncertainties given in table 3.6.

Height of measuring instrument	Combined expanded uncertainty
2 m	$\pm 0.4^\circ\text{C}$
1.25 m	$\pm 0.5^\circ\text{C}$
0.55 m	$\pm 0.5^\circ\text{C}$

According to WMO (2018), the distribution of humidity values is not Gaussian, and the expanded uncertainty can therefore not be calculated for humidity. A different approach was therefore taken when finding the relative humidity measurements' uncertainties. The maximum and mean values of the absolute values of the difference between relative humidity measured by the travelling normal, and the experiment's instruments, are given in table 3.8. As mentioned in section 3.2.3, the field control in February 2020 revealed problems with the humidity measuring instrument at the location with cut grass at 2 m. The underlined values in table 3.8 are calculated by including the field control from 2020, and the non-underlined values were calculated by excluding these values.

**Table 3.8:** This table shows the maximum and mean values of the absolute values of the difference between relative humidity measured by the experiment's instrument and by the travelling normal,  $(X_i - \bar{X})$ . All  $(X_i - \bar{X})$  values can be found in appendix B. C represents the location with cut grass and U represents the location with uncut grass. The heights are the heights at which the instruments are mounted. In the leftmost column, the underlined values have been calculated by including the field control from 2020 and the non-underlined values were found by excluding those values.

Location and height	C, 2 m	C, 1.25 m	C, 0.55 m	U, 2 m	U, 1.25 m	U, 0.55 m
Maximum absolute value	<u>26.15</u> / 3.70	4.91	4.70	5.20	4.70	4.70
Mean absolute value	<u>11.38</u> / 2.17	2.64	2.48	2.18	3.01	3.20

Since expanded uncertainty could not be calculated for relative humidity, a more generalized approach was taken when determining the uncertainties of these measurements. Based on the maximum and mean values of the absolute values of the difference between relative humidity measured by the travelling normal and by the experiment's instrument, given in table 3.8, an uncertainty of  $\pm 3$  p.p. was chosen for the measurements. This resulted in combined uncertainties of  $\pm 6$  p.p. when evaluating the difference between relative humidity measurements, as presented in table 3.9. The combined uncertainty of  $\pm 4$  p.p. is included for the difference between relative humidity measurements at 2 m. This is because the mean values for the instruments at this height were the lowest and an evaluation of this combined uncertainty will be done in addition to the combined uncertainty of  $\pm 6$  p.p.

**Table 3.9:** This table presents the combined uncertainties of the difference between or relative humidity measurements at the location with uncut (U) and cut (C) grass at the three heights in the experiment behind this thesis. The combined uncertainties are based on the individual measuring instruments' uncertainties given in 3.8. p.p. is the abbreviation for percentage point.

Height of measuring instrument	Combined uncertainty
2 m	$\pm 6/\pm 4$ p.p.
1.25 m	$\pm 6$ p.p.
0.55 m	$\pm 6$ p.p.

### 3.3 Data processing

A thorough quality control of the experiment's data was needed because it had not undergone MET's automatic quality control. The automatic control was only applied to temperature measuring instrument at the location with cut grass (C) at 2 m. The raw data were sent to MET and the easiest way to access all the data was to retrieve it all together and then process it manually. Because of this, a quality control of the data was put together and a discussion of this and what actions were taken will now follow.

The analysis started by analyzing the data sets from the summer of 2019; from 23/5/2019 00:00 until 30/10/2019 12:00. When these data sets have been imported into Python using Spyder, holes and duplicates in the data sets were discovered. The duplicates were evaluated first, and a code was written to find the duplicates in the data set for cut grass (C) and for uncut grass (U). It was found that both data sets had one duplicate on 27/10/2019 02:00 and that the U data set had six duplicates on 31/5/2019 between 15:00 and 20:00. By plotting the data from 31/5/2019 with the first and second duplicate, it was clear that the second duplicate deviated by an abnormal amount from the C data set. The second duplicate was therefore deleted. For the duplicate that both data sets had on 27/10, the last duplicate was kept because the values of the last duplicate matched the previous and following data most closely.

After deleting the duplicates, the data sets did not have the same number of rows. The creation of a simple Python function allowed for examination of rows in two separate data sets based on their timestamp. This function was used to locate the holes in the two data sets. This again allowed for easy removal of data for specific analyses. In the C data set, rows were missing between 2/7/2019 10:00 and 3/7/2019 12:00 and between 11/10/2019 20:00 and 13/10/2019 09:00. In the U data set, rows were missing between 1/6/2019 09:00 and 1/6/2019 16:00.

The rows missing between 11/10/2019 20:00 and 13/10/2019 09:00 in the C data set were due to a power outage. The instruments were turned on again between 09:00 and 10:00 on 13/10/2019. The maximum and minimum temperatures were affected in the data from 10:00 on 13/10/2019, while the data for average values were not. Because of this, all values from 11/10/2019 20:00 until 13/10/2019 10:00 were removed from the C and U data sets.

After the duplicates between 15:00 and 20:00 on 31/5/2019 in the U data set, values distinctly different from C's data were logged. Figure 3.6a show the hourly temperature values at 2 m between 15/5/2019 and 15/6/2019 for C and U, and figure 3.6b show the difference between the values. Figure 3.6b illustrates how significantly different the values logged at C and U were during some hours on 31/5 and 1/6. This resulted in them being classified as poor quality data and removed from the data sets. Notably, this happened right before the missing rows between 09:00 and 16:00 on 1/6/2019 in the U data set. In conclusion, all values in both data sets were removed between 31/5/2019



21:00 and 1/6/2019 08:00 when analyzing temperature data at 2 m.

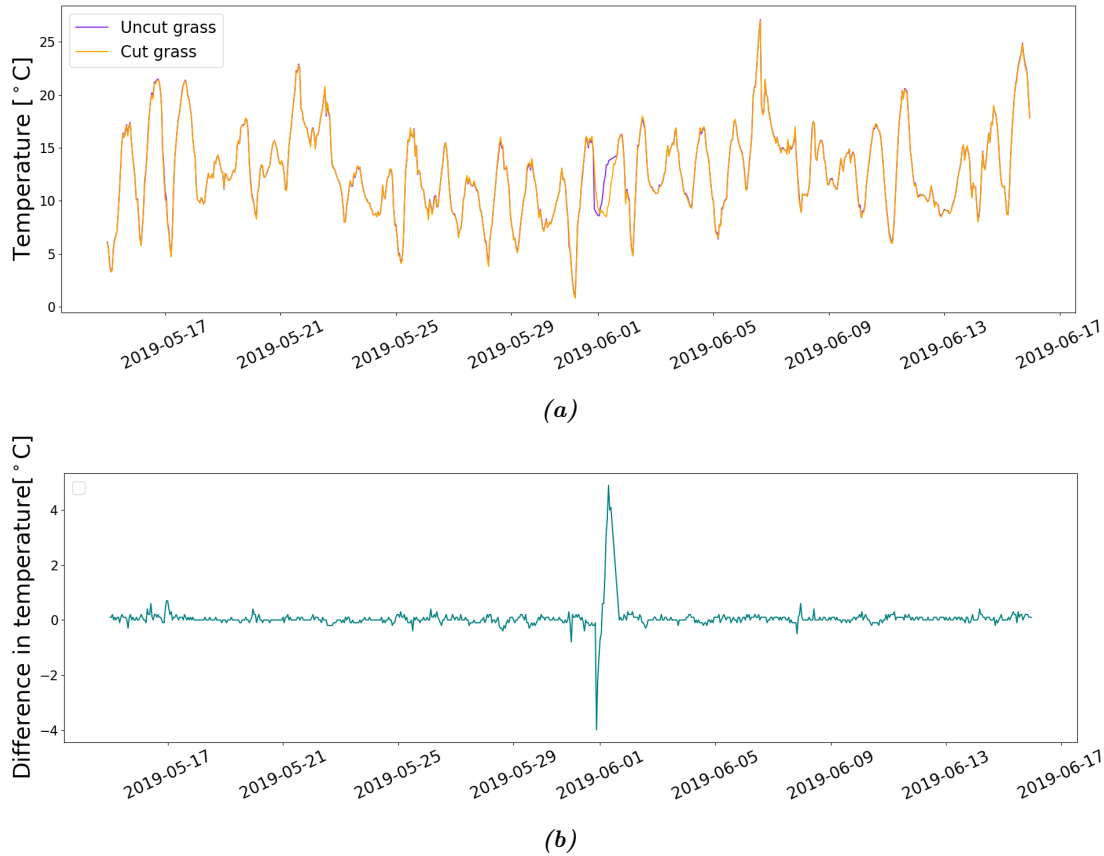


**Figure 3.6:** Temperature data measured at 2 m between 15/5/2019 and 15/6/2019 is shown in this figure. (a) shows the temperature values and (b) shows the difference between them. Because of the size of the difference in temperature for some values logged on 31/5 and 1/6 in 2019, the data are considered poor quality data and are removed from the data set.

The test cite used for the experimental setup discussed in this thesis experienced vandalism the summer of 2019. A cable was cut and this affected the temperature measuring instrument at 0.55 m at C. The damage was repaired by soldering the cable ends together. This seemed to work at first, but because of the summer holidays in Norway, it was not discovered until much later that this was not effective. Missing values were marked as -99.9 and about 97.5% of the data were lost between 1/7/2019 15:00 and 21/8/2019 13:00, when the measuring instrument got replaced. The 2.5% of the data not marked as -99.9 are unusable data because of their scattered occurrence in this time period.

The humidity measuring instrument at 2 m at C fell out for unknown reasons on 16/7/2019. The instrument was switched with the humidity instrument at 1.25 m on 6/8/2019 between 09:00 and 10:00. This should have solved the problem, but the values from 2 m differ significantly from the values at U up until 21/8/2019. This can be seen in figure 3.7. The humidity instrument at 1.25 m was replaced on 21/8/2019 and values after 13:00 can be used when evaluating the humidity at this height. To summarize, humidity data from C at 2 m between 16/7/2019 00:00 and 21/8/2019 13:00 had to be discarded and the same was true for the humidity data from C at 1.25 m between 6/8/2019 10:00 and 21/8/2019 13:00.

Around 23/9/2019, the humidity measuring instruments at C at 2 m started logging vastly different values than the five other humidity instruments. A difference in humidity between the instruments at 2 m as high as 77 p.p. was found. This was not discovered until the field control on 27/2/2019, as discussed in section 3.2.3 and showed in table

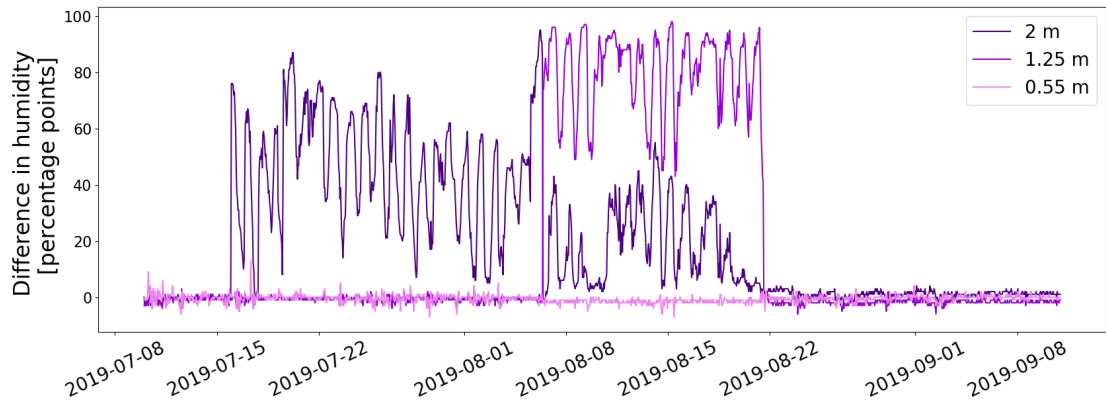


**Figure 3.7:** Plot of the difference between relative humidity logged at the location with uncut grass and that with cut grass. The time period is 10/7/2019-10/9/2019.

3.4. The variation between the values logged at C at 2 m and the five other humidity instruments can be seen in figure 3.8a. The difference between measured relative humidity at U and C at all three heights is given in 3.8b. In this plot, the significant deviation is evident and this resulted in all relative humidity values at C at 2 m being removed from 23/9/2019 until 30/10/2019.

With so much data missing for temperature and humidity at different times, heights, and positions, the data processing became complex. Data had to be removed from the data sets depending on what analysis was being conducted. The goal was to use data sets that were as large as possible. Therefore, the sizes of the data sets were maximized within the constraint of only including data that was usable within the context of the given analysis. Following is an example of how this was done: data from 1/7/2019 15:00 until 21/8/2019 13:00 were removed when looking at the difference between temperature at U and C at 0.55 m, however it were included in the data sets for temperature data from 2 m and 1.25 m.

A data coverage plot is given in figure 3.9. This plot summarizes at what times throughout duration of the experiment, data were lost from different measuring instruments, heights, and locations.

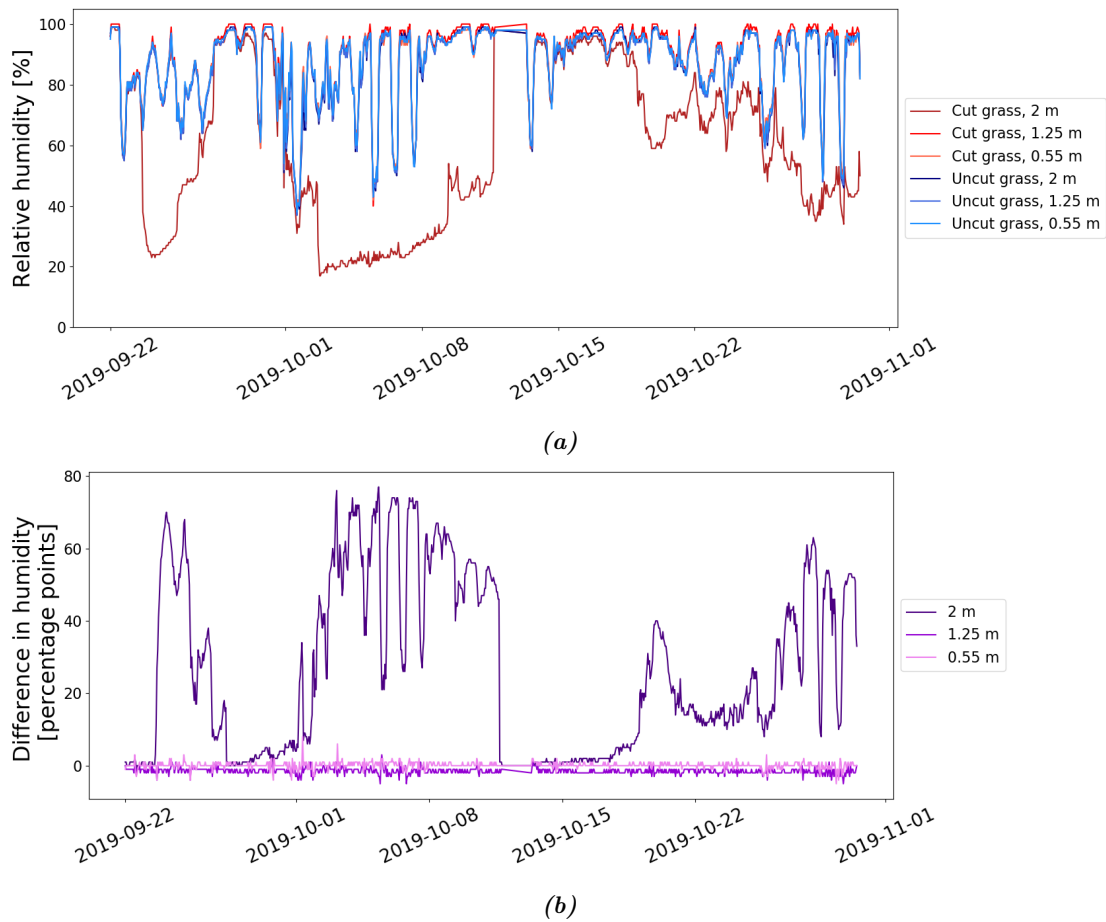


**Figure 3.8:** The plots were created using relative humidity data between 22/9/2019 00:00 and 30/10/2019 12:00 from the location with uncut (U) and cut grass (C) and from all three heights of the measuring instruments: 2 m, 1.25 m, and 0.55 m. (a) shows the relative humidity values and (b) shows the difference between the relative humidity values at the three heights.

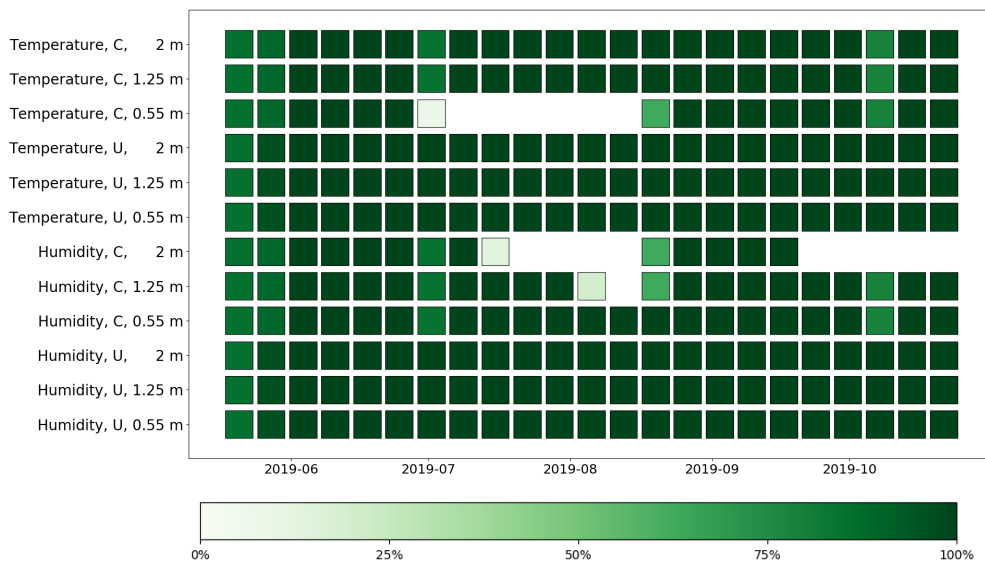


**Figure 3.9:** This is a data coverage plot that shows what data were lost or unusable in the thesis' duration in 2019. The data coverage is plotted weekly. C stands for the location where the grass was cut and U stands for the location where the grass was uncut. Humidity data logged were relative humidity.

## 3.4 Weather in 2018 and 2019

The measuring instruments for this experiment were installed in early July 2018 and started recording values on 11/7/2018 at 12:00. Because the summer of 2018 was significantly different from previous years and from 2019, the weather at the site in the summers in 2018 and 2019 must be evaluated in order to understand how the data from the two years can be compared with each other.

### 3.4.1 2018

The period between May and the beginning of August in 2018 was abnormally warm and dry in Norway. The average temperature for the May-June-July period was 3.1 °C above the normal, which is significantly higher than the previous record from 2002 of 1.9 °C. Additionally, this period had rainfall equal to 74% of the normal, which meant that the May-June-July period in 2018 was the fourth driest ever (Gangstø Skaland et al., 2019). The May-July period in Ås in 2018 was the warmest since the temperature recordings started in 1874. It was also very dry, and a third of the 167 mm of rainfall in that period occurred one day, 7/6/2018. That amount of rainfall in such a short amount of time, and the ground being as dry as it was then, resulted in most of the water draining off instead of being taken up by the soil. August also had a low amount of rainfall (44.7 mm) before September followed with heavy rain (120.7 mm) (Wolff, Thue-Hansen, and Grimenes, 2019). A picture of the location with uncut grass (U) was taken 4/7/2018 and is shown in figure 3.10. The non-green spots shows how dry it was that summer.



**Figure 3.10:** Picture of the U location in this thesis' experiment on 4/7/2018, which was before logging started. Photo: Signe Kroken.

The dryness and warmth in the summer of 2018 resulted in the grass under U not growing much before it started raining more in September. This can be seen in the pictures in figure 3.11, which were taken 20/9/2018. Figure 3.11a is of C and is included in this text to show how close the bottom instruments are to the ground when the grass is cut. In figure 3.11b, one can see that the grass has grown a few centimeters. However, when comparing figure 3.11a to figure 3.11b, one can see that the difference in grass height is only a few centimeters. The height of the grass under U in figure 3.11b is probably close to what it is under C right before maintenance at BIOKLIM cuts the grass.

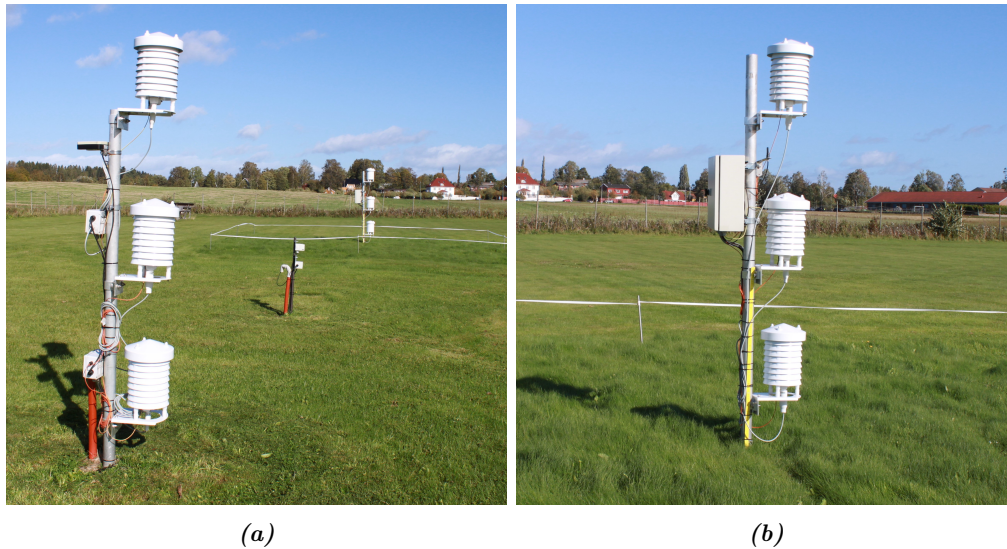


**Figure 3.11:** Pictures of the test site from 20/9/2018. (a) is a close-up of the pole where the grass was kept short and (b) close-up of the pole where the grass was not cut. Photo: Signe Kroken.

### 3.4.2 2019

In 2019, the measuring instruments logged data the whole year. This year was not as dry and warm as 2018. In May, the rainfall amount was 95 mm, which is 50% more than the normal. June had plenty of rainfall and a mean temperature close to the average, while July was quite dry and ended with a heat wave. August was also warmer than normal, with an mean temperature of 1.3 °C above the average (Wolff, Thue-Hansen, and Grimenes, 2020).

## 3.5 The use of the 2018 data set

Because the grass under U and C was very similar in 2018 and very dissimilar in 2019, there was a desire to be able to compare data from the two years. Due to the aforementioned weather effects on the grass height in 2018, there was a time period within the duration of the experiment where grass height at the two locations was effectively the same. In theory, this provided an opportunity to compare data from the two locations with the grass height being equal. The goal of the evaluation of this data was to determine the natural variations in temperature and humidity data between the two locations, with the grass height held constant.

The grass height in 2018 was kept functionally the same due to weather conditions. This made it favorable to compare data from the two locations within the same year. However, these same weather effects created problems when trying to compare data from the location between the two years (e.g. comparing the temperature at the U location at 2 m between 2018 and 2019).

Furthermore, due to complications with the 2018 data set, only hourly data between 11/7/2018 12:00 and 15/9/2018 13:00 were determined to be usable. Hourly data from the same interval in 2019 were used when directly comparing the two years. The purpose of this decision was to keep factors associated with time of day, such as the position and influence of the sun, as consistent as possible between the two years. This would, in theory, ensure that calculations better represent an evaluation of the influence of grass height alone.

## Part 2

The second part of this chapter describes the methods of data analysis used in the thesis. Two specific methods of analysis is explained first: the statistical tests used is described in section 3.6 and section 3.7 explains the theory behind of box and whisker plots. Section 3.8 details the weather categories used in the data analysis, and section 3.9 explains how single days in different weather categories were found.

### 3.6 Statistical tests

One method used to examine the data in this thesis was to apply the Kolmogorov-Smirnov (KS) test. This is a nonparametric test, which means that it does not assume that the data follow any certain distribution. A KS test is used to evaluate the following null and alternative hypothesis:

- $H_0$ : The samples come from the same distribution
- $H_1$ : The samples do not come from the same distribution

A sufficiently low p-value will lead to a rejection of the null hypothesis and conclude that the two samples are not from the same distribution (Kawwa, 2020).

In the KS test, the empirical distribution function (EDF) is used. The EDF is an estimate of a sample's cumulative distribution function (CDF). The CDF indicates the probability of a value being less than or equal to a specified value. The CDF and EDF are found by sorting all the values in the sample in ascending order and then for each value,  $x$ , the probability of any value in the sample being equal to or lower than  $x$  is calculated (Kirkman, 1996). The CDF and the probability density function (PDF) of a distribution are shown in figure 3.12. In a PDF, the area under the curve indicates the probability (Dolan, 2019). In figure 3.12, the area under the PDF curve to the left of 0 is half of the total area, which means that there is a 50% chance of a value being equal to or smaller than 0. The plot of the CDF shows that when  $x=0$ , then  $y=0.5$ . This means that there is a 50% chance of  $x$  being equal to or smaller than 0. Figure 3.13 shows an EDF. The distribution shows that there is a 50% probability of a value being equal to or lower than 0 and a 95% probability of  $x \leq 0.5$ .

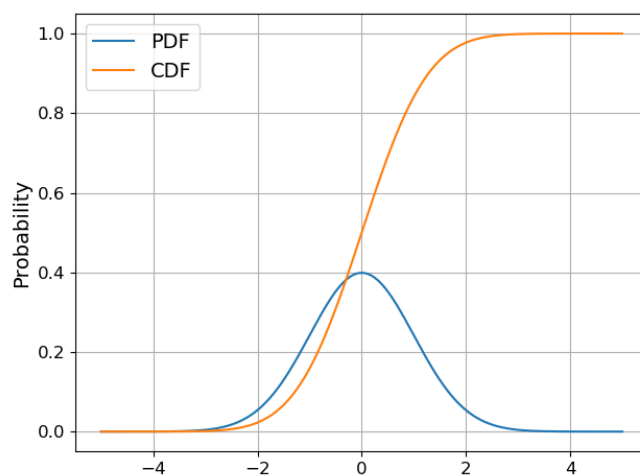


**Figure 3.12:** A plot of the probability density function (PDF) and the cumulative distribution function (CDF) of the normal (Gaussian) distribution with mean value of 0 and standard deviation equal to 1.

The KS test can be run both as a one-sample and a two-sample test. In a one-sample test, the EDF of a sample is compared with a CDF of a reference distribution,

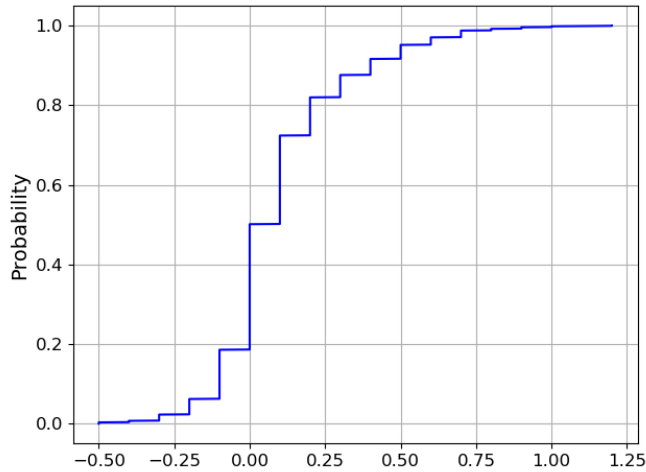


**Figure 3.13:** A plot of the empirical distribution function (EDF) of the difference between temperature measured at 2m and 1.25m at the location with uncut grass ( $U$ ) in this thesis' experiment.

for example the normal distribution. In a two-sample KS test, the EDFs of two samples are compared against each other. The KS test then compares the differences between the EDFs for the two samples and finds the largest divergence. This difference is the test statistic of the test. Based on the size of the samples and the chosen significance level, the p-value is found and one can then either confirm or reject the null hypothesis (Kawwa, 2020).

The Mann-Whitney U (MWU) test is also a non-parametric test. Its null hypothesis is that the distributions of two samples are identical. If the null hypothesis of a MWU is correct, then there is a 50% chance that a randomly selected value from the first distribution is greater than a randomly selected value from the second distribution (Perry, 2019). In this thesis, this test was used to confirm the test statistic from the KS test.

The chosen significance level for the tests performed in this report was a 95% significance level. This means that the p-value must be below  $5\%=0.05$  to be able to reject the null hypothesis and conclude that the two data sets are different.

### 3.7 Box and whisker plot

Box and whisker plots illustrate the spread of the data in a data set. A figure illustrating this type of plot where the different parts are marked is shown in figure 3.14. In a box and whisker plot, at least 50% of the data are within the interval of the box, called the interquartile length (IQR), and the median of the data set is represented by a line. In the box and whisker plots in this report, the median is represented by an orange line. The whiskers show the interval of all other data in the data set, except for the outliers. A data point is considered to be an outlier if its value is further away from the box than 1.5 times the length of the box (Galarnyk, 2018). This is shown in figure 3.14. The outliers will therefore lay outside of the whiskers and will be marked as small circles in this thesis' results.

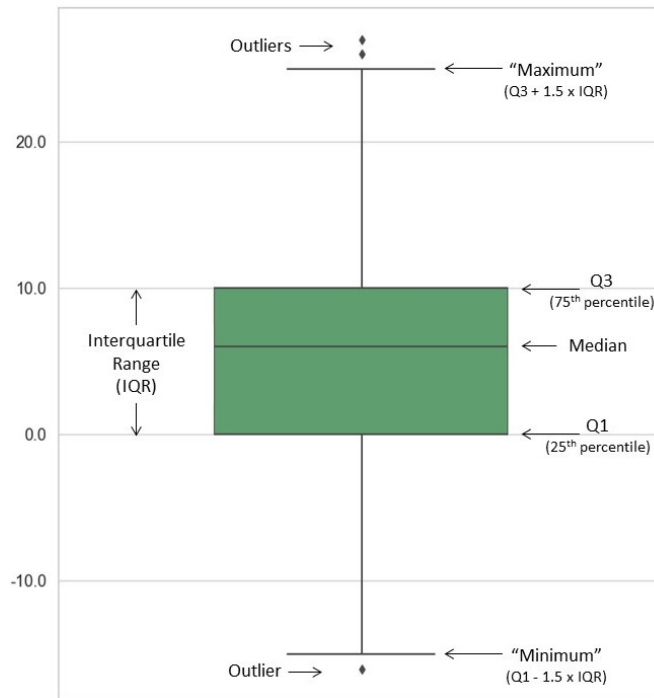


**Figure 3.14:** An illustration of the different aspects of a box and whisker plot. Adapted from Galarnyk (2018)

### 3.8 Weather categories

The weather greatly affects how much the air temperature is affected by the surface properties, which was explained in section 2.4. This section will detail how the weather categories were decided and argue their limits.

When creating the solar radiation exposure limits, the theory in section 2.4, in combination with evaluation of radiation data, from the test site were used. The solar radiation exposure was categorized as overcast or considerable cloudiness, partly cloudy, or cloud-free. The ratio of diffuse to global radiation tells us how much solar radiation is reaching the ground. This tells us how cloudy it is. The lower the diffuse to global radiation ratio is, the smaller is the area of the sky that is covered by clouds. A plot was created using hourly global and diffuse radiation values from Søråsjordet from July 2019. This plot can be seen in figure 3.15. Figure 3.15a shows the global and diffuse radiation values, and figure 3.15b shows the ratio of diffuse to global radiation. It can be seen that days like July 5, 10, 11, and 12 have low diffuse radiation values compared to the global radiation values, and are therefore days with clear skies. Days like July 6 and 19 have similar values for diffuse and global radiation and can be identified as days with overcast weather. On July 20, the peak for diffuse radiation is around half of that of global radiation and can therefore be classified as a partly cloudy day. Some days are not as easy to classify into one of the three categories by evaluating this plot, but from the theory from section 2.4 and analysis of this plot, the limits were set as presented in table 3.10

**Table 3.10:** The limits for the ratio of diffuse to global radiation for the three solar radiation exposure categories.

	Cloud-free	Partly cloudy	Overcast or considerable cloudiness
Ratio = $r = \frac{\text{Diffuse radiation}}{\text{Global radiation}}$	$0 \leq r \leq 0.25$	$0.25 < r < 0.6$	$0.6 \leq r \leq 1$



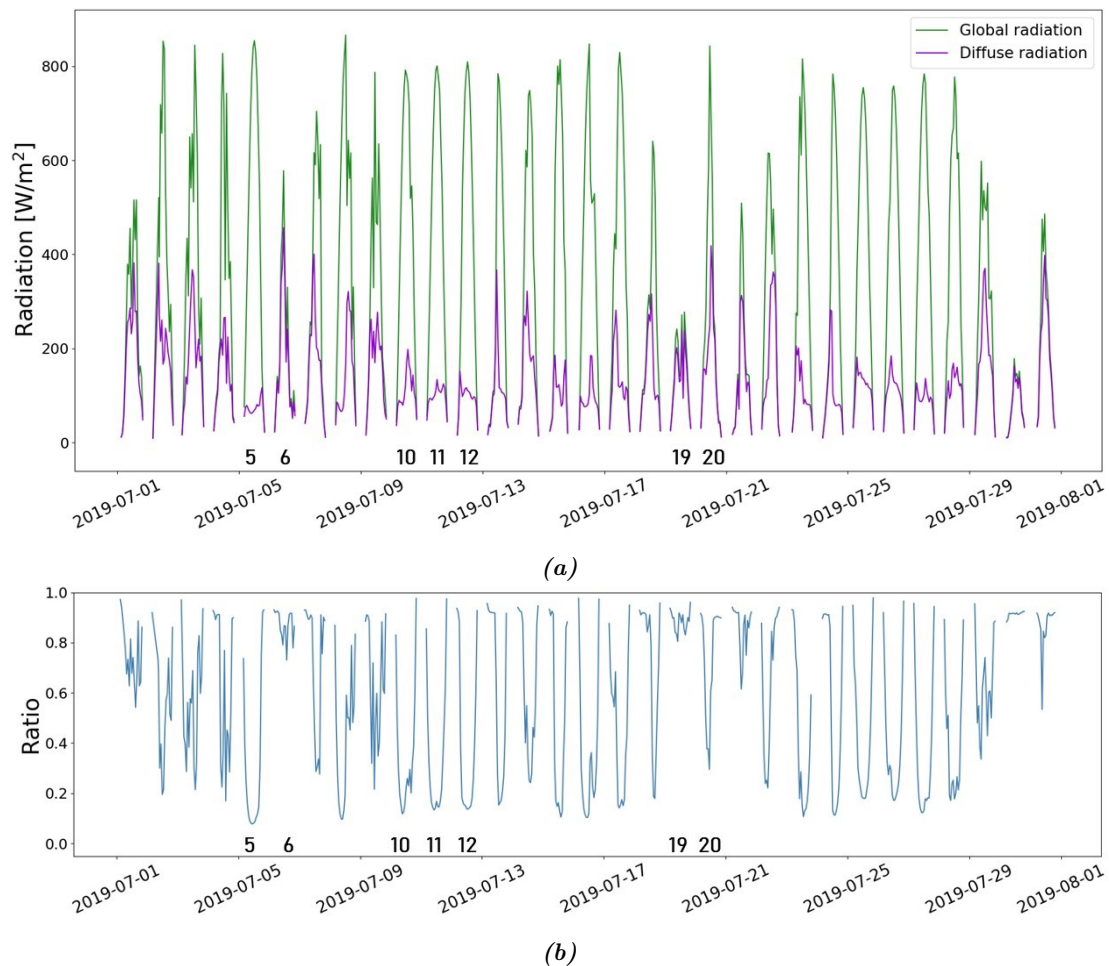


**Figure 3.15:** The figures in this plot have been made using radiation data from Søråsfeltet in Ås, Norway in July 2019. (a) shows the global and diffuse radiation values and (b) shows the ratio of diffuse to global radiation. These values are 0 during the night. The 5<sup>th</sup>, 10<sup>th</sup>, 11<sup>th</sup>, and 12<sup>th</sup> are examples of days with low diffuse to global radiation ratio, the 6<sup>th</sup> and 19<sup>th</sup> are examples of days with high diffuse to global radiation ratio, and the 20<sup>th</sup> is an example of a day where the diffuse radiation values are around half of the global radiation values.

According to the suggestions in section 2.4, the situation is considered a light wind situation when the wind speed is lower than or equal to 5 m/s. This threshold is shown in table 3.11.

**Table 3.11:** *The limits for what is considered high and light wind speed. The surface properties' influence on the air is larger when the wind speed is low because light wind result in less mixing of the air.*

	Light wind	High wind
Wind speed	$\leq 5$ m/s	$> 5$ m/s

### 3.9 Weather's influence

Analyses of single days in different weather categories were done in this thesis in order to better understand the data. Days with heavy and low influence by the surface were looked at to evaluate effect of the increased grass height U. In order to find specific days with low and high solar radiation exposure, the limits in table 3.10 were used. Diurnal and hourly radiation and wind data from Søråsjordet were evaluated and the ratio of diffuse to global radiation was calculated.

A simple Python code was written where hours with overcast or considerable cloudiness were put into one data table and cloud-free hours were put into another. The data tables with the selected data were then evaluated manually. If there was a notable amount of values from the same day in one of the categories, the weather data from that whole day were evaluated. Specifically, the global and diffuse radiation values and the wind speed values were looked at. This was done to get the best possible picture and overview of what the solar radiation exposure and wind conditions were on those days.

Both single days with generally cloud-free conditions and light wind throughout the whole day, and days with overcast or considerable cloudy conditions were found. Data from these days were analyzed individually to get a better picture of how the grass under U influenced air, and to analyse the development of the vertical temperature profile throughout the experiment's duration.

# Chapter 4

## Results

This chapter presents the main results of the thesis. Plots that have been made using the data from the test site will be presented. The plots will be used to evaluate the influence of increased vegetation height on air temperature and humidity. Results from analysis of the temperature data is presented first. An overview of the data is given and statistical tests are used to compare data from 2018 with data from 2019. Data from the experiment's duration in 2019 will then be examined. The influence of weather on the difference between temperature measured at the location with uncut (U) and with cut (C) grass will be examined, as well as the difference between measured temperature at day and night hours. Difference in daily temperature will be evaluated before a closer look at single days will be presented. Vertical temperature profiles and tables showing data from the site on specific days makes it possible to compare data and evaluate the development of the difference in temperature between U and C throughout the summer of 2019. Lastly, results from humidity evaluation will be presented.

In the results presented in this chapter, analyses were performed using data relevant to the task. In each analysis, the goal was to maximize the size of the data set that was used. This meant that some data sets were larger than others when evaluating the same parameters, but at different heights or positions. In section 3.3, it was argued thoroughly what data can be excluded from the data sets. This was summed up in figure 3.9.

This chapter presents many plots of the difference in temperature and humidity measured over uncut and cut grass. In several of these plots, the combined uncertainty of this difference is marked. The combined expanded uncertainty for the difference in temperature at 2 m is  $\pm 0.4$  °C, for 1.25 m and 0.55 m it is  $\pm 0.5$  °C. For the difference in relative humidity measurements, the combined uncertainty is  $\pm 6$  percentage points (p.p.). The combined uncertainty of  $\pm 4$  p.p. for the difference between measurements at 2 m will also be evaluated. The reasoning for this was discussed in section 3.2.4.

### 4.1 Overview of the data

This section aims to give a good overview of the data measured at the test site during the experiment's duration in 2019. Time series plots and the results of simple statistical measures are presented.

#### 4.1.1 Timelines of temperature measurements

Time series plots of the temperature measured over uncut (U) and cut (C) grass, and the difference between these values using data from the last two weeks of June and September, are given in figures 4.1 and 4.2 respectively. The real temperature data from the two time periods give a representative impression of the temperature variations throughout a day and over longer periods. Furthermore, the difference between  $T_U$  and  $T_C$  can give indications to how the increased grass height at U influence measured air

temperature. The time series were chosen randomly, but the three months difference between them is important because in that time, the grass at U increased in density and possibly in height.

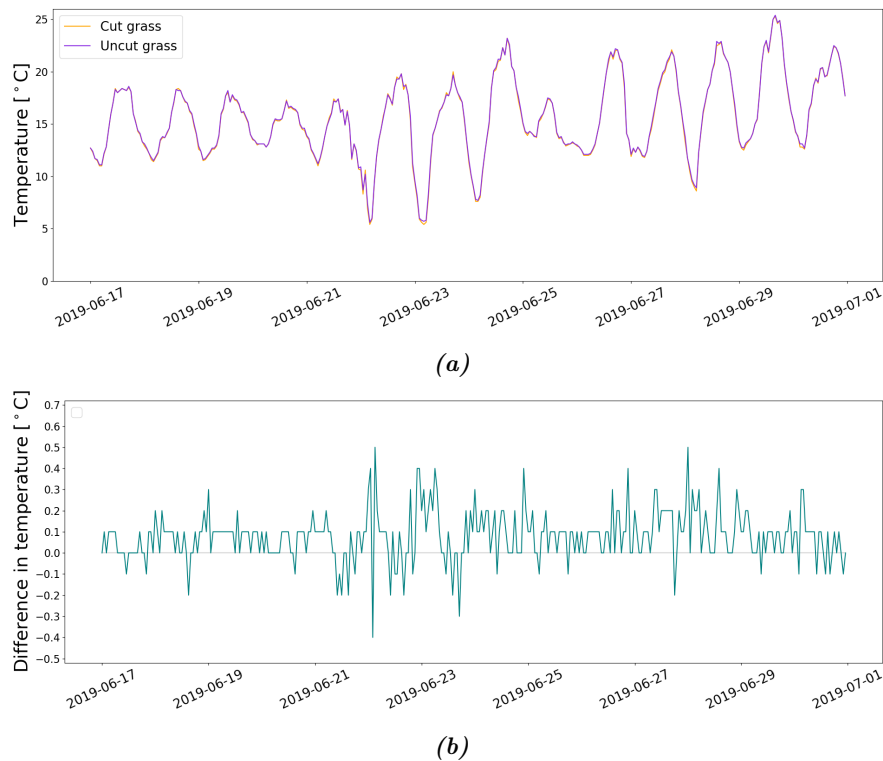


**Figure 4.1:** The plots were made using temperature data from the thesis' setup. The data set used is from 17/6/2019 until 30/6/2019. (a) Temperature measured at 2m over uncut and cut grass. (b) The difference between temperature measured at 2m over uncut and that over cut grass.

The values of the difference in temperature between U and C in both June (figure 4.1b) and October (figure 4.2b) were concentrated around 0.0°C. However,  $(T_U - T_C)$  was equal to 0.1°C more often than 0.0°C at the end of June. This was not the case for these values at the end of September, where the most common  $(T_U - T_C)$  value was 0.0°C. Nonetheless, for both time periods, 93% of the  $(T_U - T_C)$  values were in the  $\pm 0.2^\circ\text{C}$  interval. 99.4% of the  $(T_U - T_C)$  values from the June period were in the  $\pm 0.4^\circ\text{C}$  interval, while 98.2% of the values from the September period were in this interval. The largest positive and negative  $(T_U - T_C)$  values were 0.7°C and -0.5°C and were both in the September interval. Whether it was by chance that the largest  $(T_U - T_C)$  values (in both directions) were in September, or due to the increased grass height and density at U, cannot be concluded from analysis of these plots alone. Further evaluation of this will follow in the coming sections where different types of statistical tools will be used on large time series.

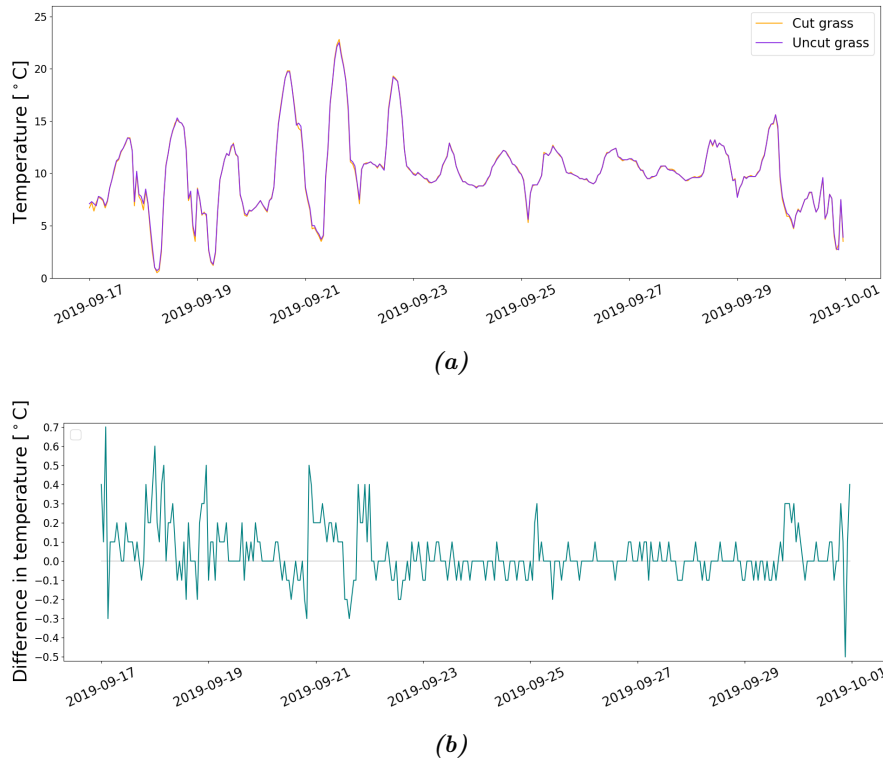


**Figure 4.2:** The plots were made using temperature data from the thesis' setup. The data set used is from 17/9/2019 until 30/9/2019. (a) Temperature measured at 2 m over uncut and cut grass. (b) The difference between temperature measured at 2 m over uncut and that over cut grass.

#### 4.1.2 Difference in temperature over uncut and cut grass in 2019

The mean and standard deviation values of the difference in temperature over uncut (U) and cut (C) grass, at the three heights the measuring instruments were placed at, are given in table 4.1. The values were calculated using data from the thesis' experiment in 2019. The mean value for all three heights is 0.0 °C. Standard deviation is 0.1 °C for the difference between temperature measured at U and C for the instruments at 2 m, while it is 0.2 °C for the difference between the values measured by instruments at 1.25 m and 0.55 m.

**Table 4.1:** This table presents the mean and standard deviation values for the difference in measured temperature over uncut and cut grass between 23/5/2019 and 30/10/2019. The three heights are the heights at which the measuring instruments of this thesis' experiment were mounted at.

Height	Mean [°C]	Standard deviation [°C]
2 m	0.0	0.1
1.25 m	0.0	0.2
0.55 m	0.0	0.2

In order to get an overview on how the temperature difference developed throughout 2019, the monthly means and standard deviations of the temperature difference in 2 m were calculated. The results are shown in table 4.2. The means are 0.0 °C in July, August, and September and are 0.1 °C in June and October. The standard deviations are 0.1 °C for all months.

**Table 4.2:** This table presents the monthly mean and standard deviation values in 2019 for  $T_U - T_C$  at 2 m, which is the difference in temperature between the location where the grass was not cut (U) and the location where the grass was cut (C) at 2 m.

Month	Mean [°C]	Standard deviation [°C]
June	0.1	0.1
July	0.0	0.1
August	0.0	0.1
September	0.0	0.1
October	0.1	0.1

## 4.2 Comparisons of data from 2018 and 2019

In this section, results from comparisons of data from 2018 and 2019 will be presented. The purpose of this is to get an overview of the difference in the data sets between the two years, and to use that information to evaluate the influence of increased grass height in a broad perspective. As mentioned in section 3.4, the weather situation in the two years was very different. Section 3.5 explained how this influences the use of the data from 2018. The time period between 11/7 12:00 and 15/9 13:00 will be used when evaluating data from 2018 and comparing data directly between 2018 and 2019, as explained in section 3.5.

### 4.2.1 Difference in temperature over uncut and cut grass

Mean and standard deviation are statistical tools that can be used to get an overview of the data and the data's dispersion. The mean and standard deviation of the difference in temperature at 2 m between U and C in the period 11/7 12:00 and 15/9 13:00 in 2018 and 2019 are given in table 4.3. The mean values are 0.0 °C. The standard deviation is 0.1 °C in 2019, while it is 0.2 °C in 2018.

**Table 4.3:** This table presents the mean and standard deviation of the difference in temperature between the measuring instruments over uncut and that over cut grass, ( $T_U - T_C$ ), at 2 m in the time period between 11/7 12:00 and 15/9 13:00 in 2018 and 2019.

Year	Mean [°C]	Standard deviation [°C]
2018	0.0	0.2
2019	0.0	0.1

### 4.2.2 Test statistics to evaluate how different the years were

The two-sample KS and MWU tests are used to decide if two data sets are from the same sample, i.e. whether they are significantly different or not. The tests were presented in section 3.6. A sufficiently small p-value lets you conclude on a given significance level that the samples are different. The chosen significance level in this thesis was 95%, which means that a p-value of 5%=0.05 is needed to reject the null-hypothesis,  $H_0$ . The results from the KS and MWU tests are given in table 4.4.

The null-hypothesis for the tests in row a and b in table 4.4 was that there was no significant difference in the difference between temperature measured at 2 m and 1.25 m between the two locations U and C in 2019 (row a) and 2018 (row b). If there was a difference between  $T_{2m}$  and  $T_{1m}$ , the influence by surface properties reach higher than what is assumed by WMO. This means that if there was a difference between

**Table 4.4:** The table presents test statistics from KS (Kolmogorov-Smirnov) tests and MWU (Mann-Whitney U) tests on data from the test site. U is the location with uncut grass under it and C the location with cut grass under it. 2m and 1m represents the measuring instruments mounted at 2 m and 1.25 m respectively.

	Input x	Input y	KS test p-value	WMU test p-value
a	$(T_{2m} - T_{1m})_U$ , 2019	$(T_{2m} - T_{1m})_C$ , 2019	$8.23 \cdot 10^{-5}$	$6.85 \cdot 10^{-5}$
b	$(T_{2m} - T_{1m})_U$ , 2018	$(T_{2m} - T_{1m})_C$ , 2018	0.125	0.203
c	$(T_U - T_C)_{2m}$ , 2019	$(T_U - T_C)_{2m}$ , 2018	$2.44 \cdot 10^{-23}$	$1.95 \cdot 10^{-22}$
d	$(T_U - T_C)_{1m}$ , 2019	$(T_U - T_C)_{1m}$ , 2018	$1.31 \cdot 10^{-10}$	$4.97 \cdot 10^{-5}$
e	$(T_{2m} - T_{1m})_U$ , 2019	$(T_{2m} - T_{1m})_U$ , 2018	0.115	0.531
f	$(T_{2m} - T_{1m})_C$ , 2019	$(T_{2m} - T_{1m})_C$ , 2018	0.003	0.094

$(T_{2m} - T_{1m})$  in two different locations, the surface properties at one location influenced the air at 1.25 m temperature to a higher degree than at the other location. The p-values in row a have an order of magnitude of  $-5$ , and one can then say that the data sets with  $(T_{2m} - T_{1m})$  with data from U and C were significantly different from each other in 2019. When using data from 2018 instead, the p-values for the two tests were 0.125 and 0.203, which are larger than 0.05. These test statistics are in row b. It can therefore be said with 95% significance that  $(T_{2m} - T_{1m})_U$  and  $(T_{2m} - T_{1m})_C$  were different in 2019, but not in 2018. In addition, due to the very low p-values in row a and the relatively high p-values in row b,  $H_0$  is rejected at all common significance levels for 2019 and fails to be rejected for 2018.

In row c and d in table 4.4, the data sets with the difference between temperature measured at U and C at a specific height, is compared between 2018 and 2019. The null-hypothesis is therefore that there was no difference between  $(T_U - T_C)$  at a specific height between the two years. In row c, data from 2 m are compared and in row d, data from 1.25 m are compared. The p-values in row c are much smaller than 0.05, both having an order of magnitude of  $-23$ . This means that the data sets consisting of  $(T_U - T_C)_{2m}$  in 2019 and 2018 can be said to have been significantly different from each other according to the KS and MWU tests. The p-values in row d have orders of magnitude of  $-10$  and  $-5$ , and the same can therefore be said for the difference in temperature at 1.25 m,  $(T_U - T_C)_{1m}$ , between the two years.

In row e and f, the data sets consisting of  $(T_{2m} - T_{1m})$  at a specific location is compared between the two years. The null-hypothesis is therefore that there was no significant variation in the difference between temperature measured at 2 m and 1.25 m at a specific location between 2018 and 2019. It is shown in row e that the p-values are 0.115 and 0.531 when doing this test on data sets from U. This means that it cannot be concluded on a 95% level, or any common significance level, that there was a difference between the temperature profile from 1.25 m up to 2 m at U between 2018 and 2019. In row f, the results from comparing the  $(T_{2m} - T_{1m})_C$  values from 2018 and 2019 are shown. The p-values from running the KS and MWU tests on these two data sets are 0.003 and 0.094. In the KS test,  $H_0$  is rejected on a 95% significance level, while it fails to be rejected in the WMU test. 0.094 is below 0.10, which means that  $H_0$  would have been rejected on a 90% significance level. This means that according to the KS test, it can be concluded on a 95% significance level that there was a difference between the temperature profile from 1.25 m up to 2 m at C between 2018 and 2019.

### 4.2.3 The difference in temperature at three heights

In figure 4.3, the differences between temperature at U and C at the three heights 2 m, 1.25 m, and 0.55 m are plotted as box and whisker plots. In figures 4.3a and 4.3b, the

hourly temperature difference from 2018 and 2019 are shown respectively. Figure 4.3a shows that the interval of the  $(T_U - T_C)$  values at 1.25 m and 0.55 m were  $[-0.8^\circ\text{C}, 1.5^\circ\text{C}]$  and  $[-1.0^\circ\text{C}, 2.3^\circ\text{C}]$  in 2018. Figure 4.3b show that these intervals were reduced to  $[-0.6^\circ\text{C}, 1.0^\circ\text{C}]$  and  $[-1.0^\circ\text{C}, 1.4^\circ\text{C}]$  in 2019. Additionally, the interval of the box for the  $(T_U - T_C)$  values at 1.25 m is reduced by  $0.1^\circ\text{C}$  from 2018 to 2019. This means more values were contained within a smaller range in the data set for 2019. In appendix C, box and whisker plots of the diurnal variation of the difference in temperature in 2018 are shown. These plots further demonstrate that the variation in the  $(T_U - T_C)$  values was larger for all heights in 2018 than in 2019.

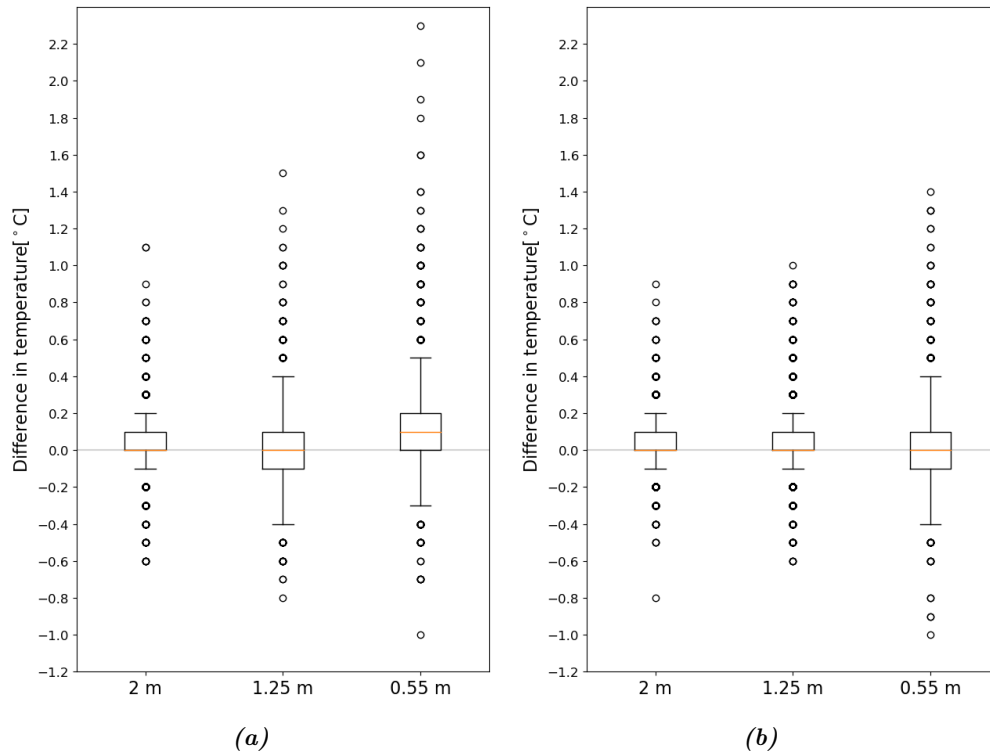


**Figure 4.3:** These plots show box and whisker plots of the difference in temperature measured over uncut grass ( $U$ ) and cut grass ( $C$ ) at three heights above the ground: 2 m, 1.25 m, and 0.55 m. (a) displays the difference in temperature in 2018, while (b) displays the difference in temperature in 2019. For 2018, the data set is from 11/7/2018 12:00 until 15/9/2018 13:00. For 2019, the data set is from 23/5/2019 00:00 until 30/10/2019 12:00.

Table 4.5 presents the percentage of data points of the value  $(T_U - T_C)$  that are in the ranges  $\pm 0.2^\circ\text{C}$ ,  $\pm 0.3^\circ\text{C}$ ,  $\pm 0.4^\circ\text{C}$ , and  $\pm 0.5^\circ\text{C}$  for the three heights, 2 m, 1.25 m, and 0.55 m, in both 2018 and 2019. The percentage numbers in the table demonstrates that more  $(T_U - T_C)$  values are closer to  $0.0^\circ\text{C}$  in 2019 than in 2018, just like what was seen in figure 4.3.



**Table 4.5:** This table displays the percentage of data points that are within a given interval for the difference in temperature between the location with uncut (U) and cut (C) grass.  $\pm 0.4^\circ\text{C}$  is the combined expanded uncertainty for the difference in temperature between the two locations, U and C, in this experiment at 2 m.  $\pm 0.5^\circ\text{C}$  is the combined expanded uncertainty for this difference at 1.25 m and 0.55 m. For 2018, the data set is from 11/7/2018 12:00 until 15/9/2018 13:00. For 2019, the data set is from 23/5/2019 00:00 until 30/10/2019 12:00.

		$\pm 0.2^\circ\text{C}$	$\pm 0.3^\circ\text{C}$	$\pm 0.4^\circ\text{C}$	$\pm 0.5^\circ\text{C}$
2018	2 m	85.1%	93.3%	96.4%	97.9%
	1.25 m	79.1%	87.8%	93.3%	96.1%
	0.55 m	71.8%	81.8%	88.0%	91.7%
2019	2 m	92.9%	97.4%	98.9%	99.6%
	1.25 m	87.5%	93.4%	96.2%	98.4%
	0.55 m	83.5%	88.5%	94.0%	96.4%

### 4.3 Diurnal variation in temperature difference

Box and whisker plots give a deeper understanding of the spread of the data. Plotting the diurnal difference in temperature measured over uncut (U) and cut (C) grass is useful to evaluate the development of this value. A thorough explanation of box and whisker plots was given in section 3.7. These kinds of plots will be presented in this section for the three heights and for different weather conditions.

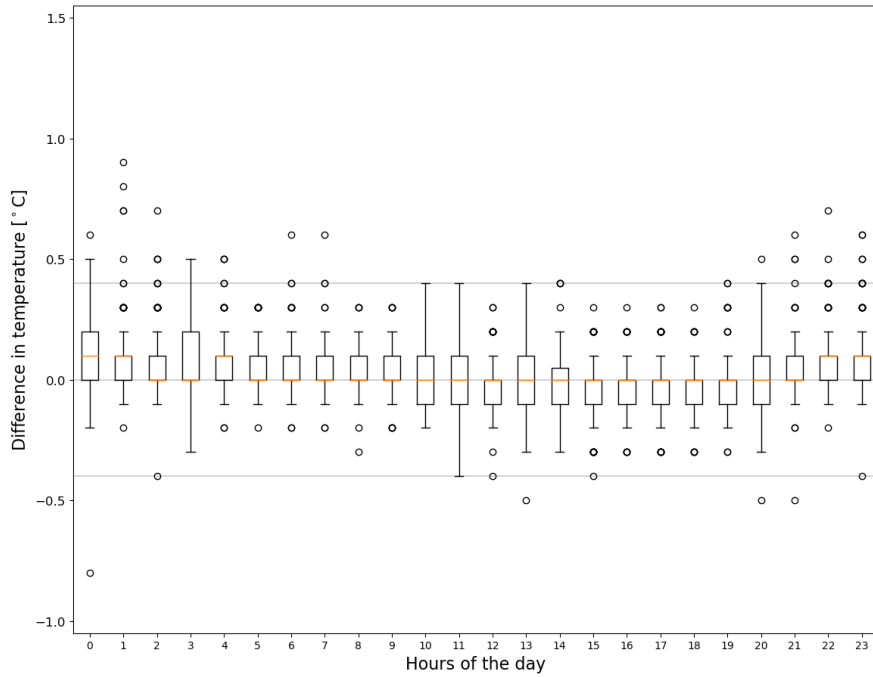
#### 4.3.1 Overview

The diurnal difference in hourly temperature at 2 m between U and C in 2019 is evaluated in figure 4.4. For all hours of the day, the boxes (containing at least 50% of the data) are within the  $[-0.1^\circ\text{C}, 0.2^\circ\text{C}]$  interval. Furthermore, the median values are either  $0.0^\circ\text{C}$  or  $0.1^\circ\text{C}$  for all hours of the day. No whiskers are outside of the  $[-0.4^\circ\text{C}, 0.5^\circ\text{C}]$  interval. The largest positive outlier is  $0.9^\circ\text{C}$  and the largest negative outlier is  $-0.8^\circ\text{C}$ .

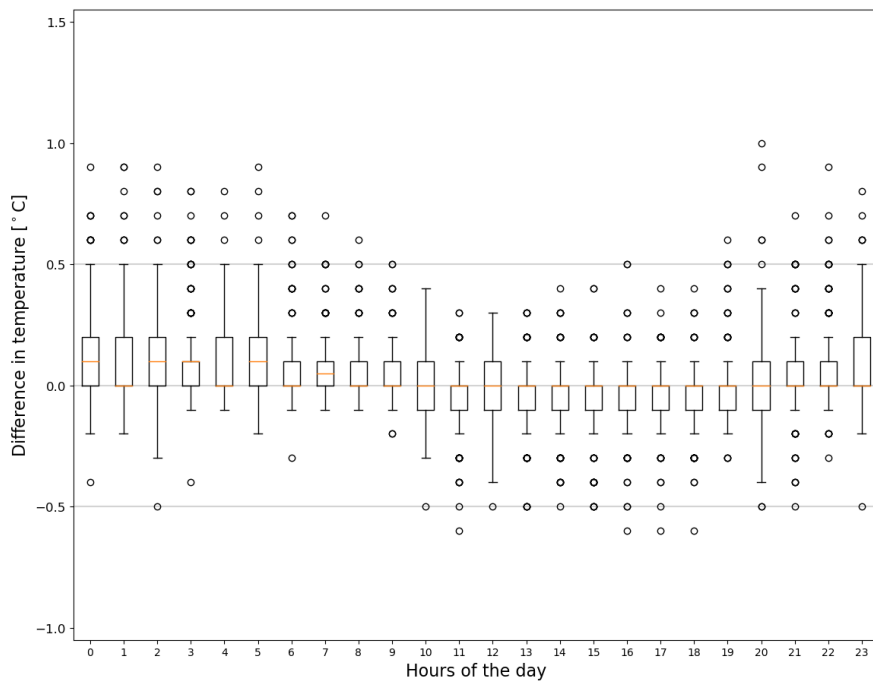
Figure 4.5 shows the same as figure 4.4, but for 1.25 m instead. Just like the plot of the diurnal difference in temperature between U and C at 2 m, all the hours' boxes are within the  $[-0.1^\circ\text{C}, 0.2^\circ\text{C}]$  interval, and all whiskers are within the  $[-0.4^\circ\text{C}, 0.5^\circ\text{C}]$  interval. The main difference between the difference in temperature at these two heights is the amount of, and the pattern in, the outliers in the plot for  $(T_U - T_C)$  at 1.25 m. The outliers are more in number and there is an indication of a diurnal pattern. The largest negative and positive  $(T_U - T_C)$  values at 1.25 m were  $-0.6^\circ\text{C}$  and  $1.0^\circ\text{C}$ .

Figure 4.6 shows the same as figures 4.4 and 4.5, but for 0.55 m. There are more and larger outliers for the difference in temperature between U and C in this plot than in figures 4.4 and 4.5. The largest negative and positive  $(T_U - T_C)$  values at 0.55 m were  $-1.0^\circ\text{C}$  and  $1.4^\circ\text{C}$ . This indicates that the temperature measurements at 0.55 m were more affected by the ground than the measurements at 2 m and 1.25 m. This is in line with the theory presented in section 2.4. However, the boxes for all hours are within the  $[-0.1^\circ\text{C}, 0.2^\circ\text{C}]$  interval, just like for the difference in temperature at 1.25 m and 2 m. Contrary to the results from the comparison of the instruments at 1.25 m, no obvious diurnal pattern was found in this plot for 0.55 m.

Additionally, similar analyses were performed separately for the temperature data at 2 m in the months June–October. The plots can be found in appendix D. No significant difference between the months could be detected. Median differences ranged from  $-0.1^\circ\text{C}$  to  $+0.1^\circ\text{C}$ , and the boxes (containing at least 50% of the data) were all within the interval  $[-0.2^\circ\text{C}, 0.2^\circ\text{C}]$ , with only a few exceptions. The mean values of the hourly



**Figure 4.4:** This plot shows box and whisker plots for the difference between the temperature at 2m over uncut grass and that over cut grass for each hour of the day. The data set used is from 23/5/2019 00:00 until 30/10/2019 12:00.



**Figure 4.5:** This plot shows box and whisker plots for the difference between the temperature at 1.25m over uncut grass and that over cut grass for each hour of the day. The data set used is from 23/5/2019 00:00 until 30/10/2019 12:00.

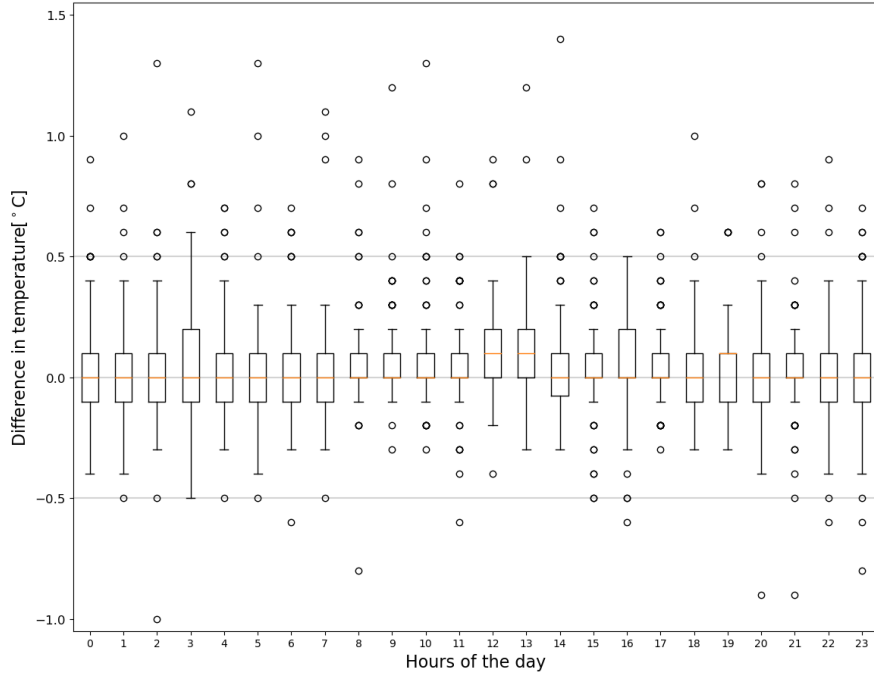


**Figure 4.6:** This plot shows box and whisker plots for the difference between the temperature at 0.55 m over uncut grass and that over cut grass for each hour of the day. The data set used is from 23/5/2019 00:00 until 30/10/2019 12:00.

median values of  $(T_U - T_C)$  for each month are given in table 4.6. They are all either 0.0 °C or 0.1 °C.

**Table 4.6:** The table shows the mean of the hourly median of the difference between temperature measured over uncut (U) and cut (C) grass at 2 m. The data set used is from 23/5/2019 00:00 until 30/10/2019 12:00.

Month	Mean of hourly median
June	0.1 °C
July	0.0 °C
August	0.0 °C
September	0.0 °C
October	0.0 °C

### 4.3.2 Radiation categories

In this section, the diurnal box and whisker plots of the difference in temperature measured over uncut (U) and cut (C) grass are separated into the three cloudiness categories described in section 3.8, and given in table 3.10: “overcast or considerable cloudiness”, “partly cloudy”, and “cloud-free”. Cloud-free conditions result in more influence by the surface properties on the air, as explained in section 2.4.1.

In figure 4.7, cloud-free, partly cloudy, and overcast or considerable cloudy hours are separated, and the  $(T_U - T_C)$  values at 2 m are plotted hourly in box and whisker plots. Figures 4.8 and 4.9 show the same as figure 4.7, but for 1.25 m and 0.55 m respectively.

It can be seen from the plots for all three heights that overcast or considerable cloudiness leads to smaller variations between the temperature measured at U and C. In the plots of  $(T_U - T_C)$  for all three heights in overcast or considerable cloudy conditions (figures 4.7c, 4.8c, and 4.9c), the maximum reach of the boxes, containing at least 50%

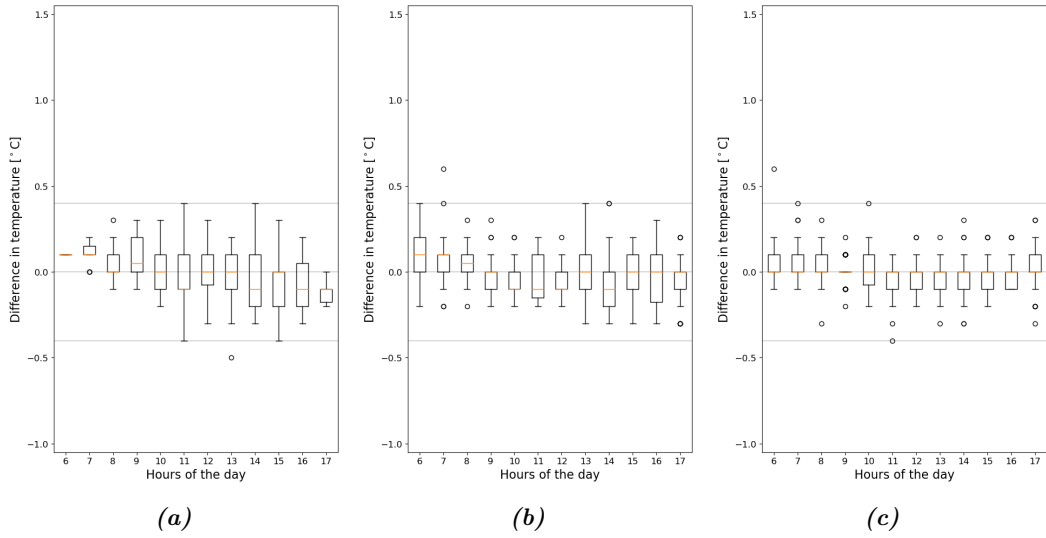


**Figure 4.7:** The diurnal difference in the temperature measured over uncut and cut grass at 2m is here plotted as box and whisker plots during day hours. The plot is separated into three solar radiation exposure categories: (a) cloud-free, (b) partly cloudy, and (c) overcast or considerable cloudiness. These categories were presented in section 3.8 and table 3.10. The data set used is from 23/5/2019 00:00 until 30/10/2019 12:00.

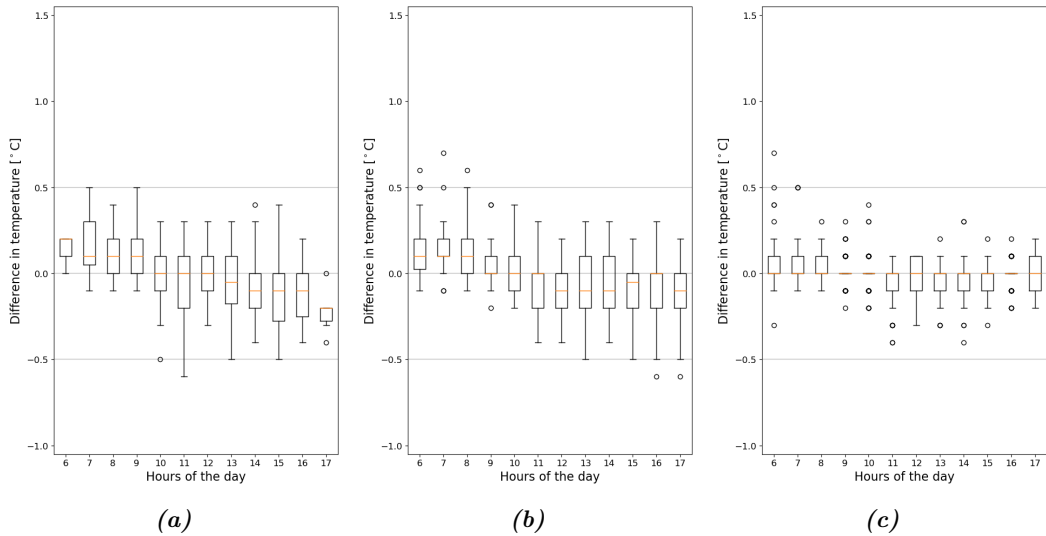


**Figure 4.8:** The diurnal difference in temperature measured over uncut and cut grass at 1.25 m is here plotted as box and whisker plots during day hours. The plot is separated into three solar radiation exposure categories: (a) cloud-free, (b) partly cloudy, and (c) overcast or considerable cloudiness. These categories were presented in section 3.8 and table 3.10. The data set used is from 23/5/2019 00:00 until 30/10/2019 12:00.

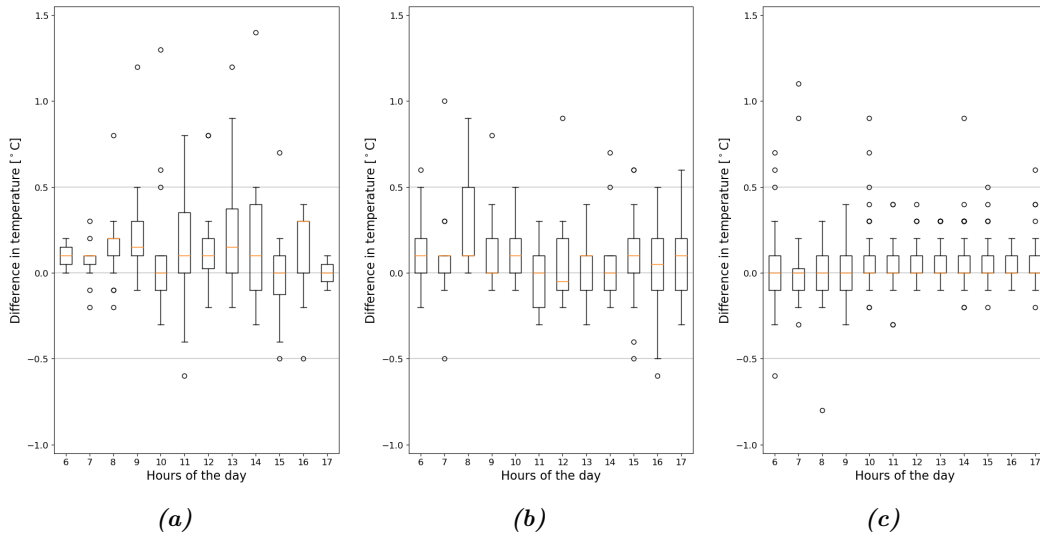


**Figure 4.9:** The diurnal difference in temperature measured over uncut and cut grass at 0.55 m is here plotted as box and whisker plots during day hours. The plot is separated into three solar radiation exposure categories: (a) cloud-free, (b) partly cloudy, and (c) overcast or considerable cloudiness. These categories were presented in section 3.8 and table 3.10. The data set used is from 23/5/2019 00:00 until 30/10/2019 12:00.

of the data, is  $\pm 0.1$  °C. In cloud-free conditions, the maximum reach of the boxes in the plot for 2 m (figure 4.7a) is  $\pm 0.2$  °C, for 1.25 m (figure 4.8a) it is  $\pm 0.3$  °C, and the interval is  $[-0.125$  °C,  $0.4$  °C] for 0.55 m (figure 4.9a).

In the plot of the difference in temperature at U and C at 2 m for overcast weather in figure 4.7c, the maximum reaches of the boxes and the whiskers are half of what they are in the plot for cloud-free weather in figure 4.7a. The maximum reach of the whiskers in the plot for  $(T_U - T_C)$  in cloud-free conditions at 1.25 m is  $[-0.6$  °C,  $0.5$  °C] in figure 4.8a and decreases to  $[-0.2$  °C,  $0.3$  °C] in the plot for overcast weather in figure 4.8c. In the same plots for 0.55 m is figures 4.9a and 4.9c, the reaches of the whiskers decrease from  $[-0.4$  °C,  $0.7$  °C] to  $[-0.3$  °C,  $0.4$  °C].

In appendix E, plots are given that are of the same temperature differences and are divided into the same categories as in figures 4.7, 4.8, and 4.9, but data from 2018 are used instead. The same patterns regarding how less cloud cover results in larger  $(T_U - T_C)$  values can be seen, but the general spread in the data was larger in 2018 than in 2019.

The number of observations in each radiation category and the percentage of total observations in the periods plotted for 2018 and 2019 are given in table 4.7. Due to a longer time period for data retrieval in 2019, a significantly higher number of observations could be considered: 2007 observations in 2019, while only 962 observations in 2018. 51% of the hours in 2018 had overcast or considerable cloudy conditions, while this number was 61% in 2019. The percentages for cloud-free weather (22% in 2018 and 16% in 2019) demonstrate the difference in weather in the two years, with it being more sunny in 2018 than in 2019. This difference was discussed in detail in section 3.4.

**Table 4.7:** This table presents the number of observations and percentage of total observations in 2018 and 2019 in the three solar radiation categories. The data are from BOKLIM at Søråsfeltet in Ås, Norway. The time period for the 2018 data is from 11.07 12:00 until 15.09 13:00. The time period for the 2019 data is from 23/05 00:00 until 10/10 23:00.

Category	2018		2019	
	Number of observations	Percent	Number of observations	Percent
<b>Cloud-free</b>	209	22%	330	16%
<b>Partly cloudy</b>	260	27%	457	22%
<b>Overcast or considerable cloudiness</b>	493	51%	1252	61%

### 4.3.3 Wind categories

In this section, the values of difference in temperature measured over uncut (U) and cut (C) grass are plotted hourly in box and whisker plots and are separated into the two wind speed categories given in table 3.11. This is plotted for data from 2 m, 1.25 m, and 0.55 m in figures 4.10, 4.11, and 4.12 respectively. It is important to note that in the plots for strong wind, the hours 00:00-06:00 only have three or less data points. This is because the wind speed is reduced during the night, as explained in section 2.4.2.

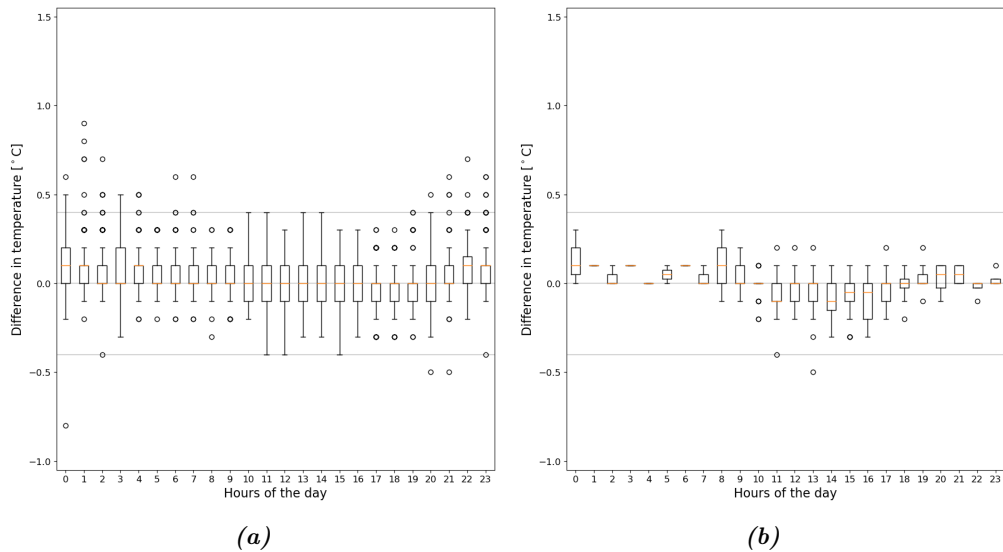


**Figure 4.10:** The difference in temperature measured over uncut and cut grass at 2 m is here plotted as hourly box and whisker plots. The plot is separated into two wind categories: (a) light wind ( $\leq 5$  m/s) and (b) strong wind ( $> 5$  m/s). The data set used is from 23/5/2019 00:00 until 30/10/2019 12:00.

Stronger wind results in more mixing, which results in less influence by the surface properties on the air. This was explained in section 2.4.2. It can be seen in figures 4.10, 4.11, and 4.12 that the amount of outliers are significantly lower in the plots of  $(T_U - T_C)$  in strong wind conditions, than in the plots of  $(T_U - T_C)$  in light wind conditions. Additionally, the reaches of the boxes and whiskers is lower for most of the hourly plots of  $(T_U - T_C)$  in strong wind conditions in comparison to light wind conditions. For  $(T_U - T_C)$  in light wind conditions at 2 m, the maximum negative and positive reaches of the whiskers are  $-0.4$  °C and  $0.5$  °C, while for strong wind conditions, these values are  $-0.3$  °C and  $0.3$  °C. Another example of this is that for  $(T_U - T_C)$  at 0.55 m at 11:00

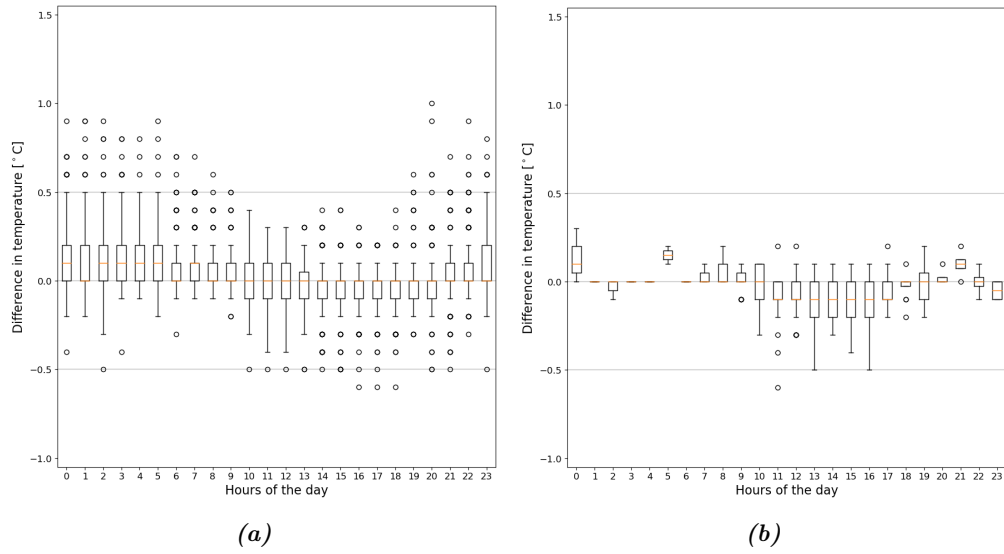


**Figure 4.11:** The difference in temperature measured over uncut and cut grass at 1.25 m is here plotted as hourly box and whisker plots. The plot is separated into two wind categories: (a) light wind ( $\leq 5$  m/s) and (b) strong wind ( $> 5$  m/s). The data set used is from 23/5/2019 00:00 until 30/10/2019 12:00.

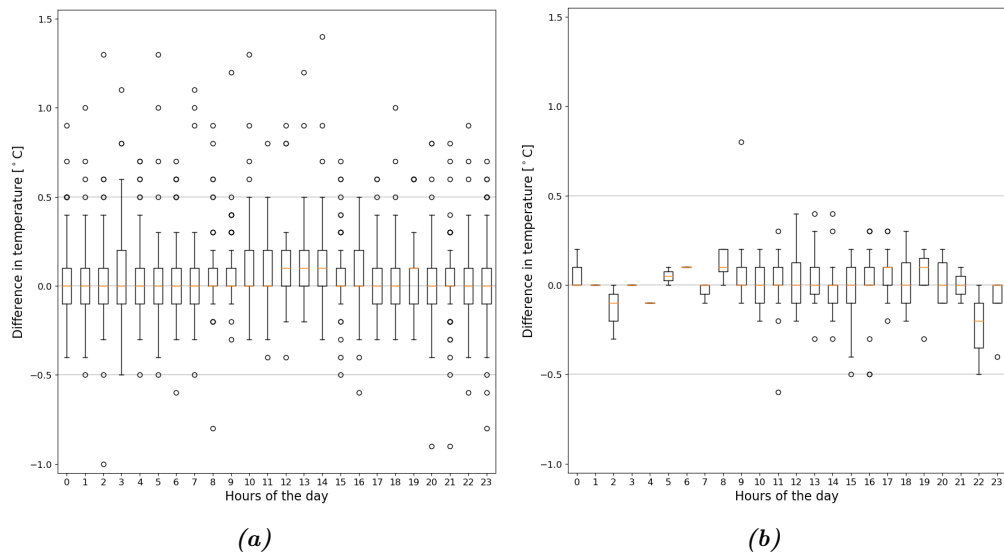


**Figure 4.12:** The difference in temperature measured over uncut and cut grass at 0.55 m is here plotted as hourly box and whisker plots. The plot is separated into two wind categories: (a) light wind ( $\leq 5$  m/s) and (b) strong wind ( $> 5$  m/s). The data set used is from 23/5/2019 00:00 until 30/10/2019 12:00.

in light wind conditions (figure 4.12a), the reach of the box and is  $[0.0^\circ\text{C}, 0.2^\circ\text{C}]$ . In strong wind conditions (figure 4.12b), this interval has decreased to  $[0.0^\circ\text{C}, 0.1^\circ\text{C}]$ .

The  $(T_U - T_C)$  values at 1.25 m at 11:00 in light wind conditions are between  $-0.5^\circ\text{C}$  and  $0.4^\circ\text{C}$  (figure 4.11a), while these values are between  $-0.3^\circ\text{C}$  and  $0.1^\circ\text{C}$  for strong wind conditions (figure 4.11b). The  $(T_U - T_C)$  values at 0.55 m are in the interval  $[-0.6^\circ\text{C}, 0.8^\circ\text{C}]$  for strong wind and in the interval  $[-1.0^\circ\text{C}, 1.4^\circ\text{C}]$  for light wind conditions.

Consequently, it can be claimed that the concept of influence of wind is clearly visible in all three figures. Hours with strong wind have lower variation in the difference in temperature between U and C.

#### 4.3.4 High influence conditions

The values of the difference between temperature measured over uncut (U) and cut (C) grass in hours with cloud-free conditions (diffuse to global radiation of 0.25 or lower) and light wind (wind speed values of 5 m/s or lower) are shown in figure 4.13. The  $(T_U - T_C)$  values measured at 2 m, 1.25 m, and 0.55 m are plotted. Situations with the combination of these characteristics are the times with the highest influence by the surface properties on the air. Despite this, no  $(T_U - T_C)$  value measured at 2 m was outside the  $\pm 0.4^\circ\text{C}$  interval (figure 4.13a), and no temperature difference value at 1.25 m was outside the  $\pm 0.5^\circ\text{C}$  interval (figure 4.13b). The spread in the  $(T_U - T_C)$  values was larger at 0.55 m in figure 4.13c, but this is to be expected considering those measuring instruments were at a height where significant influence by the surface was expected.

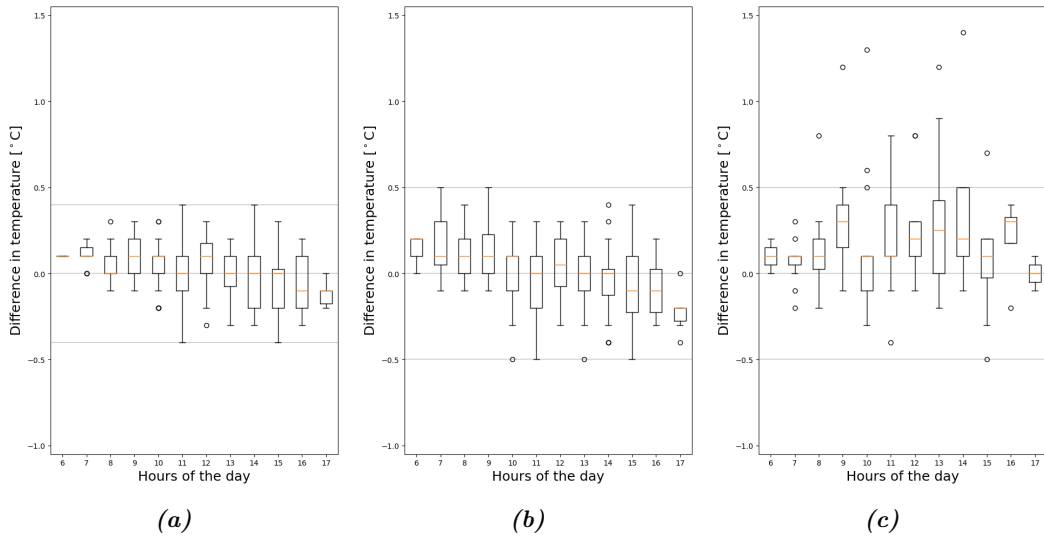


**Figure 4.13:** The figure shows box and whisker plots of the difference between temperature measured over uncut (U) and cut (C) grass at (a) 2 m, (b) 1.25 m, and (c) 0.55 m. The values are from times when the sky was considered cloud-free (see table 3.10) and light wind (5 m/s or lower), which means that the influence by the surface properties was high. The data set used is from 23/5/2019 00:00 until 30/10/2019 12:00.

## 4.4 Difference in daily values

Investigations into different daily temperature values were done because in many applications, daily mean temperature is utilized instead of hourly temperature values. This was discussed in section 2.8. Additionally, further insight into the data could be achieved by doing this.

As explained in section 3.1. three temperature values were logged every hour: actual, maximum, and minimum. The daily mean temperature was found by calculating the



average of the hourly temperature values. Daily maximum and minimum temperature values were the largest and smallest hourly maximum and minimum values of each day. In figure 4.14, the difference between these values from the location with uncut (U) and from the location with cut (C) grass are plotted as box and whisker plots. The figure shows that the boxes, containing at least 50% of the data, for all three plots include 0.0°C. It is important to note that this plot has a much smaller y-axis scale than the other box and whisker plots presented so far.

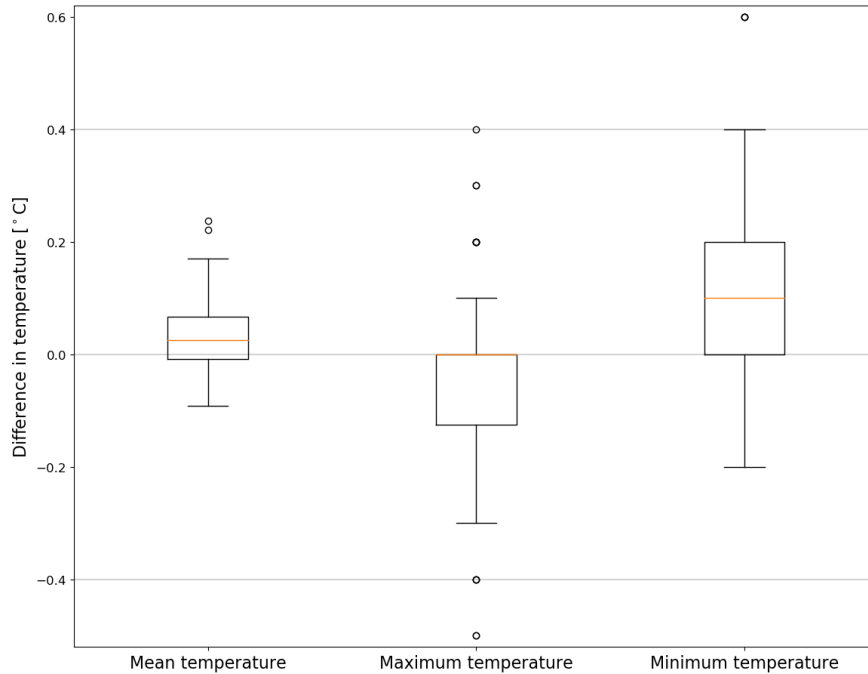


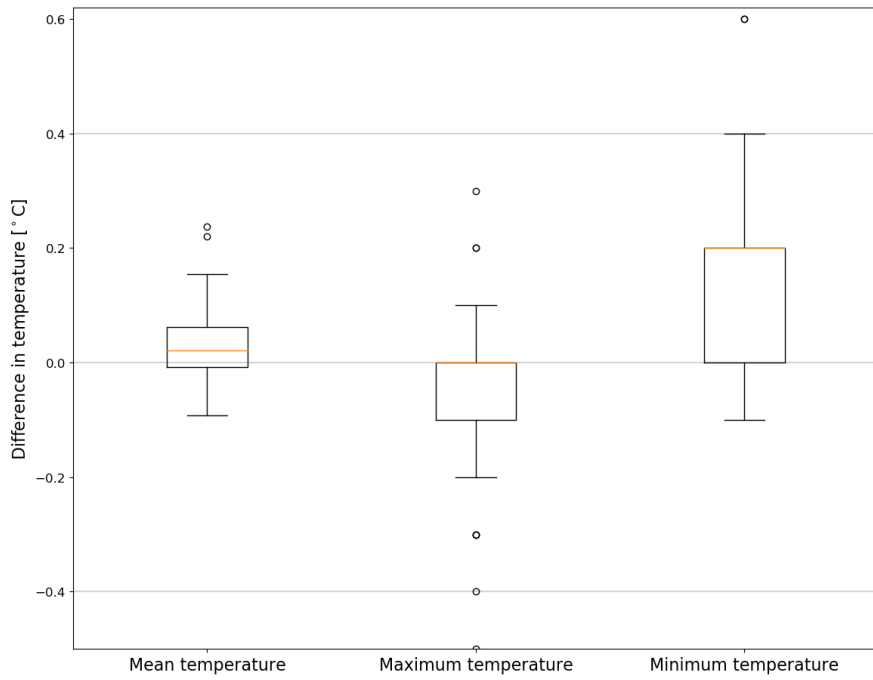
**Figure 4.14:** This plot shows three box and whisker plots of the difference in daily temperature at 2 m between the location where the grass was uncut (U) and where it was cut (C). The leftmost plot is of the difference in daily mean temperature, where the daily mean is the average value of all hourly mean values. The middle plot is of the difference in daily maximum temperature and the rightmost plot is of the difference in daily minimum temperature values. The data set used is from 23/5/2019 00:00 until 30/10/2019 12:00.

The most notable aspects of figure 4.14 are the shifts away from 0.0°C in the plots for difference in daily maximum and minimum temperature. The difference in daily maximum temperature has a downward shift with whiskers between -0.3°C and 0.1°C, while the difference in daily minimum temperature has an upward shift with whiskers between -0.2°C and 0.4°C. This means that the tendency is that daily maximum temperature at U was lower than at C, and that that daily minimum temperature at U was higher than at C.

The box and whisker plot for the difference in daily mean temperature has the smallest range out of the three plots. Except for the two outliers with values between 0.22°C and 0.24°C, all values of this difference are in the [-0.1°C, 0.2°C] interval.

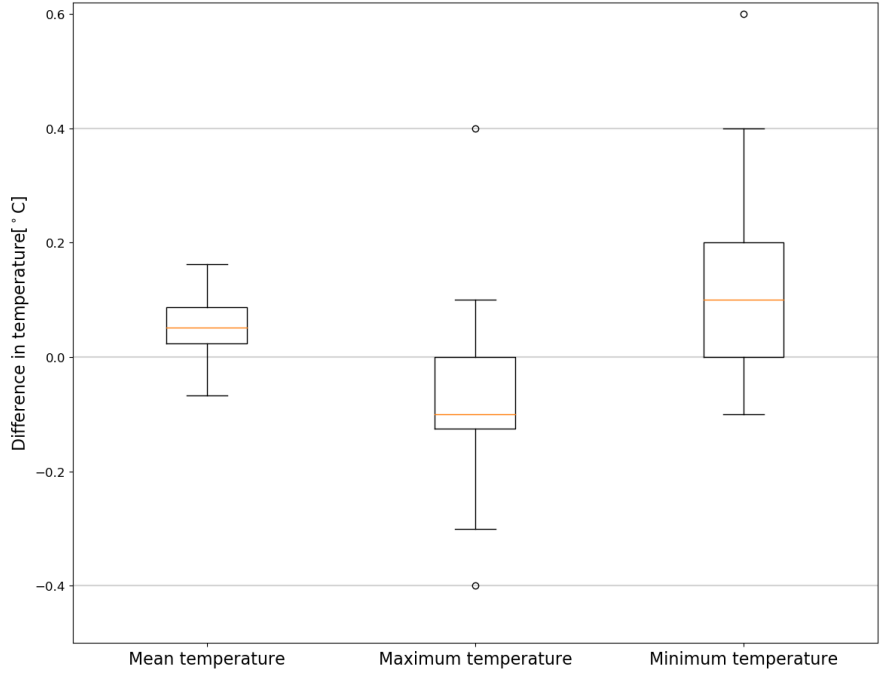
Figure 4.15 shows the same as figure 4.14, but only data from August, September, and October were used. The grass height of the uncut area was well above the WMO CIMO siting classification limit of 25 cm during that whole time period. The differences between the three box and whisker plots of the difference in temperature values in 4.14 and 4.15 are minimal, with the biggest difference being the median value for difference in daily minimum temperature shifting from 0.1°C in figure 4.14 to 0.2°C in figure 4.15.

Figure 4.16 shows the same as figures 4.14 and 4.15, but only data from May and June were used. These were the two months with the lowest grass height and density.



**Figure 4.15:** This plot shows three box and whisker plots of the difference in daily temperature at 2m between the location where the grass was uncut (*U*) and where it was cut (*C*). The leftmost plot is of the difference in daily mean temperature, where the daily mean is the average value of all hourly mean values. The middle plot is of the difference in daily maximum temperature and the rightmost plot is of the difference in daily minimum temperature values. The data set used is from 1/8/2019 00:00 until 30/10/2019 12:00.

It is assumed, as explained in section 3.1, that the grass height reached its maximum height of around 40-50 cm before the end of June. The grass density was, however, lower in May and June than in the fall months plotted in figure 4.15. Nonetheless, the plots are similar despite the median value for difference in daily maximum temperature shifting from -0.1 °C in figure 4.16 to 0.0 °C in figure 4.15.



**Figure 4.16:** This plot shows three box and whisker plots of the difference in daily temperature at 2m between the location where the grass was uncut ( $U$ ) and where it was cut ( $C$ ). The leftmost plot is of the difference in daily mean temperature, where the daily mean is the average value of all hourly mean values. The middle plot is of the difference in daily maximum temperature and the rightmost plot is of the difference in daily minimum temperature values. The data set used is from 23/5/2019 00:00 until 30/6/2019 12:00.

## 4.5 Day and night

The difference between day and night values of the difference in temperature measured at the locations with uncut ( $U$ ) and cut ( $C$ ) grass is evaluated in this section. The data set was split into two categories: day hours (06:00-17:00) and night hours (18:00-05:00). Using data from 2m, the frequency of each  $(T_U - T_C)$  value in the two categories was found. These values, in addition to the percentage of these frequencies, are given in table 4.8. The frequency percentages for both day and night hours are plotted in figure 4.17.

One can see from figure 4.17 that a higher percentage of day than night hours had negative  $(T_U - T_C)$  values, which means that the temperature at  $C$  was higher than at  $U$ . A higher percentage of night than day values have positive  $(T_U - T_C)$  values, which means that the temperature was higher at  $U$  than at  $C$ . For example, 18.3% of day values and 13.5% of night values of  $(T_U - T_C)$  are  $-0.1$  °C. 22.3% of day values and 23.7% of night values are  $0.1$  °C. Despite this pattern, the frequency of day values equal to  $0.1$  °C is higher than the frequency of day values equal to  $-0.1$  °C. This can be seen in table 4.8, where it is shown that  $(T_U - T_C)$  was equal to  $-0.1$  °C 351 times during day hours and equal to  $0.1$  °C 425 times during day hours.

The plot in figure 4.18 is the same as figure 4.17, except that only data from 15/7/2019 until 30/10/2019 were used. The same patterns as were pointed out for figure 4.17 can be seen in this plot, except that in figure 4.18, day hours have consistently higher percentages of negative  $(T_U - T_C)$  values for the same absolute values.

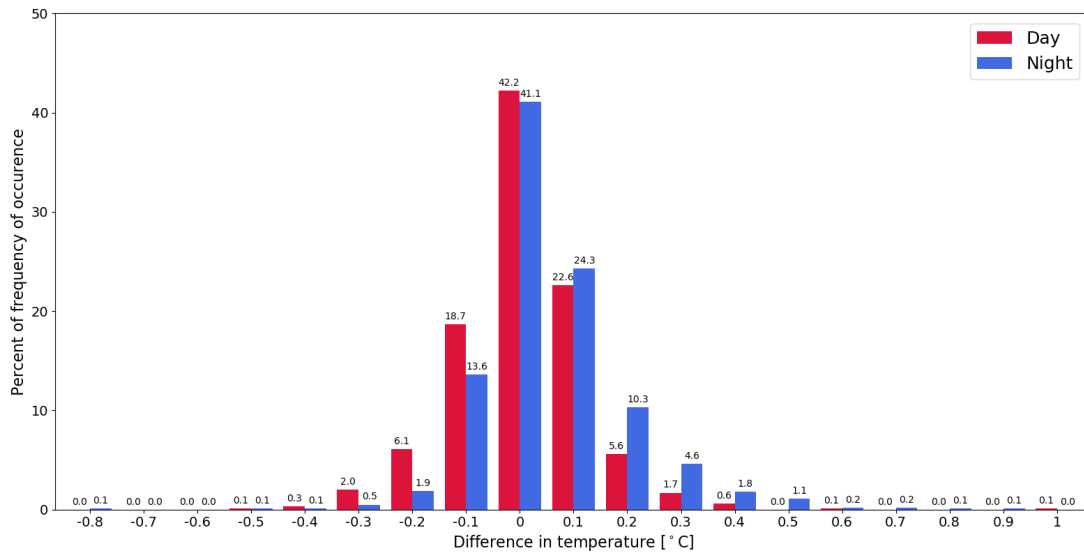


**Figure 4.17:** The data in this plot are categorized into two groups: day hours (06:00-17:00) and night hours (18:00-05:00), and the plot shows the percentage of frequency of the difference in temperature at 2m between the measuring instruments over uncut (U) and cut (C) grass in each category. The data set used is from 23/5/2019 00:00 until 30/10/2019 12:00.

**Table 4.8:** The table presents frequency of difference in average temperature over uncut and cut grass in the summer of 2019. The two categories are day (06:00-17:00) and night (18:00-05:00).

Delta T		-0.8	-0.7	-0.6	-0.5	-0.4	-0.3	-0.2	-0.1	0.0
Number of observations	Day	0	0	0	1	5	38	114	351	795
	Night	1	0	0	2	2	10	35	256	774

Delta T		0.1	0.2	0.3	0.4	0.5	0.6	0.7	0.8	0.9	1.0
Number of observations	Day	425	106	32	12	0	2	0	0	0	1
	Night	458	193	87	34	20	4	4	1	1	0

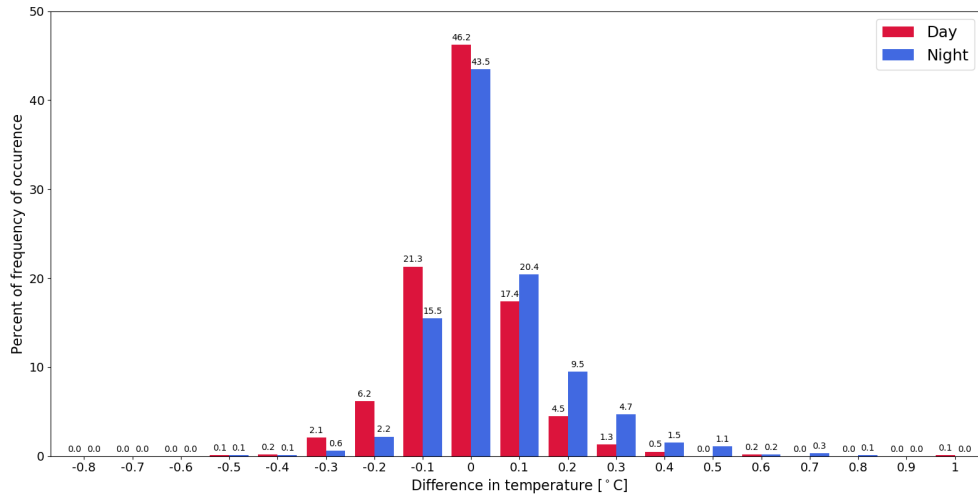


**Figure 4.18:** The data in this plot are categorized into two groups: day hours (06:00-17:00) and night hours (18:00-05:00), and the plot shows the percentage of frequency of the difference in temperature at 2m between the measuring instruments over uncut (U) and cut (C) grass in each category. The data set used is from 15/7/2019 00:00 until 30/10/2019 12:00.

## 4.6 Individual events

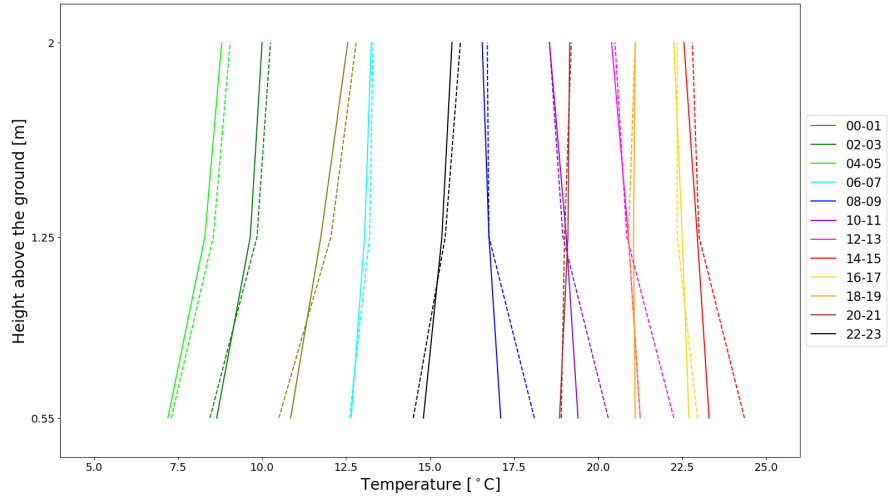
So far, results regarding long time periods have been presented. Looking at individual days and single events provides further insight into the influence of the increased grass height. This section will present data from individual days to gain further insight into the data and the influence of the increased vegetation height on temperature measurements.

### 4.6.1 Vertical temperature profiles

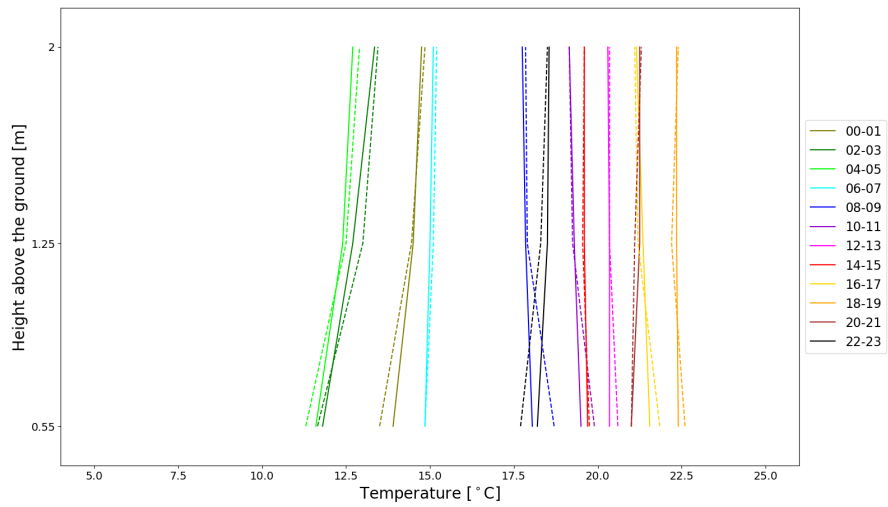
Height profiles of the bihourly temperature values were created where the temperature values from the locations with uncut (U) and cut (C) grass were plotted together. The bihourly values are the mean of the temperature measurements from two hours. The temperature measurements for each hour are the mean value of the last minute. Days in the two extremes in the solar radiation exposure categories (cloud-free and overcast: see table 3.10), were found as described in section 3.9. Additionally, the cloud-free days chosen in each month had as light wind as possible throughout the day. In each of the months in the experiment in 2019, except for May and July, the vertical temperature profile of one day in each category was plotted. As explained in section 3.1, it can be assumed that the grass had reached maximum height by the end of June, and therefore surpassed the WMO siting classification limit of 25 cm.

Figure 4.19 shows the bihourly vertical temperature profiles for temperature measured at U and C on 28/6 (cloud-free day) and 30/6 (overcast day). As expected, the difference between temperatures measured at U and C were smaller on 30/6 than on 28/6. The same result is found in the daily temperature variation. On 28/6 in figure 4.19a, it can be seen that especially in the hours from 08:00 to 15:00, the difference between the temperatures measured at 0.55 m and 1.25 m are visibly larger at U than at C. At 11:00, the difference between  $T_{0.5m}$  and  $T_{1m}$  was at U 1.0°C, while the difference between  $T_{0.5m}$  and  $T_{1m}$  at C was 0.3°C. Furthermore, it can be seen that maximum and minimum temperature values at 2 m at U were larger than at C. Other than that the daily temperature range on 30/6 was smaller, it can also be seen in figure 4.19b that the vertical difference in temperature also was smaller on this day. At 11:00 on 30/6,  $(T_{0.5m} - T_{1m})$  at U was equal to 0.5°C, while  $(T_{0.5m} - T_{1m})$  at C was 0.2°C.

Because of the lost data at C at 0.55 m (see section 3.3), the days to choose from in



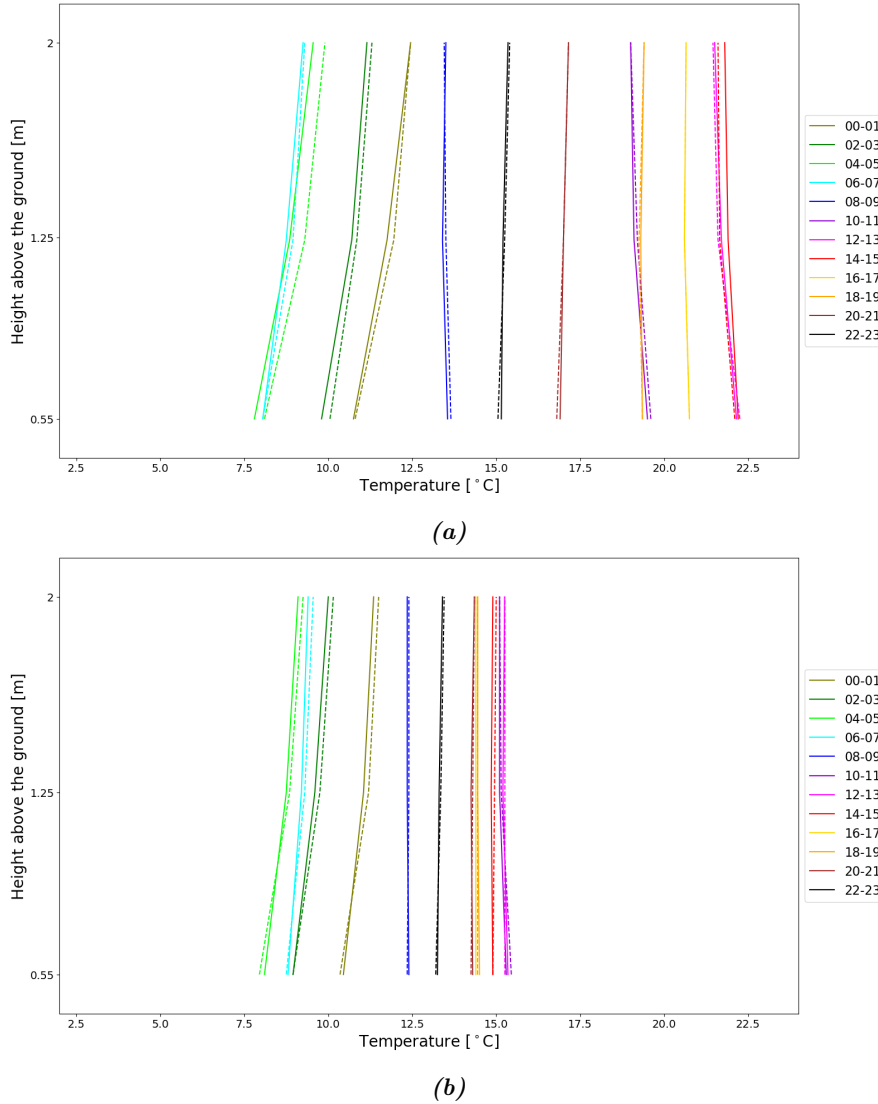
(a)



(b)

**Figure 4.19:** The plots show bihourly vertical temperature profiles over uncut (dashed lines) and cut (solid lines) grass in June 2019. In (a), a plot using data from 28/6, which was a cloud-free day is shown. In (b), a plot using data from 30/6, which was an overcast day, is shown.

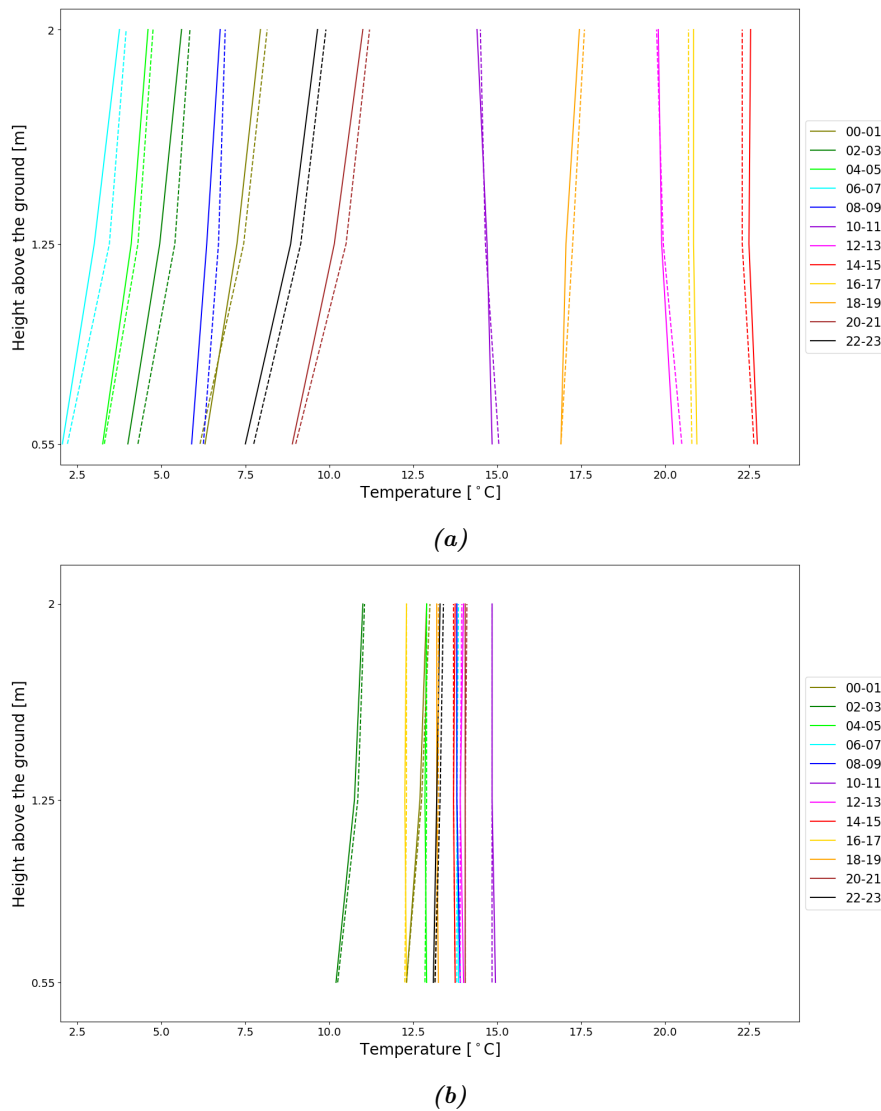
the overcast and cloud-free categories in August were limited. Figure 4.20a is a bihourly vertical temperature profile plot with data from 25/8, a cloud-free and partly cloudy day with light wind. Figure 4.20b displays how the temperature on 22/8, an overcast day with light wind, developed throughout the day. The temperature interval at C at 2 m on 22/8 was [8.0 °C, 15.9 °C], while on 24/8 it was [8.6 °C, 22.3 °C]. This makes the range 5.8 °C smaller on 22/8.



**Figure 4.20:** The plots show bihourly vertical temperature profiles over uncut (dashed lines) and cut (solid lines) grass in August 2019. In (a), a plot using data from 24/8, which was a cloud-free day is shown. In (b), a plot using data from 22/8, which was an overcast day, is shown.

The development of the vertical temperature profile over uncut and cut grass two days in September is plotted in figure 4.21. These plots demonstrate the difference between high and low solar radiation influence. Figure 4.21a is a plot using data from 21/9, which was a day with light wind (<5 m/s) and clear skies. One can see how the temperature measured at U had a smaller temperature range than the temperature measured at C, and that the maximum temperature therefore was lower and the minimum was higher at U. The maximum temperature value at 2 m at C was 22.8 °C, while the maximum value at U was 22.5 °C. Minimum temperature value at 2 m at C was 3.5 °C, while the minimum value at U was 3.7 °C. The largest difference between U and C at 2 m was 0.4 °C and the largest difference at 1.25 m was 0.5 °C. Figure 4.21b shows the temperature values on 11/9, which was a day with overcast conditions. The diurnal temperature variation

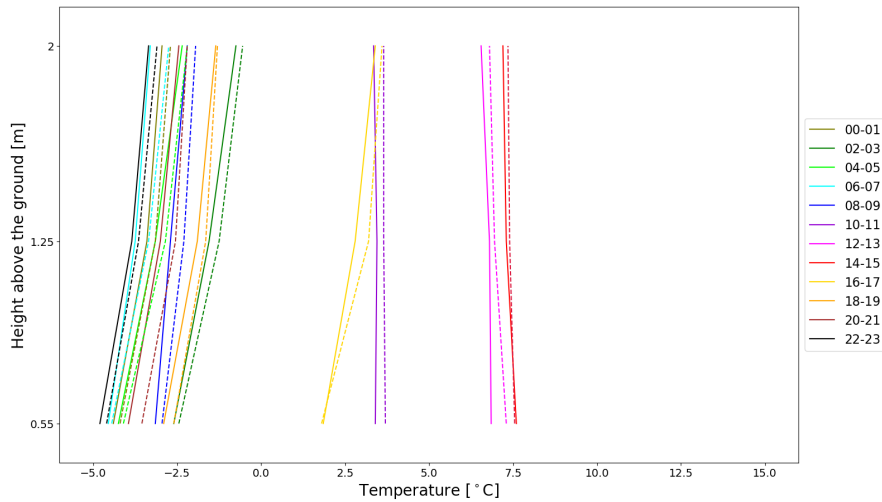
on 11/9 was small and so was the difference between temperature measured at U and C. The mean value of  $(T_U - T_C)$  at 2 m on this day was  $0.025\text{ }^\circ\text{C}=0.0\text{ }^\circ\text{C}$ , with no value outside of the  $\pm 0.1\text{ }^\circ\text{C}$  interval.



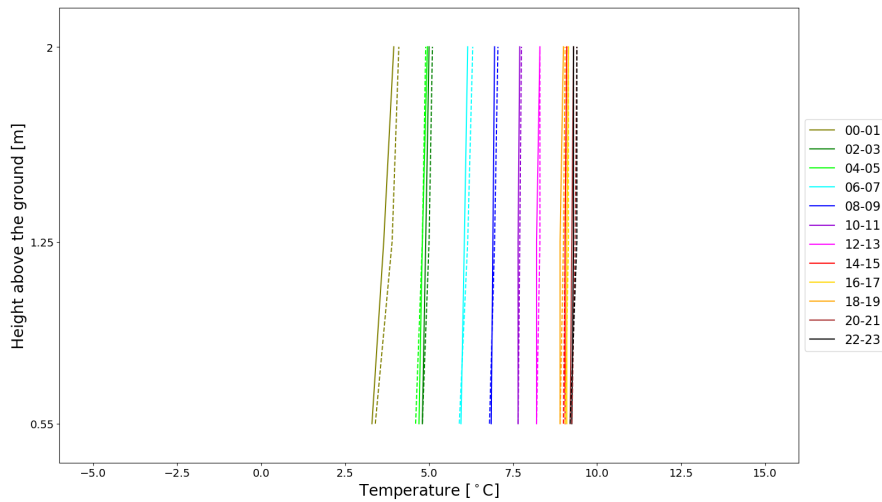
**Figure 4.21:** The plots show bihourly vertical temperature profiles over uncut (dashed lines) and cut (solid lines) grass in September 2019. In (a), a plot using data from 21/9, which was a cloud-free day is shown. In (b), a plot using data from 11/9, which was an overcast day, is shown.

Figure 4.22 shows bihourly vertical temperature profile plots over uncut and cut grass for 29/10 and 22/10, a cloud-free and an overcast day, respectively. Unlike in the plots for August and September, figures 4.20 and 4.21, the maximum temperature measured at U was not lower than the maximum temperature measured at C on these two days in October.





(a) Plot using data from 29/10, which was a cloud-free day.



(b) Plot using data from 22/10, which was an overcast day.

**Figure 4.22:** The plots show bihourly vertical temperature profiles over uncut (dashed lines) and cut (solid lines) grass in October 2019. In (a), a plot using data from 29/10, which was a cloud-free day is shown. In (b), a plot using data from 22/10, which was an overcast day, is shown.

## 4.6.2 Temperature values on individual days

Table 4.9 shows the temperature values at 2 m at the locations with uncut (U) and cut (C) grass at 14:00 on the days plotted in figures 4.19, 4.20, 4.21, and 4.22, as well as one day in May and two days in July. The table is divided into two sections: days with cloud-free and light wind conditions are highly influenced by surface properties and days with overcast conditions are not as influenced by surface properties. The largest difference between temperature measured at U and C at 14:00 was 0.4 °C on 28/6. All other ( $T_U - T_C$ ) values at 2 m had absolute values smaller than that. Days with overcast conditions all had ( $T_U - T_C$ ) values at 2 m in the  $\pm 0.1$  °C interval.

**Table 4.9:** Temperatures measured over uncut (U) and cut (C) grass at 14:00 on different days in the summer of 2019. Days with cloud-free conditions are more influenced by surface properties than days with overcast skies.

		$T_{U,2m}$ [°C]	$T_{C,2m}$ [°C]	$(T_U - T_C)_{22m}$ [°C]
Days with light wind and cloud-free skies	28/6	22.9	22.5	0.4
	27/7	27.4	27.3	0.1
	24/8	22.0	22.3	-0.3
	21/9	22.1	22.3	-0.2
	29/10	7.5	7.3	0.2
Days overcast skies	30/5	10.1	10.0	0.1
	30/6	19.5	19.6	-0.1
	22/7	19.1	19.2	-0.1
	22/8	15.1	15.0	0.1
	11/9	14.0	14.0	0.0
	22/10	8.9	8.9	0.0

Table 4.10 displays the values of hourly difference in temperature between U and C on 21/9 (cloud-free day) and 11/9 (overcast day) in 2019. These values are given for all three heights of the measuring instruments in the experiment. The bihourly temperature profiles from these days are plotted in figure 4.21. In table 4.10, it can be seen that there were smaller differences between temperature measured at U and C on 11/9 at all heights than on 21/9. Except for the difference in temperature between U and C at 2 m at 23:00, all ( $T_U - T_C$ ) values were in the  $\pm 0.1$  °C interval. The peak difference in temperature on 21/9 at 2 m was 0.4 °C, while it was 0.5 °C at 1.25 m and 0.55 m.

**Table 4.10:** Hourly difference in temperature measured over uncut ( $U$ ) and cut ( $C$ ) grass on 21/9 (cloud-free) and 11/9 (overcast) in 2019 at the three heights 0.55 m, 1.25 m, and 2 m. For all values, the unit is  $^{\circ}C$ .

Hour	21/9			11/9		
	$\Delta T_{0.55m}$	$\Delta T_{1.25m}$	$\Delta T_{2m}$	$\Delta T_{0.55m}$	$\Delta T_{1.25m}$	$\Delta T_{2m}$
00	-0.1	0.1	0.2	0.1	0.0	0.1
01	-0.2	0.3	0.2	-0.1	0.1	0.1
02	0.2	0.4	0.2	0.0	0.1	0.1
03	0.4	0.5	0.3	0.1	0.1	0.0
04	0.3	0.4	0.2	-0.1	0.1	0.0
05	-0.2	0.0	0.1	0.0	0.0	0.0
06	0.1	0.4	0.2	-0.1	0.0	0.1
07	0.2	0.5	0.2	0.0	0.0	0.0
08	0.2	0.2	0.1	0.0	0.0	0.0
09	0.5	0.5	0.2	0.0	0.0	0.0
10	0.0	-0.3	0.1	-0.1	0.0	0.0
11	0.4	0.2	0.1	-0.1	0.0	0.0
12	0.3	0.2	0.1	-0.1	0.0	-0.1
13	0.2	-0.1	-0.2	-0.1	0.0	0.0
14	0.1	-0.1	-0.2	0.0	0.0	0.0
15	-0.3	-0.3	-0.3	0.0	0.0	-0.1
16	-0.2	-0.2	-0.2	-0.1	0.1	0.0
17	-0.1	-0.1	-0.1	0.0	0.0	0.0
18	-0.3	0.0	-0.1	-0.1	0.0	0.0
19	0.3	0.4	0.4	-0.1	0.1	0.1
20	0.2	0.3	0.2	0.0	0.0	0.0
21	0.0	0.4	0.2	0.0	0.0	0.1
22	0.3	0.4	0.4	0.0	0.1	0.0
23	0.2	0.2	0.1	0.1	0.1	0.2

## 4.7 Humidity

This section presents results from analysis of humidity data from the experiment. Humidity data will be evaluated by looking at the difference between humidity values logged at the locations with uncut (U) and cut (C) grass and by more closely examining the vertical profiles. Both relative humidity ( $RH$ ), which is what the measuring instruments in the experiment logged, and absolute humidity ( $\rho$ ), which was calculated by using equation 2.5, will be analyzed.

The data will be evaluated for three time periods, listed in table 4.11. The 1<sup>st</sup> time period is from the start of the experiment and ends when the humidity instrument at 2 m at C started logging values classified as poor quality data. The 2<sup>nd</sup> time period starts when the humidity instrument at 1.25 m at C had been replaced and ends when the instrument at 2 m at C started logging poor quality data again. The 3<sup>rd</sup> time period is the entire duration of the experiment in 2019, where the data sets for each height has been maximized in size. This means that the process for determining the sizes of these data sets was the same as it was for the temperature data sets. What data were excluded and why was presented in section 3.3 and summed up in figure 3.9. In the 1<sup>st</sup> and 3<sup>rd</sup> periods, the data sets for the three heights vary in size and time periods covered. If humidity data were missing from a given height at one of the measuring instruments, the data from that time period wouldn't be looked at for that given height.

**Table 4.11:** *The table displays the three time periods in which humidity data are evaluated in this thesis.*

1.	From 23/5/2019 until 15/7/2019
2.	From 21/8/2019 14:00 until 22/9/2019
3.	The experiment's duration. The data sets are maximized in length

### 4.7.1 Difference in humidity values

This section presents the differences in humidity measured at the locations with uncut (U) and cut (C) grass at the three heights: 2 m, 1.25 m, and 0.55 m. Both the difference between the measured relative humidity values, and between the calculated absolute humidity values, are shown. The humidity differences are plotted as box and whisker plots for the three time periods presented in table 4.11. Data from period 1 are used in figure 4.23, data from period 2 are used in figure 4.24, and data from period 3 are used in figure 4.25.

The median difference of ( $RH_U - RH_C$ ) in the 1<sup>st</sup> period is 0 percentage points (p.p.) at all three heights. At least 50% of the ( $RH_U - RH_C$ ) values (represented by the boxes) are in the  $[-1 \text{ p.p.}, 0 \text{ p.p.}]$  interval for measurements from 2 m and 1.25 m, and 99.2% of these values from 2 m are inside the  $\pm 4 \text{ p.p.}$  interval. The interval of the box in the plot for 0.55 m is  $[-1 \text{ p.p.}, 1 \text{ p.p.}]$  and the whiskers reach out to  $\pm 4 \text{ p.p.}$ . The largest negative and positive ( $RH_U - RH_C$ ) values were  $-5 \text{ p.p.}$  and  $6 \text{ p.p.}$  for 2 m,  $-7 \text{ p.p.}$  and  $7 \text{ p.p.}$  for 1.25 m, and  $-7 \text{ p.p.}$  and  $16 \text{ p.p.}$  for 0.55 m.

In the 1<sup>st</sup> period, at least 50% of the ( $\rho_U - \rho_C$ ) values (represented by the box) at 2 m are contained within the interval  $[-0.07 \text{ g/m}^3, 0.08 \text{ g/m}^3]$  and the median value was  $0.00 \text{ g/m}^3$ . At 1.25 m and 0.55 m, at least 50% of the values are contained within the ranges  $[-0.12 \text{ g/m}^3, 0.04 \text{ g/m}^3]$  and  $[-0.05 \text{ g/m}^3, 0.13 \text{ g/m}^3]$  respectively. This means that a difference of  $0.00 \text{ g/m}^3$  between absolute humidity at U and C was common for all three heights.

The median of the differences between relative humidity at U and C at 2 m measured in the 2<sup>nd</sup> period is 1 p.p. It can be seen in figure 4.24a that the box stretches from 0 p.p. to 2 p.p., and the whiskers are from  $-3 \text{ p.p.}$  to  $4 \text{ p.p.}$ . This means that the extent of the

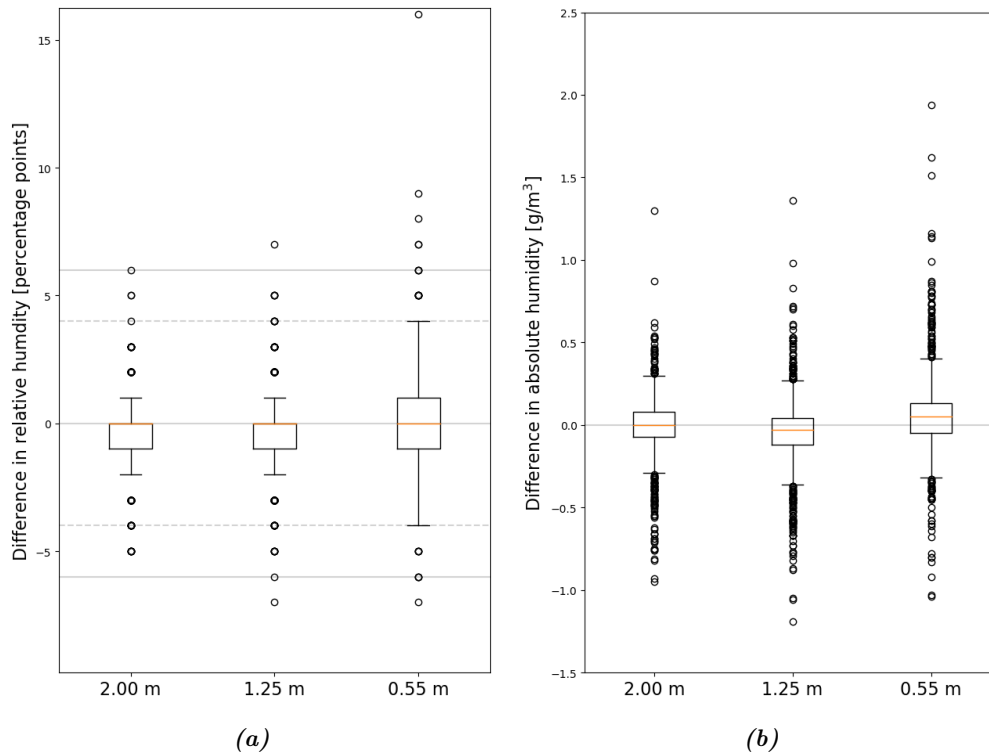


**Figure 4.23:** These plots show box and whisker plots of the difference in humidity measured over uncut grass (U) and cut grass (C) at three heights above the ground: 2 m, 1.25 m, and 0.55 m. (a) displays the difference between relative humidity, while (b) displays the difference between absolute humidity. The time period used for the data set is from 23/5/2019 00:00 until 15/7/2019 23:00.

ranges of the box and whiskers in the plot for  $(RH_U - RH_C)$  values at 2 m are larger and shifted upwards compared to the 1<sup>st</sup> period (figure 4.23a). 65.0% of the  $(RH_U - RH_C)$  values at 2 m are in fact larger than 0 p.p., meaning that the majority of the relative humidity values at this height were larger at U than at C in this time period.

The ranges of the box and whiskers of the  $(RH_U - RH_C)$  values at 1.25 m are the same in the 1<sup>st</sup> and 2<sup>nd</sup> period, but the interval has a negative shift in period 2 (figure 4.24a) compared to period 1 (figure 4.23a). In the 2<sup>nd</sup> period at 1.25 m, the median is -2 p.p. and the box interval is [-2 p.p., -1 p.p.]. Moreover, 84.4% of  $(RH_U - RH_C)$  values are below 0 p.p.

The interval of  $(RH_U - RH_C)$  values at 0.55 m was reduced from [-7 p.p., 16 p.p.] to [-5 p.p., 4 p.p.] from the 1<sup>st</sup> to the 2<sup>nd</sup> period. The median value is 0 p.p. in both time periods, but the box interval change from  $\pm 1$  p.p. to [-1 p.p., 0 p.p.].

The box in the plot of  $(\rho_U - \rho_C)$  at 2 m in the 2<sup>nd</sup> period lays above  $0.00 \text{ g/m}^3$ , while it lays below  $0.00 \text{ g/m}^3$  for these values at 1.25 m. The values therefore have the same shifts away from zero at these two heights as the  $(RH_U - RH_C)$  values did.

The  $(\rho_U - \rho_C)$  values at 0.55 m are centered around  $0.00 \text{ g/m}^3$  in the 2<sup>nd</sup> period, as was the case for the differences in relative humidity. It can be seen in figure 4.24b that the interval of the box is  $[-0.10 \text{ g/m}^3, 0.04 \text{ g/m}^3]$ , and therefore contains  $0.00 \text{ g/m}^3$ , just like it did for time period 1.

In table 4.12, the percentages of the values of the difference between relative humidity at U and C ( $RH_U - RH_C$ ) larger than and smaller than 0 p.p. are shown for the instruments at 2 m and 1.25 m. The limits for the 1<sup>st</sup> and 2<sup>nd</sup> time periods were given in table 4.11. The most notable takeaways from table 4.12 are the following changes in percentage values from the 1<sup>st</sup> to the 2<sup>nd</sup> period: the increase of values larger than zero of  $(RH_U - RH_C)$  at 2 m from 22.8% to 65.0%, and the increase of values smaller than

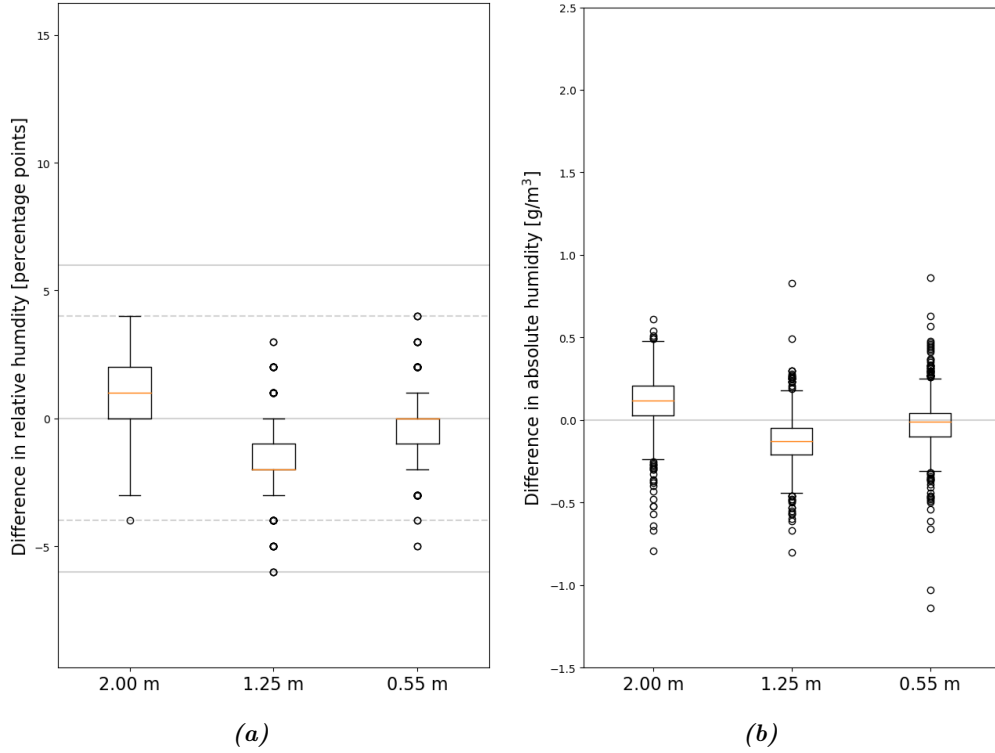


**Figure 4.24:** These plots show box and whisker plots of the difference in humidity measured over uncut grass ( $U$ ) and cut grass ( $C$ ) at three heights above the ground: 2 m, 1.25 m, and 0.55 m. (a) displays the difference between relative humidity, while (b) displays the difference between absolute humidity. The time period used for the data set is from 21/8/2019 14:00 until 22/9/2019 23:00.

zero of  $(RH_U - RH_C)$  at 1.25 m from 43.3% to 84.4%.

**Table 4.12:** The table shows the percentages of values of the difference between relative humidity measured over uncut ( $U$ ) and cut ( $C$ ) grass in the thesis' experiment larger and smaller than 0 p.p. The percentages are given for these values measured by instruments in two heights: 2 m and 1.25 m. The two time periods are 1) from 23/5/2019 until 15/7/2019 and 2) from 21/8/2019 14:00 until 22/9/2019, as given in table 4.11.

		Time period 1	Time period 2
$(RH_U - RH_C)$ at 2 m	Larger than 0	22.8%	65.0%
	Smaller than 0	31.9%	13.9%
$(RH_U - RH_C)$ at 1.25 m	Larger than 0	16.5%	15.6%
	Smaller than 0	43.3%	84.4%

The median of the differences between relative humidity at  $U$  and  $C$  at 2 m and 0.55 m in the 3<sup>rd</sup> period is 0 p.p., while it is  $-1$  p.p. for 1.25 m. As can be seen in figure 4.25b, the interval of the box for the  $(RH_U - RH_C)$  values at 2 m is [0 p.p., 1 p.p. ] and 99.5% of the values are in the  $\pm 4$  p.p. interval. The interval of the box for  $(RH_U - RH_C)$  at 1.25 m is  $[-2$  p.p., 0 p.p. ]. At least 50% of the  $(RH_U - RH_C)$  values are equal to 0 p.p. for 0.55 m.

In the 3<sup>rd</sup> period, the boxes of the difference between absolute humidity at  $U$  and  $C$  at all three heights contain the value  $0.00 \text{ g/m}^3$ . As can be seen in figure 4.25b, the interval of the box for  $(\rho_U - \rho_C)$  at 2 m is  $[-0.04 \text{ g/m}^3, 0.14 \text{ g/m}^3]$ , at 1.25 m it is  $[-0.15 \text{ g/m}^3,$

0.00 g/m<sup>3</sup>], and at 0.55 m it is [−0.06 g/m<sup>3</sup>, 0.07 g/m<sup>3</sup>].

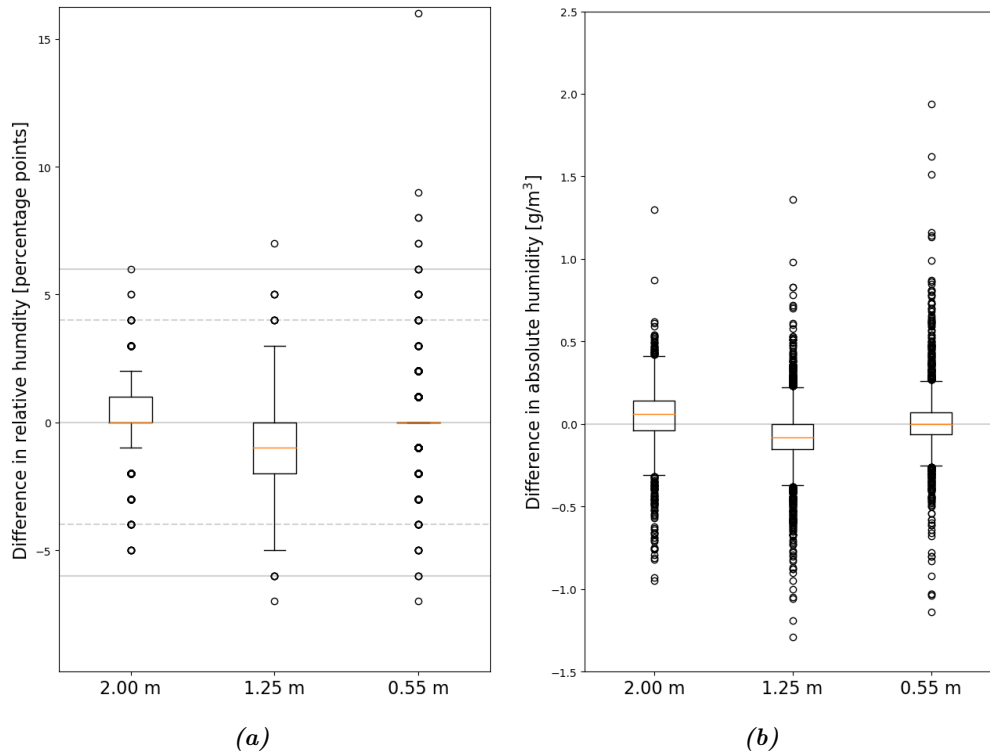


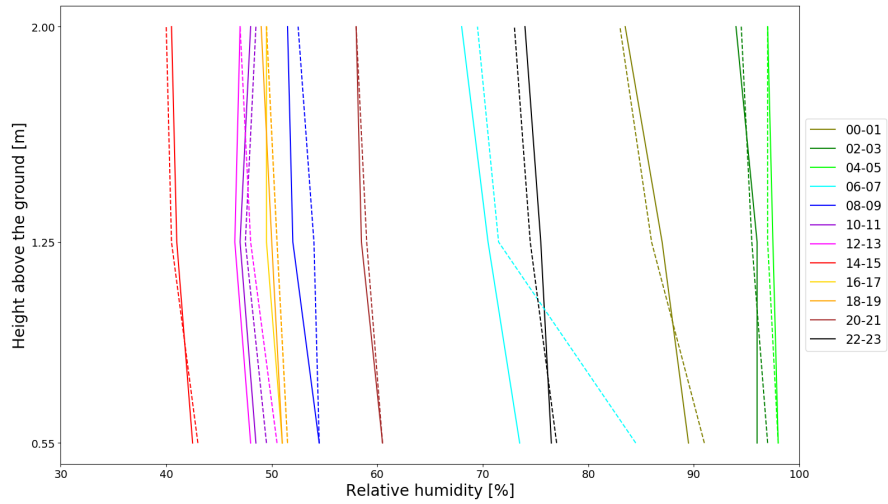
**Figure 4.25:** These plots show box and whisker plots of the difference in humidity measured over uncut grass ( $U$ ) and cut grass ( $C$ ) at three heights above the ground: 2 m, 1.25 m, and 0.55 m. (a) displays the difference between relative humidity, while (b) displays the difference between absolute humidity. The time period used for the data set is from 23/5/2019 00:00 until 30/10/2019 12:00.

Box and whisker plots of the diurnal difference between humidity measured over uncut and cut grass can be found in appendix F. These plots further demonstrate the variations in the  $(RH_U - RH_C)$  and  $(\rho_U - \rho_C)$  values presented in this section.

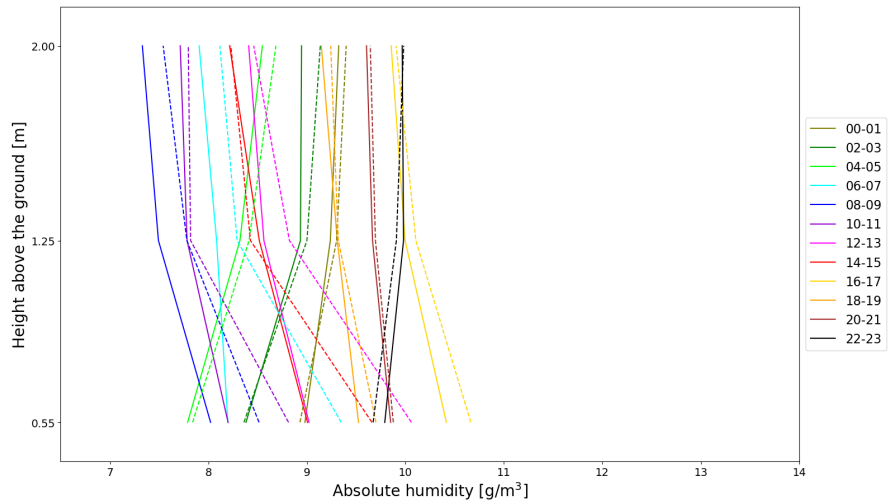
#### 4.7.2 Vertical profiles

In this section, vertical profiles of bihourly humidity values are presented. The bihourly value is the mean of the humidity measurements from two hours. The humidity measurements for each hour are the mean value of the last minute. Profiles for relative ( $RH$ ) and absolute ( $\rho$ ) humidity are plotted using data from 28/6 (figure 4.26) and 30/6 (figure 4.27).

28/6/2019 was a day with light wind (average wind speed was 2.17 m/s) and where the wind changed direction continuously all day. It was also a day with clear skies, where the average ratio of diffuse to global radiation was 0.28. The  $RH$  values at 2 m and 1.25 m increased from 00-01 until 04-05, then decreased until 14-15, and then increased until 22-23, as can be seen in figure 4.26a. This was the inverse of the development of temperature on that day, shown in figure 4.19a, which is in line with the theory that relative humidity is inversely proportional to temperature. Absolute humidity is independent of temperature. As expected, the vertical profile of absolute humidity in figure 4.26b did not follow the development of the temperature that day. Furthermore, the maximum and minimum values did not occur at the same times for the three heights, and the values did not consistently increase and then decrease throughout the day. An example of this is that the  $\rho$  values at all heights and both locations decreased from 12-13 until 14-15, then increased in value at 16-17, and then decrease again at 18-19.



(a)



(b)

**Figure 4.26:** The plots in this figure are vertical profiles of bihourly humidity values on 28/6, which was a cloud-free day with light wind ( $<5\text{ m/s}$ ) in all except for two hours. The plots show vertical profiles over uncut (dashed lines) and cut (solid lines) grass. (a) shows the development of relative humidity and (b) shows the development of absolute humidity.



On 30/6/2019, the average wind speed was 3.68 m/s, where ten hours had an average wind speed larger than 5 m/s. The wind came from the south until 14:00. After this, the wind direction changed to southwest, west, and northwest. It was a cloudy day with an average diffuse to global radiation ratio of 0.54. In the plot of relative humidity in figure 4.27a, it can be seen that the values increased from 00-01 until 04-05, and then decreased until 14-15. The values then actually increased at 16-17, before they started decreasing again and reached a minimum at 20-21. This was the inverse of the same development of air temperature values on this day (figure 4.19b). The range of the absolute humidity values was larger on 30/6 (figure 4.27b) than on 28/6 (figure 4.26b). The variation from smallest to largest values at 2 m over cut grass on 30/6 was 5.52 g/m<sup>3</sup>, while it was 3.22 g/m<sup>3</sup> on 28/6. Just like the plot for  $\rho$  on 28/6/2019, the absolute humidity values on 30/6/2019 did not consistently increase and then decrease throughout the day.

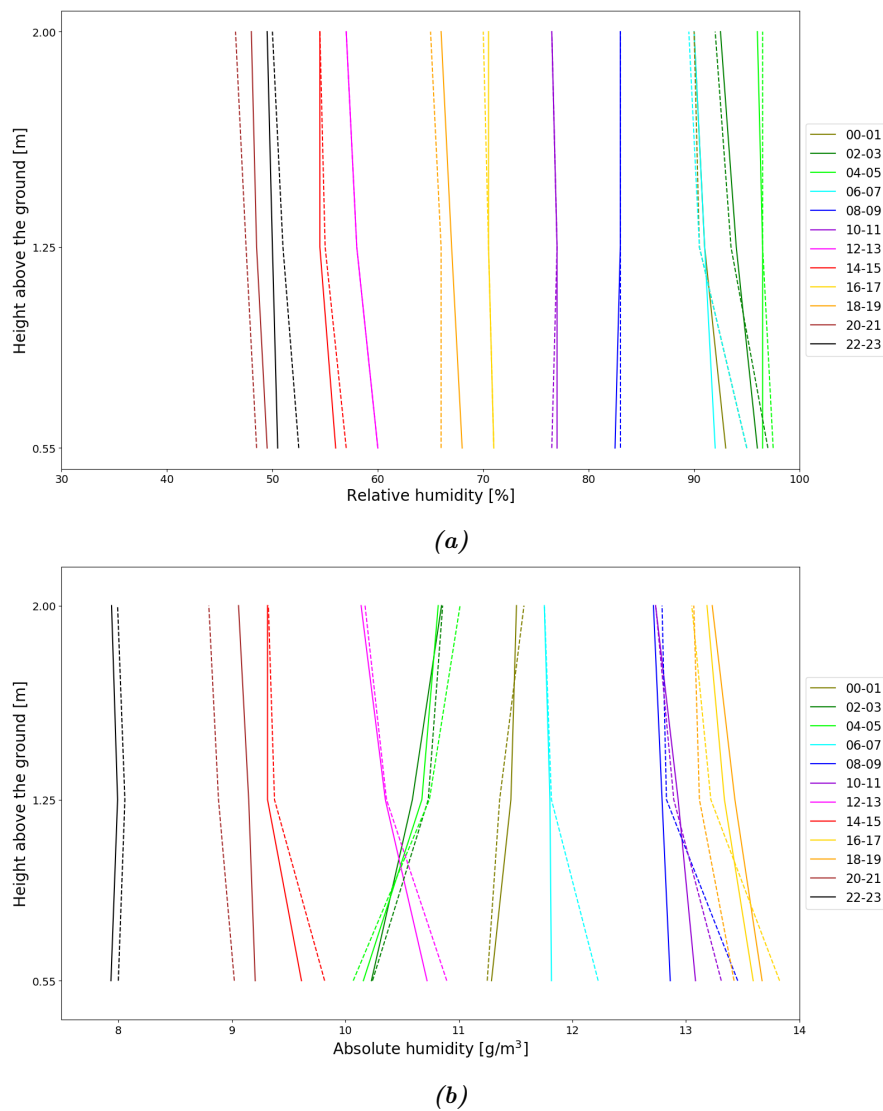


**Figure 4.27:** The plots in this figure are vertical profiles of bihourly humidity values on 30/6, which was an overcast day with strong wind (larger than 5 m/s) for ten hours out of the day and average wind speed of 3.68 m/s. The plots show vertical profiles over uncut (dashed lines) and cut (solid lines) grass. (a) shows the development of relative humidity and (b) shows the development of relative humidity.



# Chapter 5

## Discussions

This study aims to find out how air temperature measurements are affected by vegetation. The SC estimates the additional estimated uncertainty to be 2 °C for temperature measurements at meteorological stations with vegetation taller than 25 cm under the measuring instrument. The class 4 limit in the vegetation height category is 25 cm, and the additional estimated uncertainty of 2 °C is given to all class 4 temperature measuring stations.

The previous chapter presented results from analysis of the observational data from the experiment behind this thesis. In this chapter, these results will be analyzed and their significance will be discussed. The goal is to determine whether SC's claim of an additional estimated uncertainty of 2 °C can be confirmed or not. Additionally, the humidity data from the experiment will be discussed.

### 5.1 Overview of the data

On the time scale of the experiment's duration in 2019, the differences between temperatures measured over uncut (U) and cut (C) grass at all three of the measuring instruments' heights (2 m, 1.25 m, and 0.55 m), were small. The mean value of the difference in temperature between the instruments was 0.0 °C for all three heights, as could be seen in table 4.1. The mean value does not give insight into the spread of the data, which is expected to be higher for instruments mounted at lower heights. As table 4.1 shows, the standard deviation was 0.1 °C for the difference between temperature at U and C at 2 m. This is 0.1 °C smaller than the standard deviation equal to 0.2 °C for this difference at 1.25 m and 0.55 m. This tells us that by evaluating the data from the experiment's duration in 2019 (23/5-30/10), the increased grass height at U does not seem to have had a notable impact on the temperature. A more comprehensive evaluation of the temperature data that were presented in chapter 4 will follow in this chapter.

The increased vegetation height at U had no influence on the values of the difference between temperature measured at U and C at 2 m in the monthly time scale. The monthly mean and standard deviation values of  $(T_U - T_C)$  at 2 m is presented in table 4.2. No development or pattern of these values throughout the experiment's duration in 2019 can be seen. Increased grass density leads to a subdued variation of diurnal temperature. If the grass at U had a large effect on the measured temperature, one would expect the difference between temperature values measured at U and C to steadily increase. This would result in an increase in the monthly standard deviation of  $(T_U - T_C)$ . The standard deviation is 0.1 °C in all five months, meaning this expected pattern cannot be seen.

## 5.2 Comparing data from 2018 and 2019

### 5.2.1 Average and standard deviation

The difference between temperature measured at U and C was equally small in 2018 and 2019. The mean temperature difference between the instruments mounted 2 m in the period from 11/7 to 15/9 is 0.0 °C in both years, as can be seen in table 4.3. In this time period in 2019, we know that the grass at U was significantly higher than the class 3 requirement of 25 cm. In 2018, the grass height at U was always below this limit. This mean value of 0.0 °C for both years give further indication that the vegetation height has a non-significant effect on the temperature on long time-scales.

The variation in the differences between temperature measured at U and C was slightly higher in 2018 than in 2019. The standard deviation of  $(T_U - T_C)$  at 2 m was 0.2 °C in 2018 and 0.1 °C in 2019. As the results presented in section 4.2.3 shows, the variation in the difference in temperature between U and C was larger in 2018 than in 2019 at all heights. This variation between the two years was smaller at 2 °C than at 1.25 m and 0.55 m. The larger value of standard deviation in 2018 was therefore most likely due to the extreme weather in 2018.

### 5.2.2 Statistical tests

The KS and MWU tests were used to evaluate the differences in the temperature values measured at U and C between 2018 and 2019. 95% was chosen as this report's significance level.

The  $(T_{2m} - T_{1m})$  values from both locations was evaluated for the two years. According to the KS and WMU tests, the temperature gradient between 1.25 m and 2 m above the ground was different at U and C in 2019, but not in 2018. The p-value for this comparison in 2019 was low enough to conclude that the temperature values measured at U and C were significantly different (row a in table 4.4). The p-value from the KS and WMU tests using data from 2018 to see if there was a difference between U and C's  $(T_{2m} - T_{1m})$  were too high to conclude on a 95% significance level that the two data sets were different (row b in table 4.4). This tells us that in 2018, when the grass at U did not grow high, the difference between the temperatures logged at 1.25 m and 2 m at U and C was not large enough to be able to tell the two data sets apart. In 2019, when the grass did grow high, the KS and WMU test statistics tell us that the data sets differentiated enough to conclude that the temperatures logged at U and C were significantly different.

The KS and MWU tests indicate that the difference between the temperature at U and C in 2019 was significantly different from the difference between  $T_U$  and  $T_C$  in 2018. The low p-values row c in table 4.4 tell us that there was a significant difference between the data sets from 2019 and 2018 consisting of the difference in temperature between U and C at 2 m,  $(T_U - T_C)_{2m}$ . This result suggests that the data sets of the  $(T_U - T_C)_{2m}$  values in 2018 and 2019 were not the same. We see in row d that in the two years, the same can be said for the difference between U and C at 1.25 m.

Despite the conditions at C being the same in 2018 and 2019, and not at U, the statistical tests suggests that there was a difference between the air temperature at C between the two years, and no difference at U between the two years. Row e in table 4.4 shows the test statistics from comparing  $(T_U - T_C)$  at 2 m in 2018 and 2019, while row f shows the test statistic from comparing  $(T_U - T_C)$  at 1.25 m in 2018 and 2019. These tests were done to investigate if the measuring instruments at 1.25 m were affected by the increased grass to a greater degree than the instruments at 2 m. The expectation was that if the measuring instruments at 1.25 m were influenced by the grass at U in 2019, then the p-value would be low in row e and high in row f. The results from comparing the difference between the temperature at 1.25 m and 2 m at U in 2019 and 2018 (row

e), tell us that we cannot conclude on a 95% significance level that these data sets are different. However, the data sets with the same difference at C, where the grass was cut, are significantly different on a 95% level according to the KS test and different on a 90% level according to the WMU test. This result is surprising because the vegetation conditions for data measuring at C were essentially the same in the two years. This tells us that the weather in 2018 impacted the conditions at the site to such a degree that it is difficult to compare data between the two years. Because of this, the results in row c, d, e, and f in table 4.4 cannot be given much weight. The test results in row a and b, however, are from comparing data from the same year (2019 in a and 2018 in b). These test therefore do not have to be discarded.

The statistical test were run only with hourly data from a little over two months because of holes in the data set from 2018. Additionally, it was not possible to run statistical tests with data from 0.55 m because of all the data missing from that height at location C in 2019. These factors must be taken into account when considering the validity of the test results. Nevertheless, statistical tests are meticulous and p-values that indicate a difference between two data sets can be trusted.

### 5.2.3 The difference in temperature at three heights

The majority of the values of the difference between temperature at the experiment's two locations, at all three heights, were centered around  $0.0^{\circ}\text{C}$  in both 2018 and 2019. though the spread in the values was larger in 2018 than in 2019. The range of the  $(T_U - T_C)$  values was larger in 2018 than in 2019 at all three heights, as shown in figure 4.3. The percentages of the  $(T_U - T_C)$  values within an interval centered around  $0.0^{\circ}\text{C}$ , were consistently larger, at all heights, in 2019 than in 2018. Table 4.5 showed these percentages. This is inconsistent with the assumption that the conditions at the site were more homogeneous in 2018 than in 2019, and therefore further demonstrate that the extreme weather in 2018 made it inapplicable to compare data from that year with data from 2019.

## 5.3 Diurnal variation in temperature difference

The box and whisker plots of hourly values of the difference in temperature between the locations with uncut (U) and cut (C) grass for the three heights, and for different time periods presented in section 4.3, will be discussed in this section. The evaluation of these plots are essential in order to address the leading question this thesis is attempting to resolve; the influence of increased vegetation height on temperature measurements.

### 5.3.1 Overview

Even though the grass at U was taller than the SC class 3 recommendation of 25 cm throughout the majority of the experiment in 2019, the differences between temperature measured at U and C at 2 m were small. Box and whisker plots of the hourly difference in measured temperature at U and C at 2 m was shown in figure 4.4. All the boxes, which contain at least 50% of the data sets, are within the interval  $[-0.1^{\circ}\text{C}, 0.2^{\circ}\text{C}]$ . Table 4.5 showed that only 2.6% of the  $(T_U - T_C)$  values at 2 m were outside of the interval  $\pm 0.3^{\circ}\text{C}$ . This indicates that differences registered at the two instruments throughout 2019 were generally small. As explained in section 3.1, the conditions in May and June in 2019 were well suited for grass growth. The simulation in figure 3.3a shows that the grass at U surpassed the class 1 and 2's 10 cm requirement in the experiment's first week and probably grew past the class 3 requirement of 25 cm by the end of May. According to the SC, a station with vegetation height over 10 cm can expect an additional uncertainty of  $1^{\circ}\text{C}$ , and over 25 cm would result in  $2^{\circ}\text{C}$  additional uncertainty (see table 2.1). The additional estimated uncertainty that WMO CIMO predicts could not be confirmed, and

the results from the evaluation of  $(T_U - T_C)$  at 2 m (figure 4.4) indicate that the limits in the SC might be too strict.

The values of the differences between the temperature measured over uncut grass and cut grass at 1.25 m were also small in 2019, despite the increased grass height and the influence by the white logger cabinet. The variation in  $(T_U - T_C)$  at 1.25 m (figure 4.5) suggests that there was a diurnal pattern in these values. However, the  $(T_U - T_C)$  values at 0.55 m (figure 4.6) do not show indications of a diurnal pattern. Because the measuring instruments at 0.55 m are closer to the ground, they are affected more by the surface properties. It is therefore justifiable to assume that the diurnal pattern in  $(T_U - T_C)$  at 1.25 m stems from the white logger cabinet hanging close to the measuring instruments at 1.25 m (discussed in section 3.1). Despite this probable influence by the logger cabinet, all boxes and whiskers in the plot for temperature difference at 1.25 m are between  $-0.4\text{ }^\circ\text{C}$  and  $0.5\text{ }^\circ\text{C}$  and 93.4% of the values were within the  $\pm 0.3\text{ }^\circ\text{C}$  interval. Thus, the  $(T_U - T_C)$  values at 1.25 m were centered around  $0.0\text{ }^\circ\text{C}$ , just like they were at 2 m. This indicates that the instruments at 1.25 m and 2 m were equally affected by the grass at U.

The variation in the hourly  $(T_U - T_C)$  values was larger at 0.55 m than at 2 m and 1.25 m, but the values were still closely centered around  $0.0\text{ }^\circ\text{C}$ . The plot of these values for 0.55 m in figure 4.6 shows that the spread was larger at this height than for 2 m and 1.25 m in figures 4.4 and 4.5. This was expected because the air at this height is more heavily influenced by the surface properties. The maximum interval of the boxes for all three heights is  $[-0.1\text{ }^\circ\text{C}, 0.2\text{ }^\circ\text{C}]$ , while the maximum ranges of the whiskers and outliers for the hourly difference at 0.55 m are  $[-0.5\text{ }^\circ\text{C}, 0.6\text{ }^\circ\text{C}]$  and  $[-1.0\text{ }^\circ\text{C}, 1.4\text{ }^\circ\text{C}]$  respectively. These values are larger than for the hourly  $(T_U - T_C)$  values at 2 m and 1.25 m. It is simultaneously interesting to note that only 0.4% of the  $(T_U - T_C)_{0.5m}$  values were outside of the  $\pm 1.0\text{ }^\circ\text{C}$  interval even at a height this close to the ground. As can be seen in figure 3.5, a picture taken of U in August, the grass was at some points as tall as the measuring instrument itself. Despite this, the temperature difference never exceeded  $1.4\text{ }^\circ\text{C}$  throughout the entire duration of the experiment.

The similarities in the monthly mean of hourly median of  $(T_U - T_C)$  at 2 m (table 4.6) further supports the claim that there was no significant difference between this value in the months of this experiment. The grass was cut 7/5/2019 and grew at U to a height around 40-50 cm by the end of June at the latest. After this, the vegetation cover under U increased mostly in density throughout the rest of the experiment. This indicate that the grass at U did not impact the temperature on the monthly time scale.

### 5.3.2 Solar radiation

The influence of the surface properties on the air increases with decreased cloud cover. This is seen when separating the hourly difference in temperature between U and C into radiation exposure categories (figures 4.7, 4.8, and 4.9). At 2 m, all hours have  $(T_U - T_C)$  medians of  $0.0\text{ }^\circ\text{C}$  when the weather was overcast, while this value is in the interval  $\pm 0.1\text{ }^\circ\text{C}$  for partly cloudy and cloud-free hours. The same is the case for hourly medians of  $(T_U - T_C)$  at 1.25 m, other than that the medians for cloud-free hours then varies in the  $\pm 0.2\text{ }^\circ\text{C}$  interval. The variation in the hourly values of  $(T_U - T_C)$  at 0.55 m between the categories can be seen in several ways. For overcast hours, the boxes (containing at least 50% of the data) only stretch as far as  $\pm 0.1\text{ }^\circ\text{C}$ . For cloud-free and partly cloudy hours, the boxes varies in the interval  $[-0.2\text{ }^\circ\text{C}, 0.5\text{ }^\circ\text{C}]$ . These tendencies demonstrate how the surface properties influence the air temperature more when the cloud cover is small.

### 5.3.3 Wind speeds

Low wind speed results in increased influence by surface properties on air temperature. The box and whisker plots for light and strong winds for the three heights in figures 4.10, 4.11, and 4.12 show a clear interaction between wind speed and the difference between temperature measured at U and C. This supports the theory that strong winds ( $> 5 \text{ m s}^{-1}$ ) gives rise to mixing, which reduces the influence of surface properties on the air temperature.

### 5.3.4 High influence conditions

Even in conditions with the highest influence by surface properties on the air, the difference between temperature measured over uncut (U) and cut (C) grass at 2 m and 1.25 m were centered around  $0.0^\circ\text{C}$ . This can be seen in figure 4.13, where the differences between temperature measured at U and C are plotted for all the three heights of the instruments in the experiment in cloud-free and light wind conditions. The median values of the temperature difference in these conditions at 2 m and 1.25 m vary in the  $\pm 0.2^\circ\text{C}$  interval. It is interesting to note that  $(T_U - T_C)$  only varied in the  $\pm 0.4^\circ\text{C}$  interval for measurements from 2 m and in the  $\pm 0.5^\circ\text{C}$  interval for measurements from 1.25 m, despite the conditions being ideal for large influence by surface properties.

The variation in difference in temperature between U and C measured at 0.55 m in conditions with the highest influence by surface properties on the air was larger than for measurements from the higher measuring instruments. As can be seen in figure 4.13c, the median values vary in the interval  $[0.0^\circ\text{C}, 0.3^\circ\text{C}]$  and 8.9% of the values at 0.55 m were outside of the  $\pm 0.5^\circ\text{C}$  interval. None of the  $(T_U - T_C)$  values at 2 m and 1.25 m were outside of this interval in these conditions. The plots of the difference in temperature at these three heights in conditions with high impact by the surface therefore show that the air, and the measuring instruments in closer proximity to the surface features, are more susceptible to impact by these surface features.

## 5.4 Difference in daily values

As explained in section 2.8, some applications do not use hourly temperature measurements, but instead evaluate temperature on larger time scales. Daily maximum, minimum, and mean temperatures can all be used in these applications. It was therefore interesting to look at the difference in daily mean of the hourly mean temperature, the difference in daily maximum temperature measurements, and the difference in daily minimum temperature measurements.

The difference between daily mean temperature between U and C was small in 2019. In figure 4.14, it can be seen that except for two outliers slightly larger than  $0.2^\circ\text{C}$ , the difference in daily mean values at U and C were within the interval  $[-0.1^\circ\text{C}, 0.2^\circ\text{C}]$  for the entire duration of the experiment in 2019. The plot showed that there were more positive than negative  $(T_U - T_C)$  values. However, this tendency was minor, meaning that nothing can be concluded with certainty.

In the summer of 2019, the majority of daily maximum temperature values were larger at C than at U, and the majority of daily minimum temperatures were larger at U than at C. These patterns can be seen in the plots of the difference in daily maximum and minimum temperature in figure 4.14. These two patterns of difference in daily maximum and minimum temperature further supports that increased vegetation density results in a subdued daily temperature range. However, the differences between daily maximum and minimum measured at U and C are still small: the whisker-reach for difference in maximum temperature is  $[-0.3^\circ\text{C}, 0.1^\circ\text{C}]$  and for difference in minimum temperature it is  $[-0.2^\circ\text{C}, 0.4^\circ\text{C}]$ .

When analyzing separate time periods, with different grass heights at U from the experiment in 2019, the patterns in the difference in daily values between U and C did not change. Figure 4.15 shows the same plots as 4.14, but only for the months of August, September and October of 2019. From pictures taken of U in early August 2019 (figure 3.5), we know that the grass was taller than the class 3 limit of 25 cm in those months. Figure 4.16 also shows the difference in daily temperature between U and C, but the data used were from May and June of 2019. In those months, the difference between grass height at U and C was smaller than the rest of the year, but the grass at U probably surpassed 25 cm by the end of May. Both figure 4.15 and 4.16 show the same patterns as 4.14: the difference in daily mean temperature between U and C is concentrated around  $0.0^{\circ}\text{C}$ , the difference in daily maximum temperature between U and C has a slight negative tendency, and the difference in daily minimum temperature between U and C has a slight positive tendency. The plots having similar tendencies, despite the different grass height and density values at U, suggests that the grass does not need to grow much before these tendencies are evident. It further suggests that the influence on daily minimum and maximum temperature did not increase much with increased vegetation height and density. Additionally, even though the patterns are apparent, the differences are trivial. The values of the difference in daily maximum temperature exceeded  $\pm 0.4^{\circ}\text{C}$  two out of 160 days, and the values difference in daily minimum temperature only exceeded this limit on three occasions.

## 5.5 Day and night

The potential impact on air temperature measurements by increased vegetation height was further investigated by evaluating the difference in temperature values between U and C at day and night. This was done by counting the occurrences of the different  $(T_U - T_C)$  values during the day and night hours using the data from the experiment from 2019. The number of occurrences of each  $(T_U - T_C)$  value is given in table 4.8 and the percentages of these counts are plotted together in figure 4.17.

Evaluation of the difference between  $(T_C - T_U)$  values during day and night hours shows that there are indications of a decrease in the diurnal temperature variations with increased grass height and density. As the grass grew throughout the experiment's duration in 2019, this would, according to the theory, result in a higher  $T_C$  than  $T_U$  during the day when the maximum temperature occurs, and the opposite ( $T_U > T_C$ ) during the night when the daily minimum occurs. The pattern in figure 4.17 demonstrates this concept. The majority of values of  $(T_U - T_C)$  for both day and night hours were  $0.0^{\circ}\text{C}$ , but the day hours had more negative than positive  $(T_U - T_C)$  values than the night values and vice versa. However, when evaluating the day values separate from the night values, we see that the day values had more instances of  $(T_U - T_C)=0.1^{\circ}\text{C}$  than  $(T_U - T_C)=-0.1^{\circ}\text{C}$ , and almost the same amount of  $(T_U - T_C)$  values equal to  $0.2^{\circ}\text{C}$  and  $-0.2^{\circ}\text{C}$ . This was not the case for night values of  $(T_U - T_C)$ , where the values had a positive tendency, in line with the theory. An investigation into the reason for this was done by plotting values from the experiment from 15/7 until 30/10 in 2019 in figure 4.18. In the middle of July, the grass at U had reached its maximum height. As can be seen in figure 4.18, after 15/7, day hours had more negative  $(T_U - T_C)$  values and night hours had more positive  $(T_U - T_C)$  values. This confirms the theory that increased grass density results in smaller temperature variations throughout the day.

Even though the increased grass height at U seems to have influenced the air temperature, the influence was small and many values did not follow the expected pattern. In figure 4.17 and 4.18, it is interesting to note that over 40% of the data had a  $(T_U - T_C)$  value of  $0.0^{\circ}\text{C}$  and that many of the values did not follow the pattern explained in the previous paragraph.



## 5.6 Vertical temperature profiles

The bihourly vertical temperature profile plots from days with overcast and cloud-free weather in figures 4.19, 4.20, 4.21, and 4.22 give insight into the influence of increased vegetation combined with weather variations. The tendencies in these plots is that there were larger temperature variations throughout a day when the solar radiation exposure was larger and that the difference between U and C is larger on these days.

The vertical temperature profile plots show that larger cloud cover generally lead to smaller diurnal temperature variations. The difference between the daily mean temperatures at 2 m at C on 11/9 (figure 4.21a) and 21/9 (figure 4.21a) was 1.2 °C, but the temperature variation throughout the day was about 20 °C on 21/9, while it varied less than 5 °C on 11/9. This consequently demonstrated that larger solar radiation exposure leads to larger variations in temperature throughout the day.

The difference between temperature measured at U and C is larger on days with low cloud cover. This is because the surface properties influence the air more when the cloud cover is low, as discussed in section 5.3.2. As seen in table 4.10, the largest difference in temperature between U and C on 21/9 (small cloud cover) at 2 m was 0.4 °C, and at 1.25 m it was 0.5 °C. The average value of  $(T_U - T_C)$  at 2 m on 21/9 was 0.1 °C, which was four times the average value of  $(T_U - T_C)$  at 2 m on 11/9 (large cloud cover). It is shown in the table that all values of  $(T_U - T_C)$ , except for one, at all three heights on 11/9, were in the  $\pm 0.1$  °C interval. The one value that was not in that interval was equal to 0.2 °C. This shows how much smaller the differences in temperature between U and C were on the day with large cloud cover. However, the differences on 21/9 are still well below the SC's estimated additional uncertainty of 2 °C that the measuring instrument at U would have gotten (see table 2.1).

The influence by the surface properties is higher on days with low cloud cover, and the air closest to the ground is affected to a larger degree. The temperature varies more with height closer to the ground, and the measurements of temperature at 0.55 m were therefore more affected by the increased vegetation height than the measurements at 2 m and 1.25 m. This effect was higher on days with low cloud cover. 28/6 was a day with low cloud cover and the grass at U was taller than the SC class 3 limit of 25 cm. The influence that the increased vegetation height had on the vertical temperature profile can be seen in the bihourly plot of this day in figure 4.19a. The mean value of  $|T_U - T_C|$  at 0.55 m on 28/6 was 0.5 °C. This is higher than on 30/6 (figure 4.19b), where the mean value of  $|T_U - T_C|$  at 0.55 m was 0.3 °C. This demonstrates that the difference between the measured temperature at 0.55 m at U and C was larger on the day with greater influence by the surface properties.

Even though theory says that increased vegetation height and density leads to subdued diurnal temperature variations, there are many factors that affect the influence of the vegetation on the air. 28/6 was a day with light wind and cloud cover, but as figure 4.19a shows, the maximum temperature measured at U was not smaller than the maximum temperature measured at C this day. This is in contrast to what the theory says of subdued temperature variation over increased grass density. It is therefore an example of the complexity of the factors that can influence the difference between temperature at U and C, such as recent rainfall and wind direction.

It is worth mentioning that the vertical temperature profile plot for 24/8 in figure 4.20a did not show all the tendencies described in this section. This is because 24/8 was not the day with the lowest ratio of diffuse to total radiation ratio that month, but it was used because data from 0.55 m at C were lost up until 21/8/19 at 13:00. 24/8 was the day between 22/8 and 31/8 with the best combination of high solar radiation exposure and light wind. The daily range of temperature values on 24/8 demonstrates well that a day with low cloud cover has a larger temperature range, in contrast to the smaller temperature range on 22/8 (figure 4.20b).

## 5.7 Different effects in the same class

Because it is the highest class in any category that determines the site's overall class, it is essential that a class number in any category influence the measurements equally. In section 2.7, other projects' findings regarding nearby heat sources and water bodies' influence on temperature measurements were presented. In table 2.3, a summary of these studies was given and the results are somewhat divergent. However, it seems like the additional estimated uncertainty for class 3 of 1 °C given in the SC is too strict, and that the limits in the nearby heat source category need to be adjusted.

The U location in this thesis' experiment had a class 4 throughout the majority of this experiment's duration in 2019, but the largest temperature deviation at 2 m was 0.9 °C. Furthermore, this large deviation between temperature measured at U and C only occurred once and 97.4% of the  $(T_U - T_C)$  values at 2 m were in the  $\pm 0.3$  °C interval (see table 4.5). These temperature deviations indicate classifying U as in class 4 makes it account for more error than is proven to be necessary by this project. This tells us that, just like the studies evaluating the nearby heat sources have shown, the limits in the vegetation height category in the SC cannot be confirmed by this thesis' analysis.

## 5.8 Humidity

In this section, the analysis of the experiment's humidity data presented in section 4.7 will be discussed. The uncertainties of the relative humidity ( $RH$ ) measurements are described in section 3.2.4 and table 3.8. The combined uncertainties of the difference between relative humidity measurements are presented in table 3.9 and is shown to be  $\pm 6$  p.p. at the three heights in the experiment behind this thesis. Additionally, it could be argued to be  $\pm 4$  p.p. for the instruments at 2 m. There are no additional estimated uncertainties provided for humidity observations by the SC. Some relative humidity data were lost or was unusable in this study, as discussed in section 3.3.

There is a small indication that the increased grass height at U influenced the vertical profile of relative humidity ( $RH$ ) in the time period between 23/5/2019 and 15/7/2019. With 93.9% and 91.3% of the values of the difference between relative humidity measured over uncut (U) and cut (C) grass at 2 m and 1.25 m being inside the  $\pm 2$  p.p. interval in the this time period, it can be said that there is a insignificant difference between values measured at these to heights. While 90.5% of  $(RH_U - RH_C)$  values at 0.55 m were within the  $\pm 2$  p.p. interval, the interval of the difference between relative humidity measured at U and C at this height was  $[-7$  p.p.,  $16$  p.p. ]. This is in contrast to the interval of the  $(RH_U - RH_C)$  values at 2 m and 1.25 m, which were  $[-5$  p.p.,  $6$  p.p. ] and  $[-7$  p.p.,  $7$  p.p. ] respectively. Even though these results are from the beginning of the experiment, they show indications of possible impact by the increased grass height on the vertical humidity profile.

The opposite shifts away from 0 p.p. of the values of the difference between humidity measured at U and C between 21/8/2019 and 23/9/2019 at 2 m and at 1.25 m, either stems from poor data quality or unexplained factors. The plot of these values in the given time period was given in figure 4.24. Though 92.7% of values of the the difference between relative humidity values measured at 2 m were within the  $\pm 2$  p.p. interval, it is interesting to note that the values had a positive shift, resulting in 65.0% of the values being larger than 0 p.p. This means that the majority of the  $RH$  values were larger at U than at C at 2 m in this time period. This is in contrast to the time period between 23/5/2019 and 15/7/2019, where only 22.8%  $(RH_U - RH_C)$  values at 2 m were larger than 0 p.p. Furthermore, 86.5% the  $(RH_U - RH_C)$  values at 1.25 m were within the  $\pm 2$  p.p. interval. At the same time, there was a distinct negative trend in the  $(RH_U - RH_C)$  values at this height (meaning that the values were larger at C than at U), with 84.4% for the values being below 0 p.p. These shifts away from  $(RH_U - RH_C)$  values of 0 p.p.

could not be seen in the values of the difference in humidity values measured between 23/5/2019 and 15/7/2019. The positive shift for the difference at 2 m and negative shift for the difference at 1.25 m can be seen for both relative and absolute humidity. No such shift can be seen for the values of the difference in temperature in the two periods (see appendix G). This tells us that the shift in the difference in humidity values at 2 m and 1.25 m either are due to the complexity of influence on humidity, that there was something wrong with both or one of the humidity instruments, or simply due to incidental variations within the uncertainty of the sensors.

As we know from section 3.3, the humidity instrument at 2 m, at the location with cut grass, fell out on 16/7/2019. When it was switched with the instrument at 1.25 m on 6/8/2019, the problems withstood. The same day that the measuring instrument at 1.25 m was replaced (21/8/2019), erroneous values from the instrument at 2 m seemingly disappeared. This was shown in figure 3.7. On 23/9/2019, the obvious errors in the measurements returned. This continued until it was discovered in May 2020 that the issues were caused by a broken electrical cord. Therefore, the humidity instrument at 2 m at C is most heavily suspected of logging untrustworthy data in the time between 21/8/2019 and 23/9/2019. However, the deviations away from zero of the values of the difference between humidity measurements at 1.25 m are larger than at 2 m in this time period. This calls into question the reliability of the measurements by the humidity instrument at 1.25 m at C between 21/8/2019 and 23/9/2019.

The values from the 1<sup>st</sup> period (23/5/2019-15/7/2019) seem to be trustworthy, and they indicate that the *RH* measurements were not heavily affected by the increased grass height. 99.2% of the values of the difference between relative humidity measured at U and C at 2 m were inside the  $\pm 4$  p.p. interval. The alternative combined uncertainty is  $\pm 4$  p.p. for  $(RH_U - RH_C)$  values at 2 m, and this means that all the values within the  $\pm 4$  p.p. interval could potentially have been 0 p.p. Some of the values also could have reached out as far as  $\pm 8$  p.p. Additionally, 93.9% of the  $(RH_U - RH_C)$  values at 2 m were within the  $\pm 2$  p.p. interval and 84.3% of the values were within the  $\pm 1$  p.p. interval. In order for more robust conclusions to be drawn regard the influence of the grass height on humidity measurements, longer and more trustworthy data sets are needed. However, values of the differences between humidity at U and C were centered around zero and the majority of the values were smaller than the combined uncertainties of the instruments.

The diurnal variation of the vertical profiles of absolute humidity ( $\rho$ ) indicate that there are several factors that influence the air humidity. As mentioned, the development of  $\rho$  on 28/6 (figure 4.23b) and 30/6 (figure 4.24b) did not follow that of temperature on those same days (figure 4.19). On 28/6, the influence by surface properties on the air was large due to the small cloud cover and light wind. 30/6, on the other hand, was a day more characterized by the regional weather patterns, which may have transported air masses with different water vapor content into the test site area. Additionally, it was a day with low influence by the surface properties. The difference between the smallest and largest  $\rho$  values was larger on 30/6 than on 28/6, despite the temperature variation and surface influence being larger on 28/6 than on 30/6. Moreover, on 28/6, the times where the minimum and maximum values of  $\rho$  occurred were not the same at all heights. All of this highlights the complexity of factors influencing air humidity.



## Chapter 6

# Conclusions and Outlook

### 6.1 What is the influence of vegetation height on temperature measurements?

This thesis has evaluated the influence of grass height on air temperature measurements and related it to the vegetation height limits set by WMO CIMO in the SC. According to the SC, if the grass under a measuring instrument is taller than 25 cm, the additional estimated uncertainty for the site's temperature measurements is 2 °C. The analysis of the difference between temperatures measured over uncut (U) and cut (C) grass at 2 m shows that the largest negative and positive values of  $(T_U - T_C)$  at this height were -0.8 °C and 0.9 °C, but that 97.4% of the values were in the interval [-0.3 °C, 0.3 °C]. The combined expanded uncertainty for these values was  $\pm 0.3$  °C. This proves that the observed difference between measured temperatures at the two locations was smaller than would be implied by the additional estimated uncertainty that the SC claims should be applied to the site.

**The influence by increased height of vegetation on air temperature is smaller than WMO CIMO claims in their SC. The additional estimated uncertainty given in the SC cannot be confirmed by the analyses performed in this thesis.**

The variations in the  $(T_U - T_C)$  values are similar for the measuring instruments at 1.25 m and 2 m, despite the instrument at 1.25 m at U being closer to the grass than the instrument at 2 m. For the  $(T_U - T_C)$  values at 1.25 m, 93.4% were within the  $\pm 0.3$  °C interval, in comparison to 97.4% of the values at 2 m being within this interval. Whether or not the presence of the white logger cabinet was the cause of the lower percentage for the values at 1.25 m than at 2 m, or the cause was the instrument at 1.25 m being closer to the grass, cannot be determined for certain. Regardless, its presence should be taken into account when interpreting this disparity. Nonetheless, these high percentage values indicate that instruments mounted between 1.25 m and 2 m are equally affected by the ground and justifies WMO CIMO's instructions to mount air temperature instruments within these heights above the ground.

The vertical temperature profile was shown to be affected by the increased grass height. Through analysis of the experiment's data, it could be observed that the vertical temperature profile at U was affected by the increased grass height in a manner consistent with the academic understanding.  $(T_U - T_C)$  values measured closer to the ground, at 0.55 m, had a higher frequency of nonzero observations than those measured farther from the ground, at 1.25 m and 2 m. However, the largest  $(T_U - T_C)$  value at 0.55 m was 1.4 °C. Furthermore, 99.4% of the  $(T_U - T_C)$  values at 0.55 m were within the  $\pm 1.0$  °C interval. It can therefore be claimed that the impact of grass height on the vertical temperature profile in this study, even for the lowest and most impacted measurement height, is less than what the WMO CIMO says.

The increased variation in  $(T_U - T_C)$  on days with higher influence by the surface properties on the air demonstrates the influence by increased grass height on air temperature. Smaller cloud cover and lower wind speed increased the impact of surface properties on the air. It was demonstrated in this thesis that the difference between the temperatures measured at the two locations was larger during the time periods where these “high-impact” weather characteristics were present. This demonstrated that there was an influence by the grass height on the air temperature.

There was no clear development or increase in the  $(T_U - T_C)$  values at 2 m or their variation throughout the experiment. The non-existent systematic differences in the hourly values between the months of the experiment, indicate that the increase in grass height and density did not have a large enough impact on the temperature measurements at 2 m to influence the air temperature measurements.

The increased vegetation height and density at U seems to have subdued the diurnal temperature variation. The daily maximum temperature was generally lower at U than at C, and the daily minimum temperature was generally higher at U than at C. Nonetheless, the  $(T_U - T_C)$  values for both daily maximum and minimum temperature never diverged far from  $0.0\text{ }^\circ\text{C}$ . The majority of  $(T_U - T_C)$  values for daily maximum were in the interval  $[-0.3\text{ }^\circ\text{C}, 0.1\text{ }^\circ\text{C}]$  and the majority of  $(T_U - T_C)$  values for daily minimum were in the interval  $[-0.2\text{ }^\circ\text{C}, 0.4\text{ }^\circ\text{C}]$ .

Despite the limited sizes of the humidity data sets, the analysis shows that an influence on the vertical profile by the increased grass height could be observed. In the analysis of the difference between humidity values at U and C (both absolute and relative humidity), the deviations away from a nonzero difference were larger, and more in number, for the measurements done at 0.55 m than at 2 m and 1.25 m. A more detailed and thorough analysis of the influence by increased grass height on humidity is needed in order to come to more robust conclusions.

## 6.2 Final suggestions

The additional estimated uncertainty of  $2\text{ }^\circ\text{C}$  given in the SC to temperature measuring sites with vegetation height taller than 25 cm could not be confirmed in this thesis.

It was demonstrated that increased vegetation height did influence the temperature profiles. Therefore, it is reasonable to require an ideal site to have vegetation height be less than 10 cm in order to have no additional estimated uncertainty. However, the experiment showed that the influence by grass of height 40-50 cm is smaller than what is claimed by WMO CIMO in their SC. Therefore, a class 3 classification for grass between 10 cm and 50 cm, associated with an estimated additional uncertainty of  $1\text{ }^\circ\text{C}$ , is defensible. Since grass does not grow taller than this, the additional estimated uncertainty added in this class would be high enough to account for the variation in albedo between grass and other types of vegetation.

Some meteorological stations are placed in cropland with vegetation much taller than 50 cm. The vegetation itself does not seem to influence the temperature measurements unless the measuring instrument is closer to the top of the vegetation than currently assumed, as the discussion of the instrument at 0.55 m shows. Therefore, the estimated additional uncertainty of  $2\text{ }^\circ\text{C}$  associated with class 4 sites would be a high enough uncertainty value to properly account for this type of vegetation.

Based on the results from this study, new suggested vegetation height limits are as presented in table 6.1. It is the conviction of the author of this thesis that the results from this project are representative for Nordic countries, and that the limits are recommended for comparable stations to the one in this project’s experiment.

**Table 6.1:** *New suggested limits for the vegetation height category in WMO CIMO’s SC based on the results and discussion presented in this thesis. These limits are suggested for comparable*

Class	Vegetation height
1	<10 cm
2	<10 cm
3	<50 cm
4	No requirement
5	No requirement

### 6.3 Improvements

The goal of the experiment in this thesis was to evaluate the effect that increased vegetation has on measurements of air temperature and relative humidity. During the evaluation and analysis of the data from the experiment, thoughts regarding improvements to the setup and the execution of the experiment were made. Suggestions for changes and additions to the experiment that could have enhanced the credibility and significance of the results will be made in the following paragraphs.

More regular supervision of the measuring instruments would have improved the reliability of the results and given them a larger significance. Field controls of the measuring instruments were only done twice; once before the measurements started in 2018 and once after the experiment in 2019 was over. The field controls were not done by people who have much experience with the execution of these types of control. This may have affected the results from the two field controls and the reliability of them. The uncertainties of the measurements might be lower than what this thesis concludes that they were. More regular monitoring of the measurement instruments and frequent field controls would have made the calculated uncertainties more reliable.

The motivation for this thesis was to discuss and evaluate the vegetation height in WMO CIMO’s SC. In order to do that, the grass height had to be known. Pictures were not taken specifically of the experiment until August 5 in 2019. We can therefore only rely on Åshild Ergon’s expertise when assuming the grass under U had reached 40 cm by the end of June (Åshild Ergon, personal communication, 21/4/2020). The significance of the results regarding the grass height’s influence would have been improved if pictures were taken regularly.

Photographing the site regularly would have made it possible to comment on and discuss the influence of vegetation density on temperature and humidity measurements in addition to vegetation height. The grass only increases in density after it reaches its maximum height. The pictures could have allowed us to more closely examine the known phenomenon of increased vegetation density’s effect on air temperature. Vegetation density is not currently considered in the SC, and therefore observations of this could have allowed us to come to novel conclusions and strengthened the results from this thesis.

The white logger cabinet hanging at U close to the measuring instruments at 1.25 m resulted in temperature data from this height being more heavily influenced by solar radiation than the other five instruments. Part of the aim of this thesis was to evaluate whether it is the height of the vegetation or the proximity to the vegetation top that influence meteorological measurements. The background for this is that, as mentioned in section 2.6, a class 3 measuring instrument at 1.25 m could be closer to the vegetation top than a class 4 instrument at 2 m. Analysis of the influence of distance from the measuring instrument to the vegetation top could be done by analyzing the temperature at 2 m and 1.25 m and seeing if they were significantly different. However, this was not

possible because analysis of the data from 1.25 m indicates significant influence from the logger cabinet.

More significant and noteworthy conclusions regarding the increased grass height's influence on humidity could have been made if the data sets were larger and more consistent, and if the quality of the data was better. The usable data showed indications of the increased grass at U influencing the vertical profile for air humidity, but also revealed the complexity of how air humidity, especially absolute humidity, is influenced. Future work on influence on humidity should include measurements of additional meteorological variables such as leaf moisture and soil moisture at both locations in order to understand the full picture of the influence by increased vegetation height and density on humidity.

## 6.4 Further investigations

A detailed analysis of the data and investigations into grass height's influence on air temperature and humidity was performed through this research. This section will present suggestions for further investigation into other aspects of this project's research question.

Further investigations are needed in order to generalize the influence of other types of vegetation on meteorological data. The SC specifies that the vegetation needs to be "natural and [...] representative of the region" (WMO, 2018). This project has only evaluated the influence of increased grass height on temperature and humidity measurements. In order for the criteria by the SC to apply for all vegetation types in all regions, evaluations of the influence by different vegetation types on temperature and humidity measurements need to be performed.

Experiments at other geographical locations are needed in order to develop a more robust understanding of the effect of vegetation on temperature measurements. The experiment in this thesis was performed in Ås, Norway, which is a high latitude location. If more studies are undertaken at different latitudes, a meta-analysis can be performed to develop a working scientific understanding of the phenomena being examined in this thesis.

Investigations should be done in regards to the combined effects of variation in vegetation height and albedo values. Many measuring instruments are placed on cropland in order to avoid shading, and to be away from heat sources, such as buildings. This results in variation in vegetation height and ground albedo value throughout the year. When the crop is cut short, the ground is darker and will have a lower albedo value. The ground will therefore absorb more radiation, and this will influence the air temperature. Different types of crops have different maximum heights, and many will grow much higher than the 25 cm class 3 limit in the SC. Taking these factors into consideration, it is reasonable to assume that there are more variables affecting the temperature measurements at these kinds of sites than are currently encapsulated in the SC. Therefore, more studies of the influence of the complexity of surface property influence should be undertaken.

In addition to the need for novel experiments, there is also a need for variations of this project to be undertaken in order to compliment the results of this experiment. For example, investigations into the effects of vegetation on ground temperature could be done. Because air temperature is affected by ground temperature, understanding how ground temperature is affected by grass height and density will give additional context and understanding to the results and conclusions of this experiment.

Model investigations into the influence of various surface features on near-surface air properties could also give greater insight into the subject of this project. In a simulation, variables such as soil type, vegetation type, weather, geographical location, and day of the year could be varied. By doing this, the different variables' influence on air temperature and humidity, as well as radiation and energy budgets, could be evaluated. These investigations could deepen the current understanding of the conclusions reached



in this experiment, as well as come to other novel conclusions.



# Bibliography

- Barry, Roger G and Richard J Chorley (2009). *Atmosphere, weather and climate*. Routledge. Chap. 3.
- Dannevig, Petter, Knut Harstveit, and Kristin Seter (Jan. 2020). *luftfuktighet*. URL: <https://snl.no/luftfuktighet>.
- Dolan, Brian (Nov. 2019). *Probability Density Function (PDF) Definition*. URL: <https://www.investopedia.com/terms/p/pdf.asp> (visited on 05/23/2020).
- Elert, Glenn (2020). *Blackbody Radiation*. URL: <https://physics.info/planck/>.
- Engineering ToolBox (2004). *Water Vapor and Saturation Pressure in Humid Air*. URL: [https://www.engineeringtoolbox.com/water-vapor-saturation-pressure-air-d\\_689.html](https://www.engineeringtoolbox.com/water-vapor-saturation-pressure-air-d_689.html) (visited on 04/23/2020).
- Foken, Thomas (2008a). *Micrometeorology*. Vol. 2. Springer. Chap. 1.
- (2008b). *Micrometeorology*. Vol. 2. Springer. Chap. 2.
- Galarnyk, Michael (Sept. 2018). *Understanding Boxplots*. URL: <https://towardsdatascience.com/understanding-boxplots-5e2df7bcbd51> (visited on 02/14/2020).
- Gangstø Skaland, Reidun et al. (Jan. 2019). *Tørkesommeren 2018*. ISSN: 1894-759X. Norwegian Meteorological Institute.
- Geiger, Rudolf, Robert H Aron, and Paul Todhunter (2003). *The climate near the ground*. sixth. Rowman & Littlefield. Chap. 31.
- Hamagami, Takashi et al. (2012). “Field experiment on the effects of a nearby asphalt road on temperature measurement”. In: *16th Symposium on Meteorological Observation and Instrumentation, 92nd American Meteorological Society Annual Meeting*, pp. 22–26.
- Huwald, Hendrik et al. (2009). “Albedo effect on radiative errors in air temperature measurements”. In: *Water Resources Research* 45.8.
- IPCC (2014). *Climate Change 2014: Synthesis Report. Contribution of Working Groups I, II and III to the Fifth Assessment Report of the Intergovernmental Panel on Climate Change*. [Core Writing Team, R.K. Pachauri and L.A. Meyer (eds.)]. IPCC, Geneva, Switzerland, 151 pp.
- Isotech (May 2018). *Certificate of Calibration, Calibration Procedure for milliK Precision Thermometer Indicator*.
- Jianxia, Guo et al. (2012). “Experiments and simulations of sitting classification for wind and temperature observation”. In: WMO TECO 2012.
- Justervesenet (June 2019). *Certificate of Calibration, Calibration Procedure for Dew Point Mirror*.

- Kawwa, Nadim (Feb. 2020). *When to Use the Kolmogorov-Smirnov Test*. URL: <https://towardsdatascience.com/when-to-use-the-kolmogorov-smirnov-test-dd0b2c8a8f61> (visited on 05/22/2020).
- Kirkman, T. W. (1996). *Statistics to Use, Kolmogorov-Smirnov Test*. URL: <http://www.physics.csbsju.edu/stats/KS-test.html> (visited on 05/22/2020).
- Kumamoto, Mariko et al. (2013). “Field experiment on the effects of a nearby asphalt road on temperature measurement”. In: *Sola* 9, pp. 56–59.
- Musacchio, Chiara, Graziano Coppa, and Andrea Merlone (2019). “An experimental method for evaluation of the snow albedo effect on near-surface air temperature measurements”. In: *Meteorological Applications* 26.1, pp. 161–170.
- NMBU, Redaksjonen (Nov. 2019). *Om oss, Feltstasjon for bioklimatiske studier – BIOKLIM (tidligere FAGKLIM)*. URL: <https://www.nmbu.no/fakultet/realtek/laboratorier/bioklim/om-fagklim> (visited on 04/12/2020).
- Oke, Timothy R (2002a). *Boundary layer climates*. Second. Routledge. Chap. 1.
- (2002b). *Boundary layer climates*. Second. Routledge. Chap. 2.
- Perry, Kirsten (Nov. 2019). *Determine if Two Distributions are Significantly Different using the Mann-Whitney U Test*. URL: <https://towardsdatascience.com/determine-if-two-distributions-are-significantly-different-using-the-mann-whitney-u-test-1f79aa249ffb> (visited on 05/23/2020).
- Richmond, Michael W. (June 2003). *Examples of Uncertainty calculations*. URL: <http://spiff.rit.edu/classes/phys273/uncert/uncert.html>.
- Vilà-Guerau de Arellano, Jordi et al. (2015). *Atmospheric Boundary Layer: Integrating Air Chemistry and Land Interactions*. Cambridge University Press, Cambridge, UK. Chap. 3.
- Wallace, John M and Peter V Hobbs (2006). *Atmospheric science: an introductory survey*. Vol. 92. Elsevier. Chap. 3.
- Wolff, Mareile, Inna Haapa, et al. (2014). “Air Temperature Sensor Siting Classification in Nordic Countries”. In: *Wmo/cimo teco*.
- Wolff, Mareile, Gabriel Kielland, et al. (2016). “Temperature sensor siting classification in Nordic Countries”.
- Wolff, Mareile, Hildegunn Nygård, et al. (2018). “Recent results from siting classification in the Nordic Countries and Baltic States, applying a common metadata scheme for air temperature measurements.” In: WMO-CIMO TECO 2018 in Amsterdam.
- Wolff, Mareile, Vidar Thue-Hansen, and Arne Auen Grimenes (Jan. 2019). *Meteorologiske data for Ås 2018*. ISBN: 978-82-7636-032-5. NMBU.
- (Jan. 2020). *Meteorologiske data for Ås 2019*. ISBN: 978-82-7636-033-20. NMBU.
- World Meteorological Organization (2017). “WMO Guidelines on the Calculation of Climate Normals”. In: ISBN: 978-82-7636-033-20.
- (2018). “Guide to Instruments and Methods of Observation”. In: 1.8. WMO-No. 8, ISBN: 978-92-63-10008-5.

# Appendices

## Appendix A

### Travelling normal calibration

*Table A.1: Measuring table for calibration of the humidity measuring instrument Vaisala HMP77.*

Read value [V]	“True” value [%RH]	Correction [%RH]
0.1	8.4	-1.6
0.2	18.5	-1.5
0.3	28.6	-1.4
0.4	38.6	-1.4
0.5	48.7	-1.3
0.6	58.8	-1.2
0.7	68.9	-1.1
0.8	79.0	-1.0
0.9	89.0	-1.0

## Appendix B

### The field controls' results

	C 2.00 m		C 1.25 m		C 0.55 m		U 2.00 m		U 1.25 m		U 0.55 m	
	Temp.	Hum.	Temp.	Hum.	Temp.	Hum.	Temp.	Hum.	Temp.	Hum.	Temp.	Hum.
23.05.2018	-0.09	-0.85	-0.13	1.83	-0.13	3.27	-0.05	2.70	-0.01	2.50	-0.10	3.30
	-0.06	3.70	-0.13	3.46	-0.12	2.49	-0.04	1.60	0.00	3.61	-0.10	3.30
	-0.07	1.90	-0.10	3.29	-0.14	4.70	-0.06	1.27	-0.02	3.70	-0.09	4.20
	-0.18	3.39	-0.09	3.08	-0.17	2.13	-0.04	2.01	-0.12	3.70	-0.14	4.10
	-0.19	1.83	-0.09	3.80	-0.16	3.28	-0.03	0.74	-0.06	3.80	-0.12	3.32
	-0.15	2.72	-0.09	2.96	0.04	1.57	-0.04	0.50	-0.04	4.60	-0.09	4.70
	-0.11	1.26	-0.08	4.91	-0.15	2.75	-0.03	1.00	0.02	3.20	-0.02	4.30
	-0.14	2.04	-0.12	2.27	-0.14	3.50	-0.07	0.70	0.06	3.70	-0.06	3.30
	-0.15	1.85	-0.10	2.01	-0.18	4.17	-0.11	1.71	0.06	4.70	0.08	2.80
27.02.2020,	-0.05	-8.73	-0.12	3.11	-0.15	2.54	-0.24	4.13	-0.21	3.20	-0.72	4.09
	0.02	-14.65	-0.13	2.86	-0.22	1.94	-0.16	3.44	-0.10	3.69	-0.59	4.10
	0.02	-17.73	-0.06	3.20	-0.13	1.64	-0.04	3.32	-0.05	3.11	-0.52	4.18
04.05.2020 for C 0.55 m	0.05	-26.15	-0.06	1.91	-0.06	0.32	-0.05	2.25	0.12	1.66	0.14	2.76
	0.02	-25.18	-0.06	2.94	-0.06	2.67	-0.02	1.82	0.17	-0.93	0.17	1.59
	0.00	-20.36	-0.06	2.01	-0.03	1.83	-0.01	2.23	0.03	1.63	0.15	2.50
	0.05	-24.61	0.01	1.97	-0.10	3.22	0.00	5.20	0.26	2.21	0.16	1.40
	0.07	-25.57	-0.02	0.65	-0.04	-0.71	-0.03	2.13	0.24	2.35	0.24	2.02
	0.07	-22.37	0.00	1.29	-0.07	-1.95	0.08	2.53	0.30	1.84	0.18	1.72

*Figure B.1:* The table in this figure shows the real values of the difference between measured air temperature and relative humidity by the measuring instruments and the travelling normal. C is the location with cut grass and U is the location with uncut grass. Temp. is temperature and Hum. is humidity.

## Appendix C

### Diurnal box and whisker plots for 2018

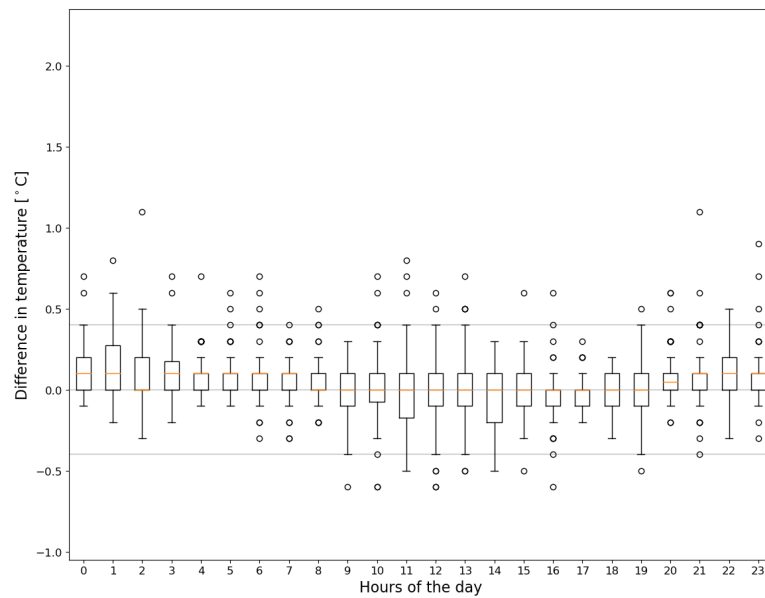


*Figure C.1:* This plot shows box and whisker plots for the difference between the temperature at 2m over uncut grass and that over cut grass for each hour of the day. The data set used is from 11/7/2018 12:00 until 15/9/2018 13:00.



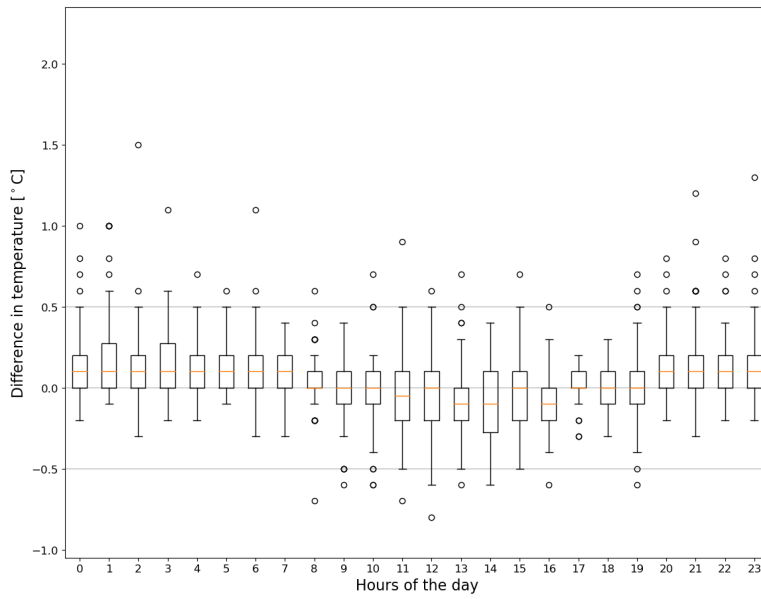


**Figure C.2:** This plot shows box and whisker plots for the difference between the temperature at 1.25 m over uncut grass and that over cut grass for each hour of the day. The data set used is from 11/7/2018 12:00 until 15/9/2018 13:00.

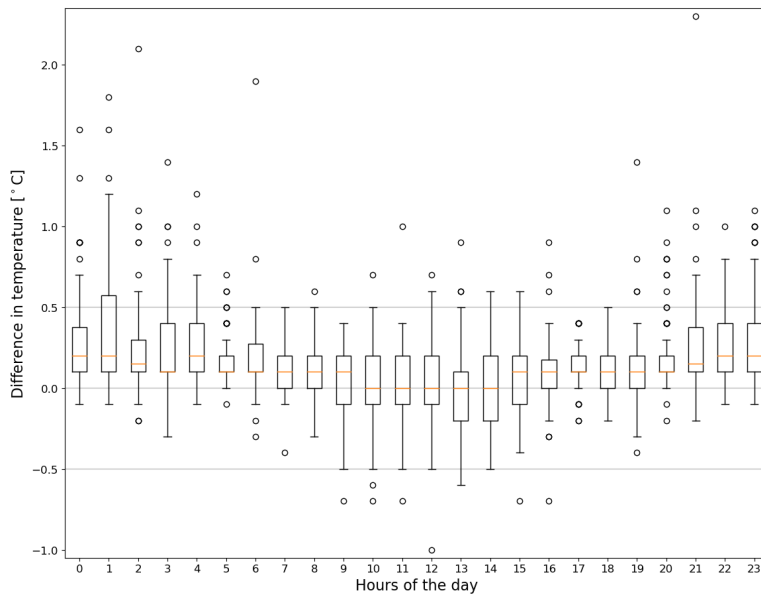


**Figure C.3:** This plot shows box and whisker plots for the difference between the temperature at 0.55 m over uncut grass and that over cut grass for each hour of the day. The data set used is from 11/7/2018 12:00 until 15/9/2018 13:00.

## Appendix D

# Monthly difference in temperature

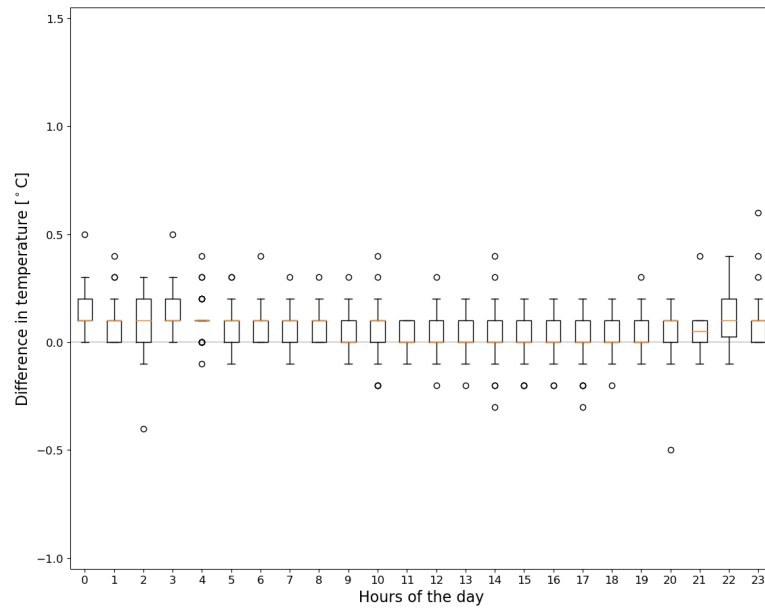


**Figure D.1:** This plot shows box and whisker plots for the difference between the temperature at 2m over uncut grass and that over cut grass for each hour of the day. The data set used is from 1/6/2019 00:00 until 30/6/2019.

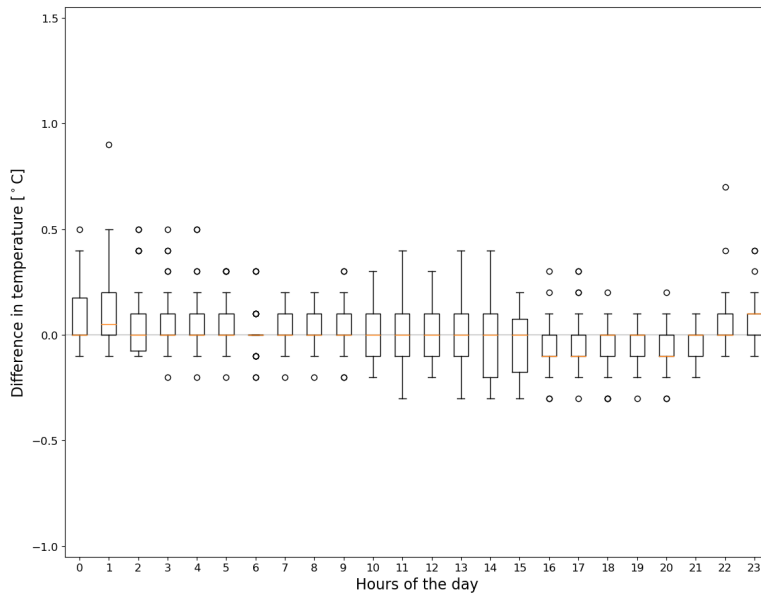


**Figure D.2:** This plot shows box and whisker plots for the difference between the temperature at 2m over uncut grass and that over cut grass for each hour of the day. The data set used is from 1/7/2019 00:00 until 31/7/2019.

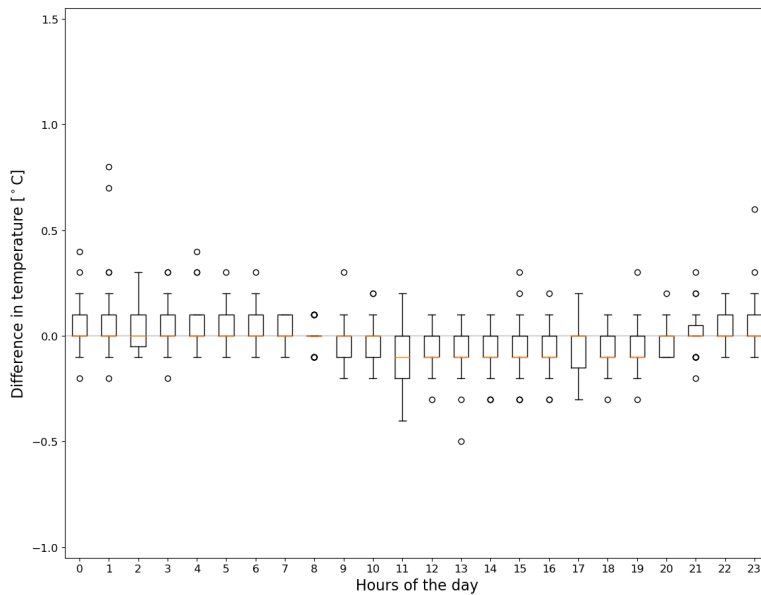


**Figure D.3:** This plot shows box and whisker plots for the difference between the temperature at 2m over uncut grass and that over cut grass for each hour of the day. The data set used is from 1/8/2019 00:00 until 31/8/2019.

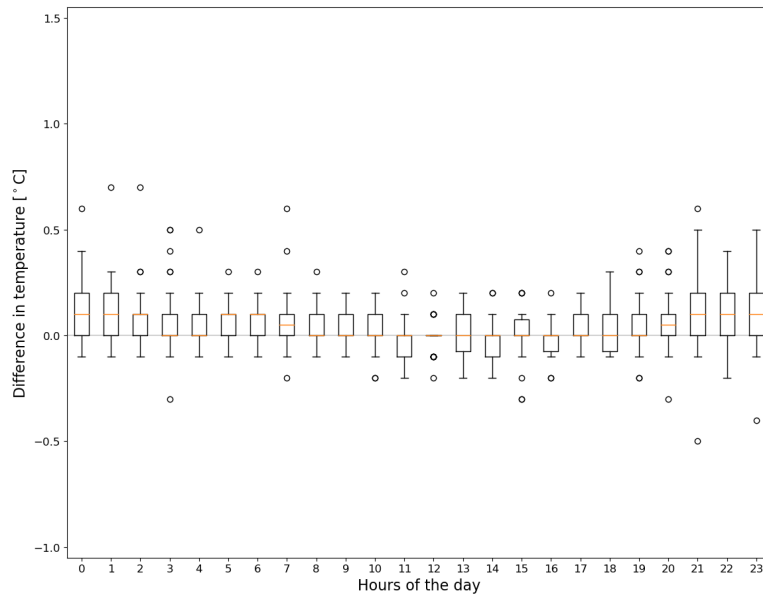


**Figure D.4:** This plot shows box and whisker plots for the difference between the temperature at 2m over uncut grass and that over cut grass for each hour of the day. The data set used is from 1/9/2019 00:00 until 30/9/2019.

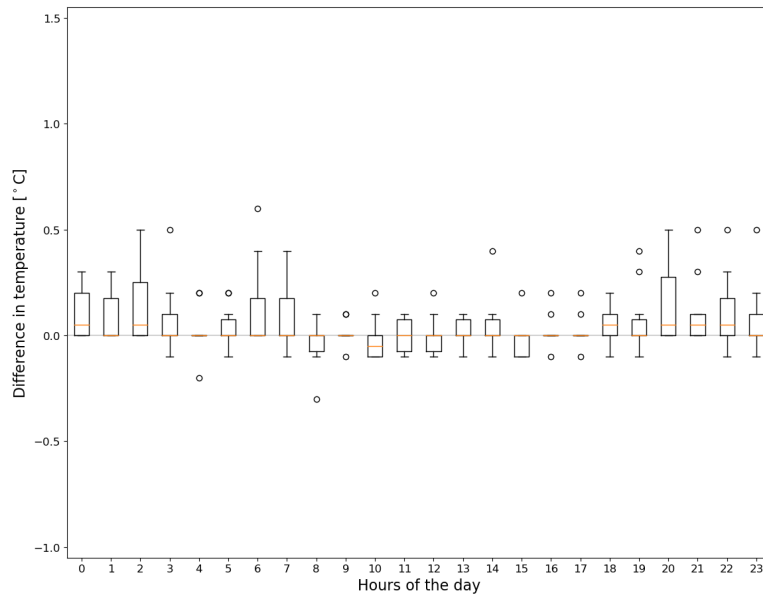


**Figure D.5:** This plot shows box and whisker plots for the difference between the temperature at 2m over uncut grass and that over cut grass for each hour of the day. The data set used is from 1/10/2019 00:00 until 30/10/2019 12:00.

## Appendix E

### Radiation category plots for 2018

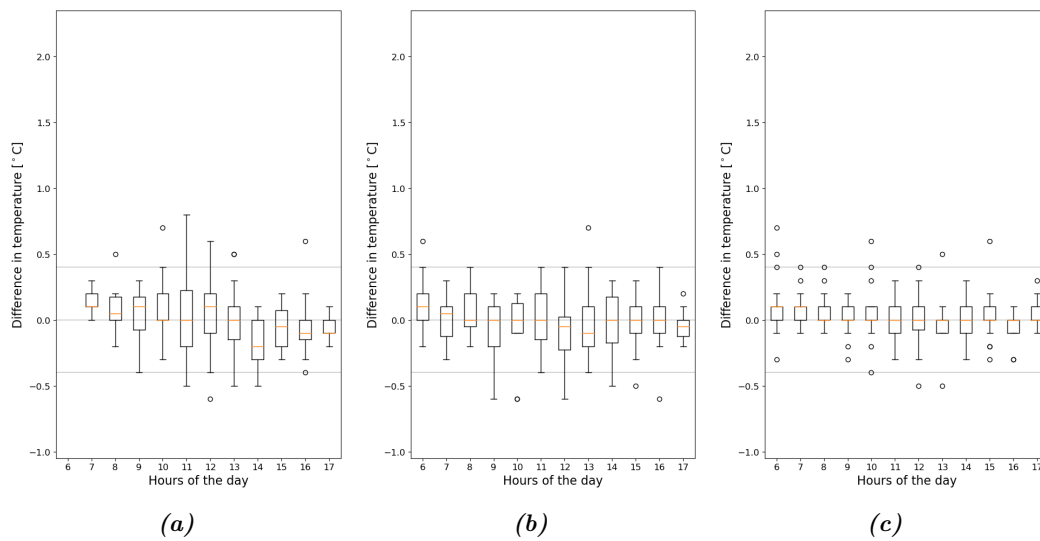


**Figure E.1:** The difference in temperature measured over uncut and cut grass at 2 m is here plotted as box and whisker plots during day hours. The plot is separated into three solar radiation exposure categories: (a) cloud-free, (b) partly cloudy, and (c) overcast or considerable cloudiness. These categories were presented in section 3.8 and table 3.10. The data set used is from 11/7/2018 12:00 until 15/9/2018 13:00.

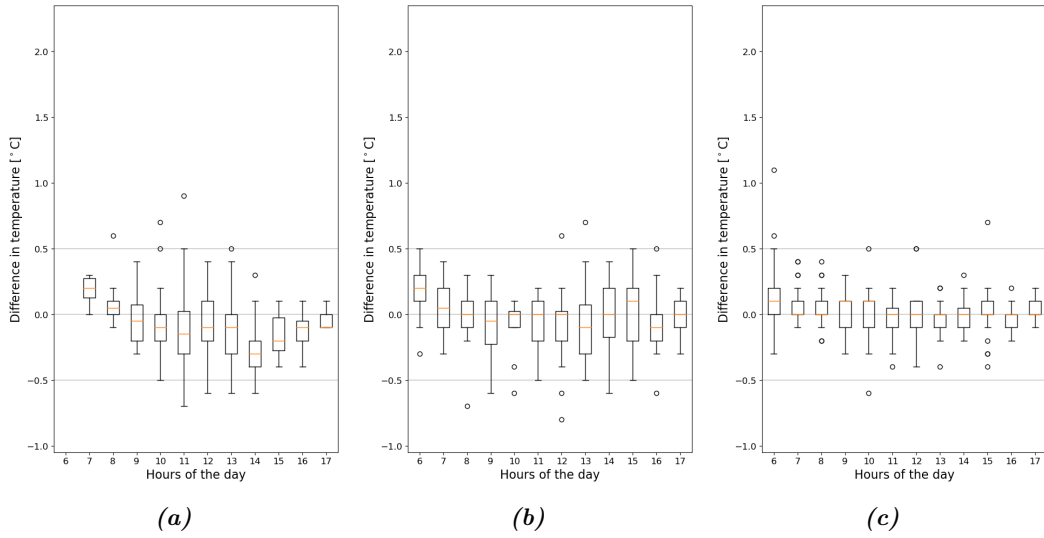


**Figure E.2:** The difference in temperature measured over uncut and cut grass at 1.25 m is here plotted as box and whisker plots during day hours. The plot is separated into three solar radiation exposure categories: (a) cloud-free, (b) partly cloudy, and (c) overcast or considerable cloudiness. These categories were presented in section 3.8 and table 3.10. The data set used is from 11/7/2018 12:00 until 15/9/2018 13:00.

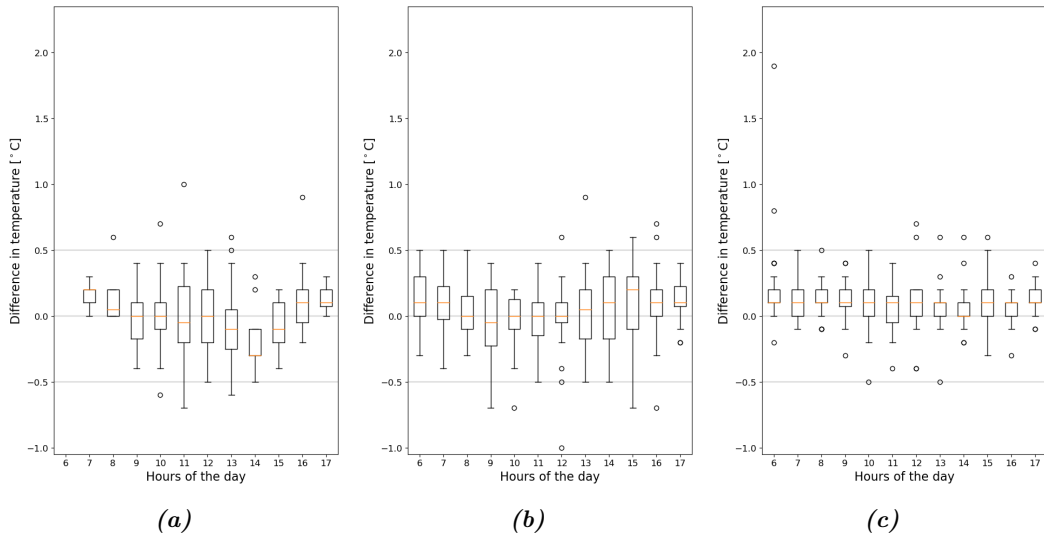


**Figure E.3:** The difference in temperature measured over uncut and cut grass at 0.55 m is here plotted as box and whisker plots during day hours. The plot is separated into three solar radiation exposure categories: (a) cloud-free, (b) partly cloudy, and (c) overcast or considerable cloudiness. These categories were presented in section 3.8 and table 3.10. The data set used is from 11/7/2018 12:00 until 15/9/2018 13:00.

## Appendix F

### Diurnal difference in humidity

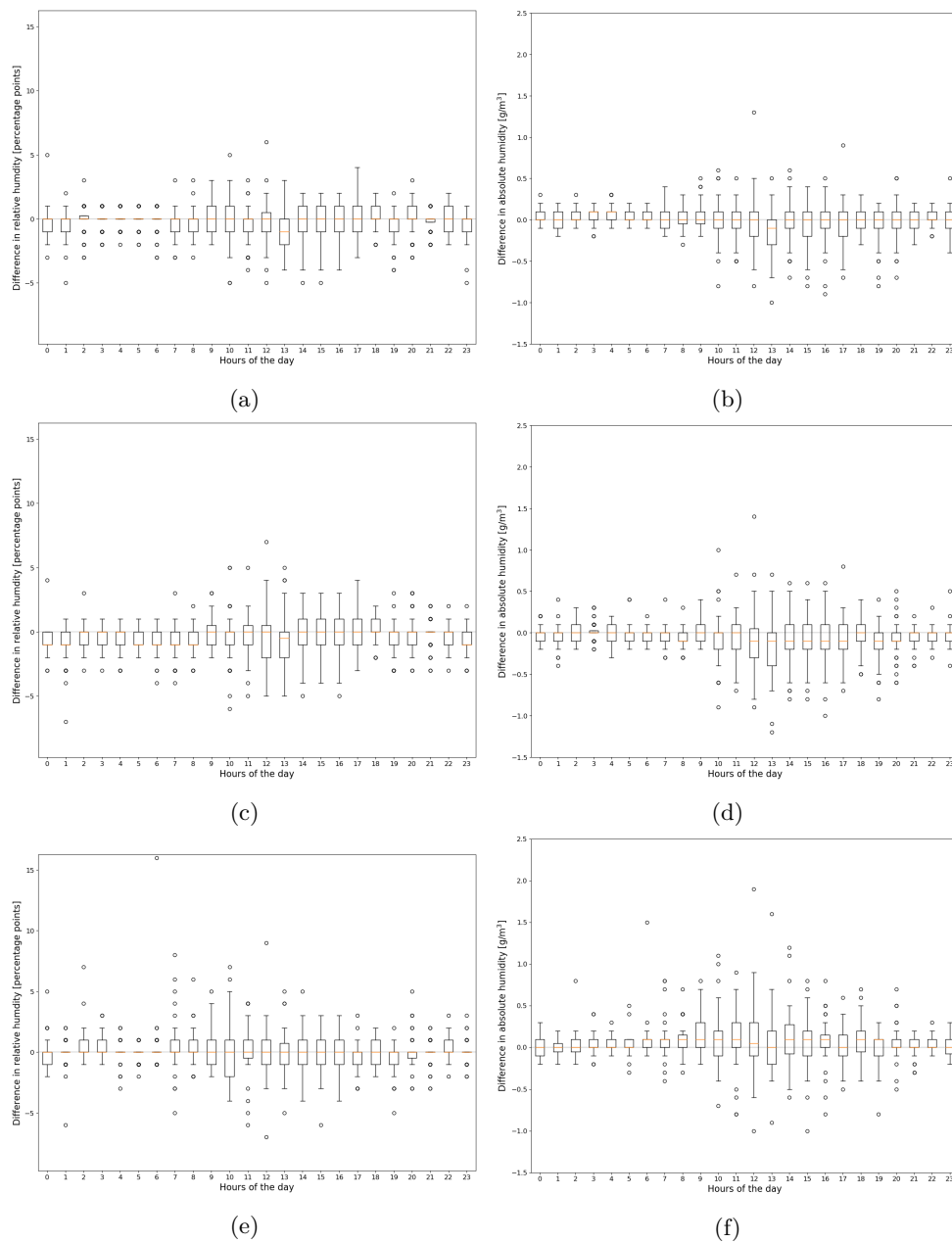


Figure F.1: These plots show box and whisker plots of the difference in humidity measured over uncut grass ( $U$ ) and cut grass ( $C$ ). The plots display the following: (a) the difference between relative humidity at 2 m, (b) the difference between absolute humidity at 2 m, (c) the difference between relative humidity at 1.25 m, (d) the difference between absolute humidity at 1.25 m, (e) the difference between relative humidity at 0.55 m, (f) the difference between absolute humidity at 0.55 m. The time period used for the data set is from 23/5/2019 until 15/7/2019

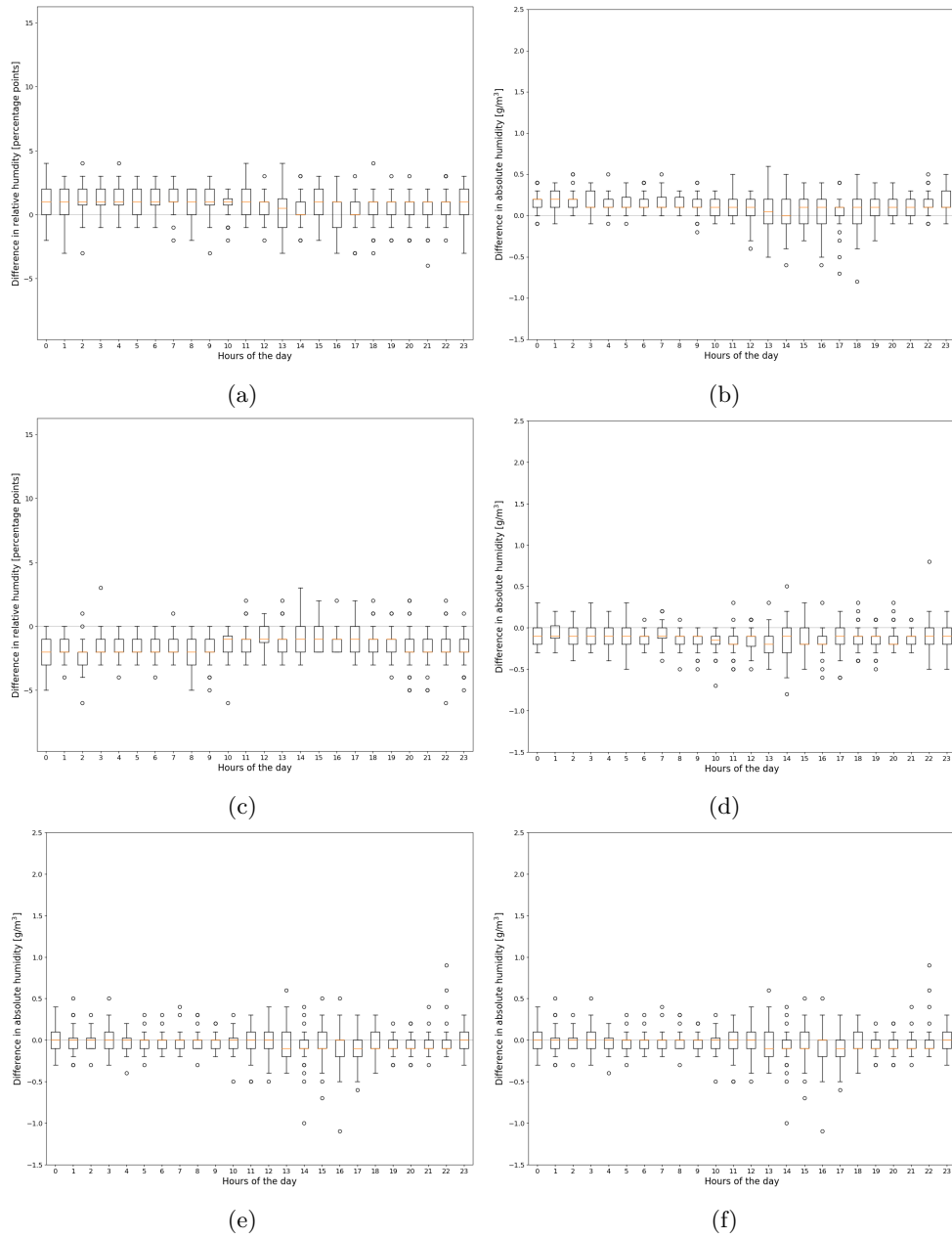


Figure F.2: These plots show box and whisker plots of the difference in humidity measured over uncut grass ( $U$ ) and cut grass ( $C$ ). The plots display the following: (a) the difference between relative humidity at 2 m, (b) the difference between absolute humidity at 2 m, (c) the difference between relative humidity at 1.25 m, (d) the difference between absolute humidity at 1.25 m, (e) the difference between relative humidity at 0.55 m, (f) the difference between absolute humidity at 0.55 m. The time period used for the data set is from 21/8/2019 14:00 until 22/9/2019



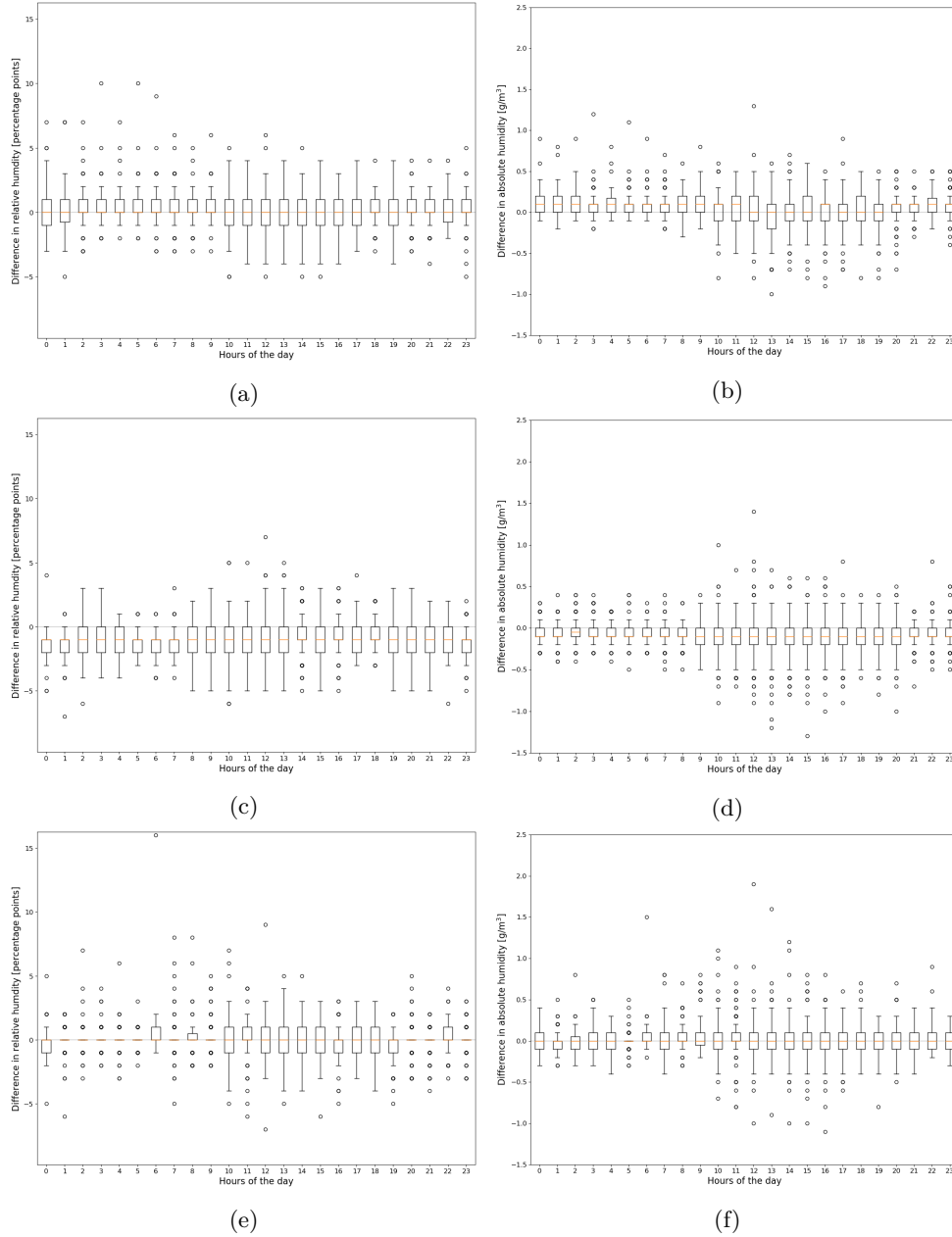
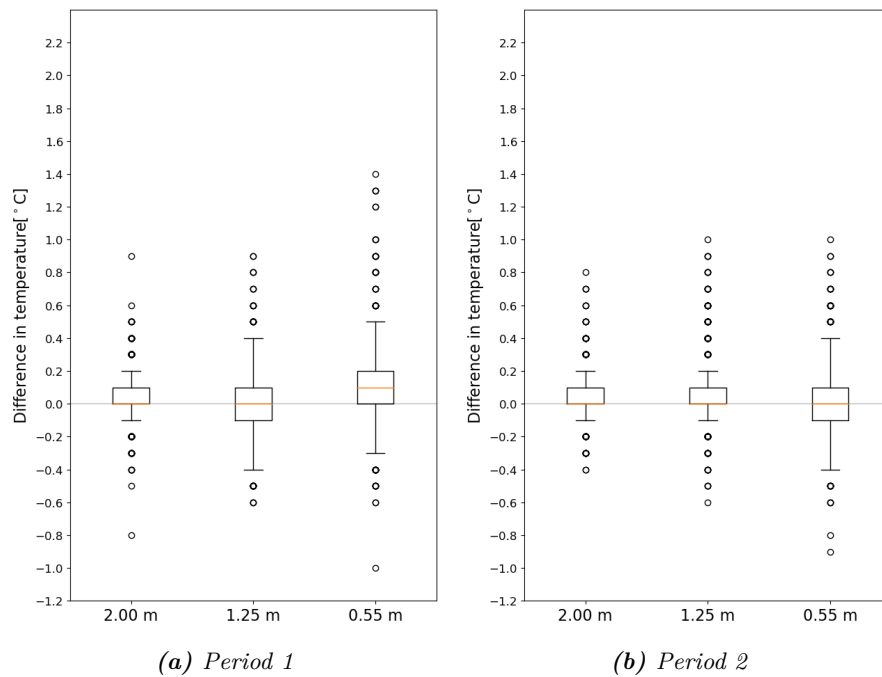


Figure F.3: These plots show box and whisker plots of the difference in humidity measured over uncut grass ( $U$ ) and cut grass ( $C$ ). The plots display the following: (a) the difference between relative humidity at 2 m, (b) the difference between absolute humidity at 2 m, (c) the difference between relative humidity at 1.25 m, (d) the difference between absolute humidity at 1.25 m, (e) the difference between relative humidity at 0.55 m, (f) the difference between absolute humidity at 0.55 m. The time period used for the data set is from 23/5/2019 00:00 until 30/10/2019 12:00.

## Appendix G

# Difference in temperature in two time periods



**Figure G.1:** These plots show box and whisker plots of the difference in temperature measured over uncut grass (*U*) and cut grass (*C*) at three heights above the ground: 2 m, 1.25 m, and 0.55 m. These values are plotted for the 1<sup>st</sup> and 2<sup>nd</sup> periods that humidity data are plotted for in section 4.7.1, presented in table 4.11. (a) displays the difference in temperature in the 1<sup>st</sup> period (23/5/2019-15/7/2019), while (b) displays the difference in temperature the 2<sup>nd</sup> period (21/8/2019 14:00-22/9/2019).







**Norges miljø- og biovitenskapelige universitet**  
Noregs miljø- og biovitenskapelige universitet  
Norwegian University of Life Sciences

Postboks 5003  
NO-1432 Ås  
Norway